12-2009

CREATION OF BIOACTIVE SURFACES TO MODULATE CELL BEHAVIOR USING SURFACE INITIATED PHOTOINIFERTER-MEDIATED GRAFT PHOTOPOLYMERIZATION

Nihar Shah
Clemson University, nmshah@gmail.com

CREATION OF BIOACTIVE SURFACES TO MODULATE CELL BEHAVIOR USING SURFACE-INITIATED PHOTOINIFERTER-MEDIATED GRAFT PHOTOPOLYMERIZATION

A Dissertation
Presented to
The Graduate School of
Clemson University

In Partial Fulfillment
of the Requirements for the Degree
Doctor of Philosophy
Bioengineering

By

Nihar Manilal Shah
December 2009

Accepted by:
Dr. Ken Webb, Committee Chair
Dr. Andrew Metters
Dr. Karen Burg
Dr. Naren Vyavahare
Dr. Andrew Mount

Abstract

Biomaterials widely used in biomedical applications still face biocompatibility issues arising from non-specific protein adsorption on the foreign surface, and the consequent undesired cell response. Emerging evidence suggests that imparting specific bioactivity to the biomaterial's surface to elicit favorable response from cells, (like osseointegration of joint implants and endothelialization of stents) can yield much better biocompatibility results when combined with passive prevention of protein adsorption. In more complex diseases like spinal cord injury and cardiomyopathy, specific biomolecules are required to elicit desired cell responses for successful regeneration. However, for success of such biomolecule-based strategies, the effects of various parameters (type of molecule, concentration, spatial and temporal distribution) on the behavior of target cells need to be thoroughly investigated.

Surface-initiated photoiniferter-mediated polymerization (SIPMP) was selected for this study, because it:

1. can graft protein-resistant polymer (like poly(ethylene glycol) (PEG), poly(hydroxyethyl methacrylate) (HEMA)) on any biomaterial surface.
2. provides excellent control over the amount of polymer grafted.
3. allows covalent immobilization of biomolecules on the polymer chains, and
4. allows creation of spatial patterns and concentration gradients of biomolecules by spatially controlling polymer grafting.

As the first step, poly(methacrylic acid) (pMAA) grafting via SIPMP was used to systematically control the hydrophilicity and the concentration of attached molecules on polyurethane surfaces by varying the iniferter concentration, monomer concentration, UV intensity and UV exposure time. In the next step, covalent conjugation of a hormone

noradrenalin (NA) to pMAA and pHEMA chains grafted on glass surfaces was achieved as a means to develop a novel anti-marine biofouling surface. Accessibility and bioactivity of conjugated NA was confirmed by its deleterious effects on viability and cell structure of oyster hemocytes. Finally, thickness gradients of pMAA and pHEMA chains were created on glass surface as a means to create protein concentration gradients and study their effects on gradient-dependent cell behaviors. Preliminary experiments for controlling cell adhesion by conjugating proteins to homogeneous pHEMA layers remain inconclusive, warranting further investigation. In summary, the results obtained in this study highlight the versatility of SIPMP for high throughput analysis of cell behavior on surfaces with a wide variety of bioactive functionalities.

Dedication

This dissertation is dedicated to the three most important people in my life, my mother, Bharati Shah, my father, Manilal Shah, and my fiancée, Bhavini Shah, who have been a perpetual source of unconditional encouragement and love. Even though they are on the opposite side of the world, their support has undoubtedly been instrumental in my success at Clemson.

Acknowledgements

I want to take this opportunity to thank all the people who have helped me over the past five years to make my journey a success. First and foremost, I would like to thank my advisors Dr. Ken Webb and Dr. Andrew Metters, who gave me the opportunity to work on a topic I love, and over the years have guided me to become a better scientist, professional and individual. They have been a constant source of knowledge and support, especially when I faced daunting roadblocks during research, but most importantly they inspired me to achieve far more than I thought I was capable of.

I would also like to thanks my committee members, Dr. Karen Burg, Dr. Naren Vyavahare and Dr. Andrew Mount, who with their vast research experience and bioengineering knowledge have helped me understand the significance of my research from multiple perspectives, and how it fits in the greater scheme of things. I want to extend a special thanks to my dear friend Dr. Neeraj Gohad, and Dr. Andrew Mount, who besides being excellent collaborators, have pushed me to think out the box when faced with seemingly insurmountable problems. Their expertise in optical imaging has been invaluable in obtaining excellent cell culture images.

I sincerely appreciate the technical and emotional support I have received from my lab members over the years. Brad Harris, Santosh Rahane and Chien-Chi Lin helped demystify polymerizations, while Rebecca Cribb, Jaishankar Kutty and Eunhee Cho frequently helped make cell culture experiments successful. I also want to thank Jeoung Soo Lee, who was always available to enlighten me on complex conjugation chemistries, and for keeping the lab atmosphere so cheerful.

I would also like to thank several people at Clemson University who have provided specific technical support and training when needed. In particular, Dr. Chris Kitchens, Dr. Douglas Hirt and Dr. Scott Husson for access to lab facilities, Dr. Delphine Dean, Dr. Alexey Vertegel, Dr. Igor Luzinov and Dr. Ruslan Burtovyy for AFM, and Dr. Brandon Moore and Dr. Abhijit Karve for fluorescent imaging. I would also like to thank Cassie Gregory for help with cell culture, and Bill Coburn and Mike Wilbanks for infrastructure support.

I want to give a special thanks to my brother Dejul Shah, who has constantly encouraged me to go the extra mile to succeed. I would also like to thank my good friend Balakrishnan Sivaraman for making his personal and profession support available whenever I needed it. I am very grateful to Kumarpal Sheth for taking time out from his busy schedule to proof read this dissertation. Finally, I want to extend my gratitude to numerous friends and family members, here in Clemson, and elsewhere in the world, whom I am unable to name here, but have in some way helped me over the past five years.

Table of Contents

List of Figures

List of Tables

1. Introduction

All metals, ceramics and polymers, natural or synthetic, have a specific set of bulk (like strength, toughness, hardness, elasticity, plasticity, porosity) and surface (wettability, adhesion, friction, roughness, wear resistance, corrosion resistance) properties. Ideally, the right combination of bulk and surface properties can be designed for optimal performance of the material in the targeted application. In reality however, such combinations are rare, and due to practical and economic reasons, it becomes very difficult to develop an entire new material that has the right combination. Usually the bulk material with desired mechanical properties is first developed, followed by some form of surface treatment to improve or impart desired surface properties. This has led to development of a plethora of "surface modification" (SF) techniques applicable to a wide variety of bulk materials to improve one or more surface properties.

Chapter 2.1 discusses various SF techniques as used in common non-biomedical applications. Briefly, metals are extensively used for applications requiring good mechanical properties like strength, toughness and elasticity. However they are also very prone to corrosion at the surface, which eventually reduces their life span. Numerous techniques such as electroplating, ion implantation (II), ion-beam assisted deposition (IBAD), plasma-assisted deposition (PAD), chemical vapor deposition (CVD), etc are extensively used improve corrosion resistance of metal surfaces.[1-3] IBAD, PAD and other film deposition techniques are also commonly used to improve wear resistance of metal and ceramic surfaces[2, 3], and in some specialized applications like optical coatings[4]. The microelectronics industry almost entirely depends on numerous SF techniques like metallization, CVD, PAD and lithography for manufacturing of a wide variety of integrated circuits, diodes, printed circuit boards, fiber optic cables, etc. [5-7]

Paints and specialized cross-linked polymer coatings are now ubiquitously used to protect buildings from wear and erosion, metal surfaces like vehicles and machinery from corrosion, and in some highly specialized applications like anti-biofouling coatings[8] for the shipping industry fleet. PTFE-based coatings applied to cookware to prevent adhesion, and to metal, plastic and paper food containers to prevent toxic chemical reactions are another example of the widespread use of polymer-based SF.[9-11] Polymer grafting, has emerged as the technique of choice to graft nanometer-scale fouling-resistant polymer brushes on the surface of micro- and nano-porous filtration membrane, without affecting their performance.[12]

Metallic, ceramic and polymeric biomaterials are under intense research for replacement, augmentation and regeneration of diseased tissues in human. Biomaterials are already used to completely replace heart valves, joints, intro-ocular lenses, pacemakers, etc, and support limited regeneration of some tissues like bones, cartilage and skin. The two primary requirements of any biomaterial are suitable mechanical properties and biocompatibility. It may not always be possible to obtain the right combination of various mechanical properties, (strength, modulus and wear resistance) for a specific application. Even if meticulous and expensive designing helps meet all the mechanical requirements, biocompatibility may suffer. Therefore, SF for biomedical applications is usually targeted towards improving the mechanical properties and/or biocompatibility of the biomaterial. In fact, many of the SF techniques used for non-medical applications discussed above have also been adapted for biomedical applications (Chapter 2.2). The poor wear, abrasion and corrosion resistance properties of widely used titanium implants[13-16] are now routinely improved using several techniques like nitrogen ion implantation, plasma nitriding[15, 16], laser-annealed nitriding[16], IBAD and

CVD[16]. Similarly, plasma bombardment is used to improve wear resistance of UHMWPE joint sockets[17] This has lead to significant improvements in the biocompatibility and usable life-span of such implants.

SF for improving mechanical properties of biomaterials is largely restricted to load-bearing implants. Almost all other SF strategies target improving biocompatibility, either by reducing non-specific protein adsorption to prevent undesired cell responses, or impart specific bioactivity to the surface to elicit useful cell responses (like osseointegration of joints, and endothelialization of coronary stents[18]). For some complex diseased conditions, implantation of devices like joints and stents is not sufficient, but instead regeneration of the diseased tissue is required. This is especially true for tissues with intrinsically low regeneration potential such as cardiac myocytes, blood vessels and central nervous system neurons. In these cases, specific signaling molecules need to be provided to stimulate the desired regenerative response from native cells. For this strategy to be successful, effects of various parameters like the specific biomolecule, its concentration, its spatial distribution and its temporal distribution on the target cell's behavior need to be thoroughly investigated.

Numerous SF strategies have been developed to improve the surface biocompatibility and/or impart specific bioactivity to the surface, including plasma treatment and deposition of alkylthiol or alkylsilane self-assembled monolayers (SAMs).[19-22] These treatments typically involve creation of hydrophilic functional groups like hydroxyl, carboxyl, amine and thiol on the surface, which can control protein adsorption on the surface, and can also be used to covalently couple specific biomolecules to elicit desired cellular interactions.[23, 24] Some researchers have combined SAM deposition techniques with patterning techniques like microcontact printing[25, 26] or photochemical coupling[27] to create patterns and gradients of biomolecules

on the surface. Such patterns provide excellent spatial control over cell adhesion.[26, 27] However, these techniques are prone to surface defects, molecule detachment, or undesired chemical reactions that cause loss of surface activity.[28] Redundant molecules are not present on the surface to compensate for such losses. Additionally, the movement/rotation of conjugated biomolecules becomes highly restricted, which can limit access to cell receptors and prevent formation of focal adhesion clusters resulting in poor cell responses.

Grafting of flexible polymer brushes with functional groups on the surface seems to be the most promising technique, which overcomes most, if not all of these limitations (Chapter 2.3). Polymer brushes can be created on a surface by either the “grafting to” or the “grafting from” approach. In a “grafting to” approach, pre-formed end-functionalized polymer molecules react with reactive groups on the surface to form polymer brushes. The bond formed between surface and polymer chain makes the polymer brushes robust and resistant to common chemical and environmental conditions. “Grafting to” is typically achieved either by depositing SAMs of thiolated/silanated polymer chains[29, 30], or by covalently coupling the polymer chains to functional groups on the surface[31-34]. PEG and PEG-based hydrophilic polymers grafted to gold[29, 30], glass, silicon, polymer[31-33] and metal[34, 35] surfaces are able to significantly reduce protein adsorption, and cell or platelet adhesion. Unfortunately, “grafting to” is either restricted to using commercially available pre-synthesized polymers, or requires custom polymer synthesis. Furthermore, increasing diffusion barriers created by chains already grafted on the surface prevent more chains from reaching the surface, resulting in a low grafting density and low polymer layer thickness.[28, 36, 37]

The “grafting from” approach utilizes reactive species on the material surfaces to initiate the polymerization of monomers from the surface outwards. Therefore, the aforementioned

limitations do not exist as the small monomer molecules are not as prone to diffusion barriers[37], and any molecule that can be potentially polymerized can be used. The most versatile and convenient “grafting from” method is surface initiated radical polymerization (SIRP), which can either be uncontrolled or controlled. Surface-initiated uncontrolled radical polymerization has been used to graft various hydrophilic polymers from a wide variety of biomaterials, to control protein adsorption and platelet adhesion, or facilitate covalent conjugation specific biomolecules to control cell behavior.[38-50] However, SIURP techniques produce high polydispersity (PD) on the same surface, which will cause an uncontrolled variation in concentration of the biomolecules, and hence in cell behavior.

This limitation of SIURP can be overcome by using surface-initiated controlled radical polymerization (SICRP) techniques, where the radicals undergo repetitive and reversible initiation-termination so that polymerization progresses in a very “controlled” manner. This provides excellent control over the amount of polymer and hence the concentration of conjugated biomolecules on the surface. Several SICRP techniques such as atom transfer radical polymerization (ATRP)[51, 52], nitroxide-mediated polymerization (NMP)[53, 54], reversible addition-fragmentation chain transfer polymerization (RAFT), and photoiniferter-mediated polymerization (PMP)[55-57] have been used for biomedical applications, with ATRP and PMP being the most prominent. ATRP offers low PD and excellent control over the amount of grafted polymer. However, the creation of spatial patterns[58] and/or gradients[59] on the surface requires extremely elaborate procedures.

Photoiniferter-mediated polymerization (PMP) uses UV light to graft polymer chains. By controlling the UV location, intensity and exposure time across the surface, complex spatial patterns and gradients of grafted polymer chains can be created on the surface. Grafting via

PMP is much faster (minutes rather than hours), can be performed at room temperature with or without solvent (pure monomer), requires no catalyst/ligand system, and is compatible with a wide range of vinyl monomers. Surface-initiated PMP (SIPMP) depends on the presence of special dithiocarbamate-derived iniferter (INItiator-transFER agent-TERminator) molecules on the surface, which generate reversibly terminable radicals on UV exposure to graft polymer chains. Such concentration gradients of biomolecules can also be used to quantitatively analyze other gradient dependent cell behaviors like growth and migration. Furthermore, gradients can be also combined with patterned photomasks to create multiple sets of gradients with different profiles on the same surface. Such versatile surfaces can be used to study cell behavior on different gradient profiles in an extremely high throughput manner.

Therefore, the central hypothesis of this study was that SIPMP can be used to

1. modify surface properties of different materials,
2. covalently attach biomolecules to the polymer chains,
3. create gradients on the surface, and
4. maintain accessibility and bioactivity of the immobilized biomolecules.

The surface modification of PU substrates is discussed in Chapter 3. Specifically, SIPMP was made possible by incorporating the iniferter tetraethylthiuram disulfide (TED) into a photocrosslinked PU network. The goal was to improve the hydrophilicity of the PU surfaces, and provide a means to attach small molecules on the surface. It would also be advantageous if the level of hydrophilicity and amount of biomolecule attached on the surface can be easily altered for specific applications. To achieve these goals, the amount of hydrophilic polymer poly(methacrylic acid) grafted on the surface was systematically varied using four parameters, TED concentration, monomer concentration, UV intensity and exposure time. The effect of

polymer grafting on substrate hydrophilicity was monitored by water contact angle measurements. As proof of principle, the ability to attach small biomolecules was simulated using electrostatic attachment of the positively charged dye toluidine blue. The change in amount of dye attached was monitored by spectrophotometric measurements.

Chapter 4 describes the covalent conjugation of noradrenalin (NA) to homogeneous pMAA and pHEMA layers using two different conjugation chemistries. The goal was to develop novel bioactive surfaces that prevent fouling by marine organisms. NA conjugation was verified by measuring the post-conjugation thickness increase using AFM as well as XPS scans to detect formation of the amide bond. Finally, the bioactivity and accessibility of NA was verified by oyster hemocyte culture on NA conjugated surfaces. Appropriate controls were included to confirm that only immobilized NA, and not the polymer itself, was responsible for any observed change in cell behavior.

Finally, Chapter 5 presents preliminary studies in creating well-defined concentration gradients of substrate-immobilized proteins as a means to control gradient-dependent cell behaviors. Creation of pMAA and pHEMA thickness gradients was confirmed by AFM, while pMAA gradients were visualized by the covalently conjugated fluorescent dye dansylcadavarine. Some preliminary experiments were conducted to covalently conjugate either fibronectin or L1 neural cell adhesion molecule to homogeneously grafted pHEMA chains. NIH3T3 fibroblasts and B35 neuroblastoma cells were cultured on these surfaces to verify conjugation, bioactivity and accessibility of the proteins. Appropriate controls were included to confirm that only conjugated proteins, and not non-specific protein adsorption was responsible for observed cell attachment.

2. Significance of Surface Modification and Available Techniques

Every material, natural or synthetic, has a specific set of surface properties such as wettability, adhesion, friction, charge, hardness, toughness, roughness, porosity, wear resistance and corrosion resistance, which can have a significant impact on the material's performance. For optimal performance of any material, both its bulk and surface properties need to be carefully designed. Ideally, the same material selected for its desirable bulk properties should also have the requisite surface properties. Unfortunately, such combinations are rare, and due to practical and economic reasons, it is very difficult to develop an entirely new material that fulfills both these requirements. This has led to research and development of numerous surface modification technologies that can suitably modify surface properties of metals, ceramics, and polymers, which comprise most of the commercially used materials. There are a plethora of techniques already in commercial use, with others under development to address yet unmet requirements. It is also important to realize that selection of the right surface modification technique will depend not only on the surface property desired, but also on the base material and its final application. Sometimes only one particular technique will fulfill all the requirements, whereas it is very likely multiple techniques will be applicable for other applications. The following literature review, briefly discusses some of the commercially important surface modification techniques. The first part focuses on non-biomedical applications, while the second part focuses on biomedical applications.

2.1 Surface Modification Techniques in Non-Biomedical Applications

2.1.1 Paints

One of the oldest examples of surface modification is coating walls of buildings to improve aesthetics and provide protection from the elements such as water, temperature and

wind. The early coatings probably consisted of thick layers of naturally available materials like animal dung and some form of mud. These thick natural coatings have eventually progressed into thin layers of specialized paints, which not only improve aesthetics, but also keep water out, are tough enough to withstand erosion, are flexible enough to withstand temperature variations, and in extreme cases can even withstand fires. Besides large scale use on buildings, paints are now extensively used to protect metallic surfaces such as machinery, vehicles and ships from corrosion. Specifically for ship hulls, special toxic paints are currently used to prevent biofouling by marine organisms.[60] Such anti-biofouling paints save the shipping industry billions of dollars in fuel, dry-docking, cleaning and recoating costs every year.[60] The detrimental environmental effects of these toxic paints is a primary cause for them to be slowly phased out.[60] This has created tremendous pressure for the development of environmentally benign anti-biofouling coatings. New polymeric materials as well as application technologies are being developed to meet this challenge.[60] Some of these advancements are discussed further below under polymer films.

2.1.2 Electroplating and Metallization

Besides paints, electrodeposition and electroless deposition have long been used to plate a thin layer of a desired secondary metal onto the primary bulk metal surface. These techniques are primarily used for corrosion resistance, like nickel or zinc plating of copper and steels to prevent oxidation.[1] The multibillion dollar construction industry depends on coating all the steel cables, wires and rods used in reinforced concrete with zinc to prevent long term corrosion. Electroplating is also used to improve wear resistance, conductivity and aesthetic appeal.[1] Gold, platinum and palladium plating of jewelry, furniture and decorative items to improve their appearance are some common examples.[1] Lately plating of such noble metals is

being used to improve performance of electrical connectors, battery electrodes and electronic components.[1]

Metallization has been widely used over the past 40 years to coat a layer of metal on non-conductive materials. Metallization probably started with manufacturing of mirrors by coating a thin layer of silver on glass to obtain a reflective surface. In modern times, besides mirrors, metallization is used to combine the good properties of plastics/polymers (cost, moldability, dielectrics and weight) with those of metals like conductivity, polish and strength.[5] Metallization has found numerous applications in the automotive and aerospace components, toys, furniture, electronic appliances and other hardware items. Manufacturing of printed circuit boards (PCBs) is another success story of the use of metallization on a large scale.[5]

2.1.3 Ion Implantation

An alternate approach to the physical application of paint and metal layers is direct alteration of the materials chemistry and/or composition at the surface to improve desired properties. Ion implantation (II) is one such technique which allows alloying virtually any elemental species into the near-surface region (outermost micron) of any substrate by bombarding it with highly energetic ions.[2] Besides preservation of bulk properties, it does not suffer from adhesion problems since there is no interface, sample dimensions are not changed, and it provides precise control over the implantation area.[3] It is extensively used to implant nitrogen, titanium or carbon into metal surfaces tools, gears, bearings, injection molding nozzles, screws and other industrial components to significantly reduce wear.[2] Similarly, implantation of chromium (Cr), Cr plus phosphorus, or Cr plus molybdenum can virtually

eliminate corrosion of steel components, even those subjected to extreme chemical and temperature environments.[2, 3]

Ion implantation has also been used to improve surface properties of ceramics. For example, aluminum (Al) implantation increases the fracture toughness (up to 50%) and surface hardness (up to 25%) of Yttria-stabilized zirconia, an important electrolyte coating for several solid-state electrochemical devices such as fuel cells and oxygen sensors.[2] Similarly, the surface hardness of aluminum oxide, the natural protective layer on all aluminum components, can be increased by up to 40% by Cr implantation.[2] Implantation of nitrogen ions into silicon carbide (SiC) surfaces helped reduce the friction coefficient from 0.049 to 0.024 resulting in excellent tribological properties in water.[61] Such water-based lubricating technologies are under heavy investigation to bypass the environmental pollution problems posed by oil-based lubrication systems.[61]

Even polymers have benefited from the ion Implanation technique. Implantation of ions, specifically Si ions, has made possible manufacturing of organic thin-film transistors on poly(methyl methacrylate) (PMMA) and other flexible polymer films, now extensively used in liquid crystal displays and radiology capture devices.[62] Wetting property (hydrophilicity) of polymers is important because it can affect their paintability, colorability, anti-electrostatic and anti-fogging properties.[63] Oxygen ion bombardment is being used to convert hydrophobic nature of some bulk polymers to a hydrophilic nature by creating functional groups on the surface.[63, 64]

2.1.4 Metal and Ceramic Films

While ion implantation has found commercial success, sometimes the amount of ions implanted is insufficient to improve the surface properties.[65] In such cases, deposition of

thicker films may solve the problem. At the same time, it is imperative that such deposited films have excellent adhesion with the surface so that it is not dislodged over time. Plasma-assisted deposition (PAD), ion-beam-assisted deposition (IBAD) and their derivatives are commonly used techniques to deposit robust films on a variety of surfaces. PAD is frequently used to deposit yttrium-stabilized zirconium as a heat-protection coating for turbine blades and liners (valves, inner walls) of jet combustion chambers.[66] Similarly, deposition of robust chromium oxide films on steel surfaces using IBAD results in excellent protection from alkali and acid based corrosion.[3] Magnesium fluoride films exhibiting excellent structural integrity and optical properties have been deposited using IBAD.[2] Such optical coatings are used to coat surfaces of glass lens to compensate for focal and chromatic aberrations in a much easier and economical way than improving the glass itself. Additionally, special abrasion resistant hard coatings have been developed that provide protection to the lenses, while anti-reflective (AR) coatings drastically improve image quality. Newly emerging plastic optics are coated worldwide with AR films using plasma-assisted evaporation processes.[4] Optical coatings have also made possible manufacturing of high quality wavelength, intensity and polarization filters at significantly lower costs. These filters have significantly improved the function of consumer products like UV protective glasses and digital cameras, as well as scientific instruments like microscopes, spectrophotometers, ellipsometers and FTIR spectroscopes.

A special mention must be made of diamond-like carbon (DLC) coatings which exhibit excellent chemical inertness, high wear and corrosion resistance, have low friction and can be modified to withstand extreme temperatures.[11, 64, 67] Such coatings can be produced on metal, ceramic and polymer surfaces using modified versions of the PAD or IBAD techniques.[11, 64, 67] DLC coatings, especially the ones modified with fluorine, are being used to make non-

stick cookware and protective optical coatings.[11] DLC-based coatings are also under investigation for preventing paraffin deposition inside oil pipelines[11], reducing calcium scale formation inside heat exchanger coils[11], and producing aluminum components with low friction and high corrosion resistance for the automotive industry.[64]

Chemical vapor deposition (CVD) is another technique used since the last 40-50 years to deposit thin layers of metals on surfaces, conducting or otherwise.[6] In its simplest form, CVD involves passing a precursor gas or mixture of gases to be deposited into a chamber where the object to be coated has been heated. Chemical reactions occur on the surface, leading to deposition of a homogeneous thin metal film. Improvements have taken place in the CVD process over the years that make use of plasma, ions, photons, lasers, hot filaments, etc. to increase deposition rates and/or help bring working conditions to more acceptable temperatures and pressures.[6] The early applications of CVD were mainly for corrosion prevention, but since the above mentioned improvements, it is also used extensively to create surfaces which have specific active functions. CVD is the method of choice to deposit highly purified and ordered layers of semiconductor materials (like doped Si) and conductive microscopic interconnects (like tungsten, gold) in the microelectronics industry for large scale manufacturing of integrated circuits, diodes, light emitting diodes (LEDs), fiber optic cables, and more recently microelectromechanical structures (MEMS).[6] Some other applications of CVD include deposition of DLC coatings discussed above, hard carbonitride coatings and insulating ceramic films.[6]

2.1.5 Polymer Films

Advances in polymerization techniques as well as synthesis and characterization of novel polymeric materials have lead to the development of polymer-based coatings to improve

surface properties of materials. The plethora of polymer types (like PTFE, PU), their structures (like chain length, linear, branched, hyperbranched, crosslinked), functional groups (like -OH, -COOH, $-NH_2$, CH_3) and various deposition techniques (like dip coating, spraying, plasma/ion-assisted deposition, crosslinking, grafting) provide a level of control over surface properties not possible with metal or ceramic films. In fact, polymer-based materials can now match the mechanical properties of metals and ceramics while possessing much better chemical inertness, and frictional and non-fouling (non-stick) properties.

Polymer films can be deposited by techniques similar to the ones used to deposit metal and ceramic films. For example, thermal- and plasma-assisted CVD, also known as chemical vapor polymerization (CVP) is an emerging technique to polymerize coatings directly on the surface. CVP is now being exploited for microelectronics (for dielectric insulating layers), insulation (mini-transformers, motors), optical devices (LEDs), and corrosion resistance and protective coatings (o-rings, hoses, diaphragms).

Additionally, polymers are amenable to deposition by much milder techniques such as dip coating, spraying, crosslinking and advanced surface-initiated polymerization approaches. This is very important for applications where the bulk or coating material cannot be subjected to the extreme pressures, temperatures and radiation involved in the metal and ceramic film deposition techniques. Most commercial paints applied by simple spray-on techniques now contain pre-synthesized acrylic acid, urethane, epoxy or other polymers, which are responsible for the excellent durability, wear resistance and smooth textures. More recently, a polyurethane-based paint containing polytetrafluoroethylene (PTFE) polymer and silicon resin provides resistance against graffiti and adhesive materials.[11] Upon application, the silicon resin and PTFE segregate to the surface, and become interlocked with the polyurethane (PU) to

provide excellent durability and mechanical properties.[11] Temperature and wear resistant PTFE-based coatings ubiquitous on cookware to prevent adhesion, as well as on metal, plastic and laminated paper food storage containers to prevent toxic chemical reactions, are applied by simple spray-on and curing techniques.[9-11] PTFE and other PTFE-like polymers are also under investigation for anti-corrosion applications. Perfluoroalkoxy alkane (PFA) and perfluoroethylenepropylene (FEP) coatings on steel prevented corrosion even when submerged extreme pH solutions.[11]

There is a possibility that the polymer chains deposited by simple spray-on technique will start separating and eroding off after prolonged exposure to extreme environmental conditions. This is overcome by crosslinking the polymer chains, which results in creating a uniform covalently interconnected polymer layer on the surface. Such coatings are typically deposited by reacting a precursor solution on the surface. In a recent study, crosslinked coatings composed of epoxy powder and polyaniline (PANI) applied to steel surfaces exhibited self-healing properties on scratching and prevented rust formation even after prolonged exposure to saline conditions.[68] Addition of PANI increased the crosslinking density that decreased penetration of corrosion causing liquids, and also served as a radical scavenger to prevent corrosion of the underlying metal.[68] Similarly, crosslinked perfluorinated oxazoline-based copolymer films coated on steel panels performed much better than over 100 other commercial anti-biofouling coatings in long-term ocean water immersion tests.[11] There are numerous other crosslinked polymeric materials, mostly containing silicone and/or fluorine groups, under development as anti-biofouling coatings for marine applications.[11] As discussed earlier, they are being developed to overcome the environmental challenges posed by the toxic paints currently used for marine anti-biofouling applications.

Photo-curing is gaining ground to speed up the crosslinking process and allow usage of materials which otherwise do not react with each other (like examples above).[8] This is made possible by introducing acrylate groups that can be crosslinked using extremely fast radical polymerization (curing in seconds to minutes) into monomers and macromers with desirable properties.[8] UV-cured polyurethane-acrylate coatings having excellent wear, scratch, light, water and heat resistance are now very commonly used to protect outdoor materials like fences, boats, water tanks, wood floors and metal sheets.[8] All optical fibers are now coated with special optical-quality photocrosslinked polymer layers to protect the delicate glass core from external forces.[69]

In addition to accelerated cure times, use of UV light allows easy control over the location of polymerization on the surface. Advanced lithography techniques using high resolution photomasks and highly focused light beams have been widely adopted by the electronics industry to fabricate integrated circuits.[7] The circuits are etched out from special highly flat and ordered semiconducting layers deposited using CVD as discussed earlier. The size scale of these integrated circuits keeps shrinking with advancements in both the light source and surface materials from which the components are etched.[7]

Polymer chain grafting is another technique that has received considerable attention during the last two decades for surface modification. Polymer chain grafting typically involves creation of a nanometer-scale brush-like polymer layer on the surface wherein each polymer chain is attached to a single site on the surface. These attachment sites can be created on the surface by various techniques like self-assembled monolayers (SAMs), plasma treatment, ozone exposure and radiation. Grafting does not create tough polymer layers on the surface, and therefore has evolved mainly to change the surface chemistry of the bulk material such as

hydrophilicity, polarity, charge and functional groups, rather than improve mechanical properties. However, it does provide very precise control over the surface chemistry, in many cases on the molecular level.

As an example, microporous membranes are becoming the method of choice for filtration of fluids, especially water, as they do not involve any complex physical or chemical treatments. Most membranes are made from hydrophobic polymers like PTFE, nylon, polysulfone, polyethersulfone, polypropylene, polyethylene, polyvinylidenefluoride (PVDF), etc, due to their good mechanical properties and excellent chemical stability. Unfortunately, these materials are prone to rapid fouling by salts, proteins and/or microorganisms, thus quickly degrading the membranes performance.[70] Controlled grafting of nanometer-scale polymer brushes is becoming the method of choice to improve non-fouling properties of the membranes, without changing their pore size and hence performance. In a recent study, poly(sulfobetaine methacrylate) (pSBMA) chains were grafted on the surface of PVDF membranes using atom transfer radical polymerization (ATRP) by attaching the ATRP initiator molecules to functional groups created on the membrane surface by ozone treatment.[12] This pSBMA grafting improved the surface hydrophilicity and dramatically reduced bovine serum albumin (BSA) and γ-globulin adsorption, even beyond three filtration cycles, which was the normal usable limit of the unmodified PVDF membranes.[12] Such grafting techniques are also being used to prepare stimuli responsive gated membranes which allow control over the filtration rate depending on specific environmental conditions.[71] For example, pH and temperature changes were used to control the filtration rate of polypropylene membranes by grafting poly(acrylic acid) (PAA) and poly(N-isopropyl acrylamide) (pNIPAAM) chains respectively using reversible addition-fragmentation chain transfer (RAFT) polymerization.[71] At pH values below the pKa of the PAA

chains, the chains coiled down to open the pores, while at pH values higher than the pKa, the carboxylic acid groups dissociated, extending the chains and closing the pores.[71] Similarly, at temperature values below the Lower Critical Solution Temperature (LCST) of pNIPAAM, the chains collapsed to open the pores, while at temperature values higher than the LCST, the chains extended resulting in closing of the pores.[71] A more detailed discussion of various polymer grafting techniques can be found later in this chapter.

Many of the materials used for non-biomedical applications discussed above, and numerous others, are used as biomaterials for biomedical applications. Expectedly, they too face problems in achieving the right combination of various mechanical and surface properties. Biomaterials face an additional requirement of biocompatibility, which almost entirely depends on cell behavior at the biomaterial surface. Many of the aforementioned surface modification techniques have been adapted to improve mechanical and surface properties of biomaterials. For example, ion implantation, IBAD and CVD are used to improve mechanical and corrosion resistant properties. Others like plasma treatment, SAMs and various forms of polymer grafting have been suitably adapted to address biocompatibility requirements. The following section discusses such techniques as applicable to improving surface properties of biomaterials.

2.2 Surface Modification Techniques in Biomedical Applications

Development of biomaterials for tissue replacement, augmentation and regeneration has been in the forefront for the past few decades. The main driving force has been the widening gap between the ever growing need for replacement tissues and organs, and the decreasing availability of allogenic replacements. Biomaterials have been able to cover this shortfall to some extent, with complete replacement of heart valves, joints, intro-ocular lenses, pacemakers, etc., and limited regeneration of some tissue types like bones, cartilage and skin.

These successful developments have come with, and still present, considerable challenges to meet the unique requirements of the human body. The primary requirements for any biomaterial to be successful are biocompatibility (minimal toxicity, minimal inflammatory reactions, minimal tissue damage), suitable mechanical properties (strength, elasticity, hardness, toughness, wear resistance, roughness, friction), reasonable cost, and ease of production, handling, sterilization and storage. The bulk properties of a biomaterial can be tuned to a large extent, but obtaining the right combination of modulus, strength, frictional properties, wear resistance, corrosion resistance, and chemical inertness is still a challenge. Meticulous and expensive designing may help meet all the mechanical requirements, but at the cost of biocompatibility. For example, if the bulk material has good biocompatibility, small molecules can leach out, or wear particles can be generated, which can trigger inflammatory responses inside the body. This is especially true for implants involving movement and friction like artificial joints, and needs to be addressed to prevent adverse systemic reactions.

Biocompatibility reflects the interaction of the material surface with the biological environment which includes adsorbed blood proteins, the extra-cellular matrix (ECM), and most importantly cells.[72] As soon as a foreign material comes in contact with body tissue and fluids, proteins start adsorbing on its surface. Any cell response, favorable or otherwise depends on the molecular level interactions between receptors on their membranes and chemical cues present in the environment. In case of biomaterials, chemical cues are provided by the inevitable non-specific protein adsorption on their surfaces. Protein adsorption on surfaces of biomaterials leads to conformational changes in the protein structure that alters their bioactivity.[72] This altered bioactivity is thought to contribute to undesired cell responses like fibrous encapsulation of implants[15], acute or chronic inflammatory response, and/or thrombus formation via

platelet activation[18]. These adverse responses can lead to failure and rejection of the implanted device, requiring complex and painful surgical procedures to remove and replace the implant. Since these interactions originate on the surface where proteins adsorb, early attempts at improving biocompatibility involved rendering the surface bioinert to prevent protein adsorption altogether. Coating surfaces with hydrophilic polymers like poly(ethylene glycol), and (PEG) poly(hydroxyethyl methacrylate) (pHEMA) has been successful in dramatically reducing protein adsorption.[18] However, protein adsorption in the long-term is inevitable leading to expected biocompatibility issues. Therefore, more recent efforts have focused on imparting specific bioactivity to the surface to generate more favorable cellular responses such as bone tissue integration and endothelialization.[18]

As discussed, it can be a very complex and expensive affair to develop entirely new biomaterials with bulk properties which fulfill all these requirements. An advantageous approach is to just modify the surface properties of biomaterials already approved for clinical use, to retain their good bulk properties but significantly improve their performance inside the body. Therefore, surface modification for biomedical applications is usually targeted towards improving the mechanical properties and/or biocompatibility of the biomaterial. Some examples highlighting the need for surface modification of biomaterials are briefly discussed below.

2.2.1 Surface Modification Examples of Metallic Biomaterials

Metals and their alloys have long been used in biomedical applications due to their good mechanical and machining properties.[16] They are commonly used in orthopedic surgery, craniofacial surgery, dental implantology, and plastic and reconstructive surgery for load-bearing, and bone-replacing/contacting applications.[73] Some common examples are, stainless steels used to manufacture fracture plates, screws, hip nails and total-hip replacement (THR)

stems; cobalt-based alloys used in dentistry casting and load-bearing components of total-joint replacements (TJRs); and titanium-based alloys used in THRs and nails.[16] Metals are also used for some non-load-bearing implants like coronary stents and pacemaker casings. Unfortunately, these materials have exhibited tendencies to fail after long-term use due to various reasons such as, high modulus compared to that of bone, low wear and corrosion resistance, fibrous encapsulation, inflammatory responses, and lack of osseointegration.[15]

Mismatch of the modulus between the implant metal and bone, and corrosion were major problems associated with stainless steel and cobalt alloys. Hence, they are being rapidly replaced with titanium-(Ti)-based alloys as their modulus can be tailored to closely match that of native load-bearing tissue.[13] Additionally, Ti alloys provide a high strength-to-weight ratio, good corrosion resistance and good biocompatibility.[14] However, Ti alloys have poor wear and abrasion resistance, which not only reduces the implants' service life, but also produces wear debris that causes a serious inflammatory response in the body.[14] Though much better than other metals, Ti alloys do suffer from corrosion in the long-term which can have toxic effects in the body.[15, 16] Nitrogen ion implantation and plasma nitriding of Ti alloys can produce a significant increase in corrosion and wear resistance.[15, 16] Similarly, oxygen diffusion hardening (ODH) has been shown to drastically improve wear resistance and frictional properties of Ti alloys.[15]

Laser surface treatment is gaining ground for metal implants because of the relatively rapid rate of processing, ease of automation, ability to operate at atmospheric pressure, and the ability to treat selective areas.[16] Furthermore, laser treatment can produce much more homogeneous layers on the surface and up to much greater depths. In most cases it involves annealing the metal surface in the presence of a gas to permit ion implantation to improve

surface properties. For example, wear resistance and hardness of titanium alloys improved after laser surface melting in a nitrogen gas atmosphere which created a hard TiN layer on the surface.[16] Similarly, ceramic coatings such as hydroxyapatite and calcium have also be deposited using a pulse laser deposition technique in order to improve corrosion resistance of titanium surfaces.[16]

Other common techniques like IBAD, CVD, and physical vapor deposition (PVD) have also been used to deposit ceramics (like zirconia), noble metals and TiN films on the surface to improve wear and corrosion resistance.[16] However, these films suffer from delamination in long-term physiological applications, thus limiting use of these techniques for biomedical applications.[16] DLC films discussed previously, have recently started gaining attention as coatings on metallic biomaterials.[14, 15] DLC films have been able to provide excellent corrosion and wear protection and improved frictional properties.[14, 15] More importantly, biocompatibility tests conducted on DLC films have yielded excellent results, with absence of cell cytotoxicity and inflammation.[15] Studies are currently under way to improve the adhesion strength of DLC films to metals as well as long-term hemocompatibility.[14]

2.2.2 Surface Modification Examples of Polymeric Biomaterials

Several polymeric materials have also found widespread use in biomedical devices due to their low production cost, availability in high volume, ease of molding into any shape and size, ease of sterilization and considerable shelf life. Polymers such as poly(methylmethacrylate) (PMMA), Dacron polyester, poly(tetrafluoroethylene) (PTFE), high-density polyethylene (HDPE), polyurethanes (PU), poly(lactic acid) (PLA) and poly(glycolic acid) (PGA). have undergone extensive clinical testing and found use in several biomedical applications including joints, intraocular lenses, contact lenses, large diameter vascular grafts, heart valves, electrodes and

catheters. Designing polymers with specific mechanical properties is not a problem, with various polymer types and their blends possible to meet the requirements. However, selecting polymer(s) with the combination of best mechanical properties and biocompatibility is a very difficult undertaking. For example, initial investigations resulted in manufacturing of artificial joint sockets from ultra-high molecular weight polyethylene (UHMWPE) due to its good mechanical strength, frictional properties and tolerance in the body. Unfortunately, unmodified UHMWPE has poor wear resistance, which leads to the formation and release of micron-sized wear particles, triggering inflammatory reactions around the implantation site, and wherever the particles migrate in the patient's body. Additionally, UHMWPE is also extremely hydrophobic, which leads to fouling by proteins and cells causing biocompatibility issues and degradation of frictional properties. γ-irradiation was used to crosslink the UHMWPE chains, increasing its hardness and hence wear resistance.[17] However, crosslinking also made the bulk material brittle causing fracture and failure of the material under dynamic loading conditions of joints.[17] The solution was to restrict the crosslinking reaction to the surface to obtain wear resistance while preserving the original strength.[17] Recent studies have demonstrated up to three fold increase in wear resistance by bombarding the surface of medical grade UHMWPE with energetic ions (Ar^+ or He^+).[17, 74] Unlike ion implantation in metals, ion bombardment leads to crosslinking of UHMWPE chains on the surface which increases its hardness and wear resistance.[74, 75] This increase in hardness is also attributed to formation of an oxide layer on the UHMWPE surface, which remains stable for years.[17] There is also a possibility that plasma treatment can increase the hydrophilicity of the UHMWPE surface, which can help reduce protein fouling and improve biocompatibility.

2.2.3 Surface Modification Examples to Control Cell Behavior

Some biomedical devices like pacemaker leads, electrodes, biosensors, catheters and ocular lenses suffer from fouling by protein and cells which adversely affects their functionality.[76-78] Similarly, polyurethanes (PUs), which are extensively used in biomedical applications such as heart valves and catheters due to their tunable mechanical properties, often suffer from calcification and thrombogenic biocompatibility issues that lead to long-term failure of the PU device.[79] In such cases, the surface of the biomaterial needs to made 'bioinert' to prevent such non-specific interactions.

In case of some biomedical devices, promoting cell adhesion and controlling their behavior can provide better clinical outcomes than preventing it. Osseointegration of load-bearing metallic implants by promoting tissue ingrowth and matrix deposition is absolutely critical to providing mechanical stability and preventing implant loosening.[15] Most metal implants now have some level of surface porosity to permit osseointegration. However, osteoblasts need to be stimulated to deposit bone matrix by presentation of specific physical as well as chemical cues. Cells adhesion, proliferation and growth has been shown to be partly dependent on the surface morphology. Hence, methods like machining, grinding, polishing, blasting, acid or alkali etching and anodization were used to increase the surface roughness and topography of metal implants.[73] Studies reported increased bone growth activity on such textured metal implant surfaces.[15, 73] In addition to providing physical cues, attempts are being made to impart bioactivity to the implant surfaces to further improve osseointegration. Inorganic calcium phosphate (CaP)-based coatings have been deposited on metal surfaces using dip coating, spin coating, and plasma-assisted techniques due to their similarity to native bone, which may promote bone formation and hence osseointegration.[15, 73] Numerous studies

have demonstrated improved bone formation activity on metal surfaces coated with CaP films.[15, 73] Studies are currently in progress to improve the adhesion strength, thickness and homogeneity of CaP films on metal implant surfaces.[73]

Stainless steel coronary stents have been used since the 1980s to open arteries occluded by plaque formation to restore blood supply to the heart and prevent infarction. Unfortunately, they have long encountered problems with thrombotic vascular occlusion and intimal hyperplasia (IH) leading to failure of the device.[80] Coating the stent material with antiproliferative agents has yielded limited long-term success.[80] The focus has therefore shifted to promote endothelialization as the most promising solution, since the native endothelium actively functions to prevent thrombosis inside healthy blood vessels.[81, 82] Endothelialization however, requires attaching certain signaling molecules to the stent's surface which can recruit neighboring endothelial cells to adhere, proliferate and form a healthy layer over stent's surface that will last the patient's lifespan.[81, 82] For example, a recent study reported enhanced attachment, adhesion and growth of endothelial cells on 316 stainless steel surfaces by grafted with a synthesized mussel adhesive polypeptide via PEG spacer chains compared to unmodified steel surfaces.[81] Another example is the commercial use of expanded polytetrafluoroethylene (ePTFE) and polyethylene terephthalate (Dacron) to make large diameter vascular grafts since they match the mechanical properties of native blood vessels. Unfortunately, their thrombogenic surface shortens their lifespan and prevents their usage as grafts for small diameter (<5mm) blood vessels.[82] Similar to the stent problem discussed above, current studies are investigating the immobilization of signaling molecules on the graft's surface to trigger successful endothelialization after it has been implanted in the body. Some studies have shown increased endothelial cell (EC) adhesion and proliferation when vascular

grafts are coated with peptide sequences like RGD and YIGSR, or whole ECM proteins like laminin.[82]

Before such strategies can yield clinical success, effects of various parameters like which biomolecule, its concentration, and its spatial and temporal distribution on the behavior of target cells need to be thoroughly studied. Axonal guidance for spinal cord regeneration exemplifies this need. A considerable amount of evidence points towards the need to control the spatial distribution of trophic factors presented to stimulate axonal regrowth.[83] This idea stems from the fact that axonal growth cones can be guided by concentration gradients of growth factors.[84, 85] Therefore, it has become imperative to study how gradients of different trophic factors and different concentration profiles will affect axonal guidance and growth. Diffusion gradients have been attempted to stimulate axon growth, both in vitro and in vivo, but they suffer from procedural complexities and potential to cause systemic effects.[86] A number of immobilization approaches have also been tested to create concentration gradients, such as differential evaporation and microfluidics to overcome limitations of the diffusion technique.[85, 87] However, evaporation depends on a myriad of environmental conditions, thus resulting in little control over the gradient profile. Microfluidics does allow very precise control over the gradient profile. However, they are restricted by small dimensions and require at least two proteins to form the gradient. Furthermore, microfluidics can only create linear parallel patterns, so combining gradients with complex spatial patterns is very difficult, if not impossible, to achieve.

2.2.4 Available Surface Modification Techniques to Improve Biocompatibility and Control Cell Behavior

Taking all the aforementioned factors into consideration, a technique is required that,

1. facilitates modification of surface properties to prevent non-specific interactions,
2. facilitates surface modification of polymers, ceramics as well as metals,
3. facilitates covalent attachment of any biomolecule to elicit specific responses,
4. maintains accessibility and bioactivity of the attached biomolecule, and
5. facilitates creation of concentration gradients where required.

A very important point to note is that all cellular behaviors including adhesion, proliferation, differentiation, migration, protein expression, extra-cellular matrix (ECM) production and even apoptosis depend on the interaction of receptors on the cells surface with biochemical cues present in the environment. Since these interactions take place on the molecular level, the surface modification technique should also allow precise control over the concentration of any biomolecule attached on the surface.

2.2.4.1 Changing the Bulk Material Composition

One approach to render a surface bioinert, to prevent protein adsorption, or bioactive, to control cell behavior, is to change the bulk polymer composition. For example, blending PEG-containing copolymer into the polymer bulk can potentially result in highly protein repellant surfaces due to diffusion of PEG chains to the surface.[88] Although this may be an easy method, there is a possibility of the PEG chains leaching out causing serious issues with long-term usability of this material. This can potentially be addressed by covalently linking the PEG chains to the bulk polymer backbone.[89] Similarly, biomolecules can be mixed with the biomaterial during fabrication.[90] Some biomolecules will be present on the scaffold's surface

that the cells will recognize, thus producing desired responses. This strategy has met considerable success with many commercial products currently available, including Xelma skin grafts (ECM proteins in propylene glycol alginate gel) and Extracel bone/cartilage grafts (bovine and porcine gelatin, and porcine heparin in PEG-hyaluronic acid gels).[91] The most important limitation of this technique is that it is largely restricted to polymeric materials, and nearly impossible to achieve with ceramics and metals. Furthermore, blending of bulk synthetic polymers with additive polymers or biomolecules can adversely affect mechanical properties. Additionally, it has the potential to denature or degrade the biomolecule during the fabrication process.[90] Blending is also very specific, so the material to be added, the amount to be added, and the blending technique to be used will change with the targeted bulk material and application.[92-94]

2.2.4.2 Plasma Treatment

These limitations highlight the need for a surface modification technique that is restricted to the surface of the biomaterial. Protein adsorption on surfaces is a very complex phenomenon, which depends on multiple factors including surface hydrophilicity, surface energy, surface charge, protein size, protein charge and protein concentration. In many cases it has been observed that creation of hydrophilic functional groups like hydroxyl, carboxyl, amine, and thiol on a surface can reduce non-specific protein adsorption.[95] Plasma treatment of materials by nitrogen, oxygen, methane and other gases has been investigated as a potential technique to introduce such hydrophilic groups on the surface. Plasma treatment has the added advantage of excellent penetration allowing modification of complex shapes and structures. Treatment of fluorocarbon polymers with plasma of oxygen or nitrogen-containing gases can be used to vary the surface hydrophilicity due to generation of polar groups on the surface, thus

controlling protein adsorption and cell adhesion.[19] Polystyrene (PS) surfaces treated with NH_3 plasma adsorb far less protein than untreated PS surfaces.[20] In some cases, increasing the hydrophilicity of the surface tends to promote cell proliferation, probably because the structure and hence the bioactivity of the adsorbed protein is preserved better on hydrophilic surfaces. Adhesion and proliferation of human endothelial cells is significantly increased on ePTFE vascular grafts due to creation of oxygen-based polar groups on the surface by H_2/H_2O plasma treatment.[20] In another recent study, hydrophobicity of PLA and PLGA scaffolds was significantly reduced by creation of N-containing groups on the surface by plasma treatment.[21] This increased hydrophilicity and positively charged N-containing groups on the surface helped improve infiltration of human skin fibroblast cells into the scaffold for TE applications.[21] Surfaces with extremely low surface energies like perfluoroalkyl groups also seem to prevent protein adsorption, or at least help rapid removal by low-force liquid flow.[20] For example, creation of fluorine groups on cellulose membranes used for hemodialysis by tetrafluoromethane (CF_4) plasma treatment reduced protein adsorption, leukocyte adhesion as well as complement activation.[20] Similarly, protein adsorption and the consequent inflammatory cell adhesion and debris production was significantly reduced on PMMA intra-ocular lenses by CF_4 plasma treatment.[20]

Functional groups created on the surface by plasma treatment can be used to immobilize biomolecules[95], which can then be used to stimulate cells to produce very specific responses. Several studies have reported enhanced adsorption of biomolecules on surfaces with functional groups created by plasma treatment. This is especially true when charged groups like amine ($-NH_2$) and carboxylic acid (–COOH) that can immobilize proteins due to electrostatic interactions. Alves et al. demonstrated increased BSA, Fn and vitronectin (Vn) adsorption and

bioactivity preservation by creating carbon-oxygen-based polar groups on PLA surfaces using oxygen plasma treatment.[96] Primary fetal rat calvarial cells showed increased adhesion on protein adsorbed plasma-treated surfaces compared to untreated non-protein adsorbed PLA surfaces.[96] The authors proposed that such protein treatment can be used to enhance bone matrix deposition in PLA-based bone graft substitutes.[96] In a similar study, hydrophilicity of PMMA surfaces was improved by creation of carbon-oxygen-based polar groups using oxygen plasma treatment.[97] This treatment enhanced adsorption of the antimicrobial peptide histatin 5 resulting in lowering of *C. albicans* bacterial colonization compared to untreated PMMA.[97] Such antimicrobial treatments can find applications in ocular lenses, biosensors and other biomedical implants. However, as with any physical adsorption technique, there is no control over the amount and location of the immobilized biomolecules. Furthermore, lack of covalent binding can lead to loss of biomolecules and hence bioactivity in a physiological environment. As an alternative, special crosslinking chemistries can be used to covalently couple the functional groups on the material's surface with those on biomolecules like proteins, peptides and drugs. In some studies, ammonia-based plasma treatment was used to introduce primary amine ($-NH_2$) groups on surfaces of PTFE and polyethylene substrates.[23, 98] In one study, fibronectin (Fn) was covalently immobilized to the PTFE surface using the crosslinker glutaric anhydride (GA).[23] Covalent coupling of Fn was confirmed by XPS measurements and radiolabeling assay, while bioactivity was confirmed by adhesion and proliferation of bovine aortic endothelial cells (BAECs) and ELISA.[23] Vascular grafts made from ePTFE can benefit from such protein coupling for successful endothelialization. In another study, an anti-horseradish peroxidase antibody was attached to PE surfaces using glutaraldehyde as the crosslinking agent.[98] Though bioactivity tests were not performed, such antibody immobilization on polymer surfaces can find

applications in biosensors and surface-bound assays like ELISA. Similar to $–NH_2$ groups created on the surface, -COOH groups have been used to covalently couple RGD-based peptides, collagen, anticoagulants like thrombomodulin and heparin, while –OH groups have been also been used to covalently attach heparin, glucose isomerase, etc.[99]

2.2.4.3 Monolayers

A step further from using functional groups on the material's surface for anti-fouling or biomolecule immobilization is creation of self-assembled monolayers (SAMs). SAMs can be considered to be the most elementary form of surface-bound organic thin-films. SAMs are composed of numerous short-chain molecules densely packed to homogeneously cover the surface. Each of these molecules consists of three parts: an active head group that binds strongly with the surface, an alkyl chain giving stability to the assembly by van der Waals interactions, and ω-functionality that is exposed to the environment. SAMs have attracted more attention lately because of the observation that they seem to be much better at controlling protein adsorption, even elimination in some cases, compared to functional groups created directly on the surface. This is because the molecules used in SAM formation provide much better surface coverage and can be engineered to fine tune hydrophilicity and surface energy.

Densely packed monolayers of alkanethiol short-chain molecules can be created on gold surfaces due to the high affinity of thiols for gold, a process known as chemisorption. The free terminal group can be any functional group like hydroxyl, carboxyl, amine and methyl, which can control protein adsorption, or can be further used to covalently couple specific biomolecules. Alkanethiol monolayers obviously require a thin layer of gold to be deposited on the bulk material. Gold is not really used as a biomaterial to be implanted inside the human body[37], but alkanethiol monolayers on gold films deposited on silicon, quartz, glass or metal surfaces are

extensively used to study the interaction of proteins with surface functional groups.[100] The flat and defect-free nature of gold films and the resulting SAMs permit the use of highly-sensitive surface characterization technique like contact angle, ellipsometry, surface plasmon resonance (SPR) spectroscopy and circular dichroism to study protein-surface interactions.[100] The ability to control and characterize the surface chemistry is particularly important from the biocompatibility point of view, since as discussed earlier, the cellular response depends on how proteins adsorb on the biomaterial's surface. Results from these studies are being used to engineer the type, concentration and structure of functional groups on the biomaterial's surface for better biocompatibility.[100] For example, it has been observed that SAMs prepared from alkanethiols terminated in short oligomers of the ethylene glycol group ($HS(CH_2)_{11}(OCH_2CH_2)_nOH$: $n = 2 – 7$) resist the adsorption of several model proteins, as measured by both ellipsometry and SPR spectroscopy.[95] Even SAMs that contain as much as 50% methyl-terminated alkanethiols mixed with oligo(ethylene glycol)-terminated alkanethiols, resist the adsorption of protein.[95] Elaborate screening studies have shed light on the type of functional groups that are best to resist protein adsorption[101], their characteristics being:

1. they contain hydrogen bond acceptor groups but not hydrogen bond donor groups,
2. their overall charge is neutral, and
3. they are polar.

However, investigations by Mrksich have led to the discovery that mannitol-terminated SAMs resist protein adsorption and can block cell adhesion even longer than ethylene glycol-based SAMs.[101, 102] Since mannitol has already been approved and used as a drug in humans, developing protein resistant surfaces using mannitol can speedup regulatory clearance. A recent study by McClary et al. extended the formation of alkanethiol SAMs on gold coated

poly(ethylene terephthalate) (PET) discs.[103] The SAMs presented either methyl or carboxylic groups on the surface and were tested for their interaction with Fn. It was observed that protein bioactivity was better preserved on hydrophilic carboxylic surfaces compared to the hydrophobic methyl surfaces, as confirmed by enhanced cell attachment and spreading along with increased formation of focal adhesion points and stress fibers.[103] Besides studying protein-surface interactions, alkanethiol SAMs can also provide an excellent platform to control the bioactivity of surfaces and use it to understand cell behavior. Roberts et al.. synthesized novel short-chain alkanethiol molecules that contained the RGD cell adhesion peptide sequence.[104] Attachment of bovine capillary endothelial cells was tested on mixed RGD and -OH presenting SAMs, and fibronectin and RGD adsorbed positive controls. It was discovered that cell adhesion strength, proliferation and matrix deposit on RGD SAMs was significantly different in magnitude and time scale from that on fibronectin or RGD adsorbed surfaces.[104] More recently, alkanethiol SAMs are being used to develop drug eluting 316L stainless steel (SS) surfaces, the main material used to manufacture coronary stents.[105] Hydroxyl-terminated SAMs were formed by covalent coupling of the thiol group with hydroxyl groups created on the SS surface by oxygen plasma treatment. The hydroxyl groups on the SAM were then used to covalently attach the drug ibuprofen via an esterification reaction under mild conditions.[105] Short-term controlled release of ibuprofen (21 days) was obtained via hydrolytic cleavage of the ester bond between the drug molecule and the SAM.[105] Beyond 21 days, the thiol groups start desorbing from the surface resulting in a reduction in the drug release rate.[105]

The alkane-thiol SAMs on gold discussed above are based on affinity and not covalent coupling. Therefore, while alkane-thiol SAMs are very useful to study protein-surface and protein-cell interactions, and possibly short-term drug release, their long-term use as

biosensors, or on implant materials is limited due to eventual detachment and loss of surface activity. Unlike chemisorption of thiols to gold or hydroxyl groups, silane end-groups on alkoxysilane molecules can react with hydroxyl groups to form a stable silicon oxide bond. This chemistry is also used to form SAMs on any surface which can present hydroxyl groups on the surface. Silane-based SAMs have a better potential for use on implanted biomaterials since most materials, including metals, ceramics and polymers can be modified to directly exhibit hydroxyl groups on the surface without deposition of a metal layer. The already discussed plasma treatment is universally applicable to all material types to create hydroxyl groups on the surface, but chemical treatments like acid washes can also produce similar results. A comprehensive study by Faucheux et al. created methyl (CH_3), hydroxyl (-OH), carboxyl (-COOH) and amine (-NH_2) terminated alkoxysilane SAMs on glass surfaces.[22] Hydroxyl groups for the silane reaction were created on the glass surface by treatment with a strong oxidizing piranha solution (3:1 sulfuric acid:hydrogen peroxide). As expected, –OH terminated SAMs were the most effective in resisting protein adsorption, as indicated by SDS-PAGE analysis.[22] Primary human fibroblasts culture followed the protein adsorption results wherein, cell adhesion, spreading and matrix formation was enhanced on CH_3, -COOH and –NH_2 SAMs compared to weak results on –OH SAMs.[22] Besides controlling protein adsorption, alkoxysilane SAMs have also been used to directly control cell behavior, with or without further immobilization of biomolecules. As an example of using unmodified SAMs, Bain and Hoffman demonstrated that adhesion, glucose consumption, lactate production and subsequent insulin secretion by insulinoma cell line βG I/17 can be tuned by controlling the ratio of diamine to trifluoropropyl endgroups of alkoxysilane SAMs deposited on glass surfaces.[106] A surprising discovery was made that SAMs with higher F3 surface concentration were most suitable for growth of cells and insulin

production.[106] This study has opened up the possibility of creating cell support scaffolds for artificial pancreas to be implanted in diabetic patients. Alternatively, alkoxysilane molecules were covalently pre-coupled with Hyaluronan (Hyal) to create Hyal monolayer on glass surfaces.[24] Hyal was selected as it is one of the most studied polysaccharides and has the ability to bind to cell membranes to potentially control their behavior. This can be especially useful since some polysaccharide coatings have been shown to have non-fouling characteristics.[24] It was observed that this Hyal-SAM was very smooth and hydrophilic, and was very effective In preventing human fibroblast cell adhesion.[24] In a similar but more practical example, Hyal or RGD peptide-derivatized Hyal was covalently immobilized onto epoxy-terminated silane SAMs deposited on stainless steel surfaces. The Hyal-coated surfaces were able to prevent human plasma platelet adhesion, indicating improvement in biocompatibility.[107] On the other hand, Hyal+RGD-coated surfaces did promote platelet adhesion, a result which points towards controlling adhesion of other cell types.[107] These results indicate that SAMs can be used to tune the bioactivity of metal surfaces to control cell behavior, something that can be very beneficial for cell contacting metallic implants like on vascular stents and orthopedic implants.[107]

SAMs have also received attention for development of highly sensitive biosensors since minute quantities of both the reacting enzyme on the substrate, as well as the biomolecule to be detected are sufficient for successful detection.[108] Additionally, SAMs can be easily constructed on metals used in the electrode, which in turn facilitates direct contact with the underlying electrochemical transduction mechanism for quantitative measurements.[108] Both of these factors allow considerable miniaturization of the biosensors, an ideal feature for diagnostic applications in clinics and laboratories. A wide variety of biosensors have been

successfully constructed by coupling functional end-groups of alkanethiol SAMs with enzymes such as horseradish peroxidases to detect hydrogen peroxide in ELISA, glucose oxidase to detect glucose, urease to detect urea, and acetylecholinesterase to detect acetylcholine. [108] Use of alkoxysilane SAMs for biosensor construction has been rather limited, probably because they cannot be used on gold, platinum and silver, the most common electrode metals. However, investigations into other electrode materials like indium tin oxide (ITO) and other metals, has made it a possibility. Surface hydroxyl groups necessary for silane SAM formation can be create as discussed above by plasma or chemical treatment. A recent study by Moore et al.. demonstrated the use of alkoxysilane SAMs to covalently attach complimentary DNA molecules to ITO films.[109] Oxygen plasma treatment was used to create –OH groups on the ITO film surface. These immobilized complimentary DNA molecules were able to hybridize with the target DNA molecule to produce fluorescence on the surface.[109] The transparent nature of ITO will allow spotting of the target DNA on one side, and imaging through the other side.[109] Furthermore, since ITO is conductive, both optical and electrochemical measurements can be performed for simultaneous qualitative and quantitative analysis. A novel impedimetric antibody sensor was prepared by depositing a 3-aminopropyl-triethoxysilane on silicon nitride surfaces, a new material under investigation for biosensors.[110] The anti-rabbit IgG antibody was covalently immobilized to the SAM's amine end-groups using glutaraldehyde as the crosslinker.[110] The binding between antibody and antigen (Rabbit IgG) was monitored by measuring the impedance variation of the SAM, and the sensor could detect antigen concentrations as low as 50 ng/ml.[110]

2.2.4.4 Surface Patterning

Some very simple derivatives of direct surface coupling, SAMs and physical adsorption have been developed to restrict deposition of anti-fouling molecules/polymers or bioactive molecules to certain areas on surfaces. This type of surface patterning is particularly useful to study the interactions of anchorage-dependent cells with their environment, and eventually utilize engineered patterns to control cell behaviors like adhesion, spreading and migration. For example, it can be used to create cell arrays for high-throughput monitoring of the effects of toxins and drugs on cell behavior.[111] Cell patterning is also observed in vivo, especially during fetal development to control cell growth, migration and differentiation.[112] Lately, spatial control of cell behavior has been found to be important in wound healing where a cascade of signals involving chemotactic gradients, electric field gradients, and cell adhesion receptors is tightly controlled in time and space.[112] The need for patterns and gradients of growth factors to guide neurons for spinal cord regeneration as discussed earlier is one such example.

Microcontact printing (μCP), a soft lithography technique, is one of the most widely used methods to deposit patterns on surfaces. It involved synthesis of an elastomeric stamp which is formed by casting a liquid pre-polymer solution (typically poly(dimethylsiloxane) over a microstructured master (usually silicon photoresist).[111] After curing and hardening, the elastomeric stamp's surface will have the negative image of the master's surface topography. Since the master is made by exposing silicon photoresists to UV light, extremely high resolution patterns down to a few micrometers can be created. Next, the stamp is "inked" by dipping in a solution of alkanethiols, alkoxysilanes, a polymer or the biomolecule itself. The "ink" is then transferred to the surface only where the stamp's topographical projections make contact with the surface. Typically, the non-inked areas of the surface are backfilled with a second molecule,

using solution of another alkanethiol, alkoxysilane, a polymer or a biomolecule. As an example, μCP was used to stamp square and circular island patterns of hydrophobic methyl-terminated SAMs onto gold surfaces.[113] The non-stamped regions were then backfilled with a oligo(ethylene glycol) (OEG)-terminated alkanethiol SAM.[113] After immersion in a solution of a ECM protein, the protein adsorbed only to the hydrophobic methyl-terminated regions, but not on the OEG terminated regions.[113] As expected, bovine and human endothelial cell attachment and spreading was restricted to the square islands where protein adsorption occurred, but was absent on OEG regions for periods of several days even when cultured in the presence of serum.[113] But for cells to be restricted to these islands, they need to be separated by at least 20-40μm depending on the cell type. Another very interesting observation made was that progressively restricting endothelial cell spreading by culturing them on smaller and smaller micropatterned adhesive islands transformed their behavior from growth to apoptosis. This result confirmed the significant role of cell shape on its function.[113]

For a more controlled and permanent presentation of bioactive molecules on the surface, the biomolecule can be pre-coupled to the SAM forming molecules used for stamping or backfilling. Zhang et al.. first created patterns of OEG-terminated alkanethiol SAMs on gold-coated glass coverslips.[114] Next, alkanethiol molecules containing the cell adhesion peptide sequence RADS were used to backfill the non-stamped regions.[114] These patterned surfaces produced very well-defined alignment of human epidermoid carcinoma cells, NIH3T3 mouse fibroblasts as well as transformed primary human embryonic kidney 293 cells, thus allowing creation of specific cell arrays and patterns.[114] Use of μCP to create patterns of alkylsilane SAMs to control protein adsorption for biomedical applications has been very limited. However

some studies have been conducted to spatially control protein adsorption and cell adhesion on glass and metal surfaces.[25]

Direct deposition of biomolecules using μCP is also possible by replacing the SAM molecules in the ink with the biomolecule. In this case, the biomolecules can be stamped on a homogeneous SAM or directly on the surface by eliminating the SAM layer. For example, endothelial and other cell types have been patterned on surfaces by using fibronectin as the ink.[111] Similarly, neuronal networks have been created on surfaces by directly adsorbing patterns of laminin or any of the neuron-binding peptide sequences of laminin.[111] Klein et al.. demonstrated creation of hippocampal neural networks which remained functional for over a week by printing patterns of laminin or the IKVAV-containing peptide sequence PA-22-2.[115] The neurons remained restricted to lines as narrow as 3μm. These patterns were also able to trigger differentiation of human neuroblastoma cells SH-SY5Y as well as PCC7-Mz1 stem cells into a neuronal phenotype.[115] Instead of adsorption, covalent coupling of biomolecules directly stamped on the surface can be obtained by linking them to either functional groups on the surface, or on the pre-deposited SAMs. In a study by Scholl et al.., first an aminosilane SAM was deposited on glass surfaces.[26] The heterobifunctional crosslinker N-g-Maleimidobutyryloxy]sulfosuccinimide ester (sulfo-GMBS) was then coupled to the amine groups of the SAM via its sulfohydroxysuccinimide functionality.[26] Finally, line and grid patterns (3μm to 15μm wide, with 15μm or 500μm spacing) of the peptide PA-22-2 were stamped on the surface, resulting in a covalent linkage of the peptide's thiol group to the maleimide group on the sulfo-GMBS.[26] Presence and bioactivity of PA-22-2 was confirmed by labeling with a fluorescent antibody.[26] The PA-22-2 patterns resulted in formation of hippocampal neuron patterns within 3 hours of cell seeding, and within 1 day were able to elicit

action potentials.[26] Both the above examples demonstrate a simple technique that can be used to unravel the mechanisms driving neuron growth, guidance and synapse formation for regenerative applications, and to develop novel neural biosensors.

Another method to create patterns of bioactive molecules on the surface is photochemical coupling. In this case, special bioconjugate molecules need to be synthesized which have the desired biomolecule attached to one end, and a photosensitive group at the other end. On exposure to light, the photoactive group will react with specific functional groups on the surface thus covalently attaching the biomolecule to the surface. Again, functional groups can be present directly on the surface, or on pre-deposited SAMs. The advantage of this technique over μCP is that the entire stamp synthesis process is eliminated. Since light is used for covalent coupling, custom-designed photomasks can be used to create spatial patterns, including immobilized concentration gradients. Hypolite et al.. synthesized a novel photoactive heterobifunctional crosslinker which had an N-hydroxysuccinimide group for biomolecule coupling and a photoreactive benzophenone (BP) group for selective coupling to the surface.[116] For proof of principle, the crosslinker was first conjugated to a fluorescent protein R-phycoerythrin, followed by immobilization of the crosslinker-protein conjugate to polystyrene surfaces by laser irradiation.[116] It was observed that the amount of protein immobilized on the surface can be controlled by changing the laser irradiation time. This principle was used to create concentration gradients of R-phycoerythrin on the surface.[116] The same research group also demonstrated coupling of a photoactive bioconjugate containing the RGD peptide sequence to oligo(ethylene glycol)-terminated alkanethiol SAMs on gold surfaces using laser or UV lamp irradiation.[27] It was advantageous to have a SAM as the base layer as it prevented non-specific adsorption. Fibroblast morphology (round or elongated) was controlled by seeding

them on RGD dot patterns or RGD line patterns respectively.[27] Similar to previous observations, the concentration of RGD immobilized on the surface was controlled by varying the irradiation time. Correspondingly, the number of fibroblasts adhering gradually increased from the lower end to the higher end of the RGD gradient on the surface.[27]

As discussed earlier, the focus is now shifting more and more towards controlling cell responses, and in fact using them to improve integration and/or functioning of the implanted device. Load-bearing orthopedic implants, coronary stents and vascular grafts are just few examples of devices requiring control over specific cell responses. Therefore, the need for surface modification techniques that offer ways to control biomolecule immobilization on the surface has reached a critical stage. Techniques like microfluidics, plasma treatment, monolayer formation, μCP, and photochemical coupling discussed above can potentially achieve this, and have no doubt found numerous applications where they can help obtain the desired results. Nevertheless, these techniques as a whole and individually have highlighted some very important limitations that need to be addressed.

First, they all create only a monolayer of functional groups and/or biomolecules on the surface. A monolayer of non-fouling functional groups created on the surface can be easily altered due to partial or complete detachment, or unexpected chemical reactions, leading of change of surface chemistry and loss of anti-fouling properties.[28] In the case of a monolayer of immobilized biomolecules, few molecules may get detached from the surface leading to loss of bioactivity in that area.[28] In both these cases, there are no redundant functional groups or biomolecules present on the surface to compensate for the loss.

Second, small surface defects frequently occur, especially in case of SAMs, which can either expose the bulk materials surface, or change the surface chemistry in a particular

area.[28] This can significantly alter the interaction of proteins and/or cells with the surface affecting the experimental outcome. Such defects can cause even bigger biocompatibility problems on the surface of any medical device that is implanted inside a patient's body.

Third, in all these techniques since very short or no spacer chains are used to immobilize any biomolecule, movement and/or rotation of the biomolecules will be restricted, limiting proper access by cell receptors. This restricted movement can also prevent formation of focal adhesion clusters, which are very important for controlling cell adhesion and other responses.

Fourth, techniques like microfluidics and μCP involve too many procedural complexities, and are not very amenable for non-flat contoured surfaces. SAMs by themselves cannot create patterns or gradients, requiring incorporation of other procedures. μCP can create complex 2 dimensional spatial patterns directly on surfaces or on SAMs, but it cannot create gradients. On the other hand, microfluidics can create gradients, but only in a linear and parallel fashion. Photochemical coupling of biomolecules is very quick, can be automated, can be modified easily for 3D applications, forms covalent linkages, and can create complex patterns and gradients on the surface. However, it still depends on functional groups on the materials surface or SAMs to immobilize the biomolecules, limitations of which are already highlighted above.

Finally, gradients created by any of these techniques will have its upper concentration value limited to the saturated monolayer value, thus restricting the range of slopes possible.

2.2.4.5 Physical Adsorption on Surfaces

A simple approach to overcome the above limitations is to physically adsorb polymer chains to the bulk material surface, which can be universally applied to all material types. Functional groups on this polymer layer can in turn be used to attach biomolecules to impart specific bioactivity to the surface. Simple physical coating of PEG on PU, polysulfone, PMMA and

polylactide surfaces has been shown to be very effective in reducing non-specific protein adsorption.[76, 94, 117] In a similar manner, bioactive molecules can be adsorbed on the bulk material's surface to impart bioactivity. However, long term stability is questionable as the physically coated polymer layer can be easily dislodged and lost permanently. A solution to this problem is to permanently attach the polymer chains to the surface. This has led to development and use of various polymer "grafting" techniques.

2.3 Techniques and Applications of Surface Graft Polymerization for Biomedical Applications

Polymer grafting which involves creating a brush-like layer of polymer chains on the materials surface seems to be the most promising technique, which can overcome most, if not all, limitations discussed above. First, the flexibility of long polymer chains attached to the surface will allow them to coil and collapse resulting in much higher surface area coverage per chain. This means that even if minor defect sites are present on the surface, the neighboring polymer chains can compensate by coiling and covering up the defect sites. This will prevent exposure of the bulk material surface to proteins and cells. Second, the surface density of functional groups will be significantly higher due to use of polymers with specific sidegroups. As a result, the concentration of immobilized biomolecule on the surface can be much higher. This will also considerably increase the upper concentration limit of gradients well beyond monolayer concentrations, thus significantly expanding the range of gradient slopes possible. Third, the wide variety of polymer types, chain lengths (molecular weight), chain structure (linear, branched, hyperbranched), chain densities (surface packing), and sidegroups will allow precise tuning of the surface chemistry and bioactivity. As discussed earlier, this level on control is very important because all protein and cell interactions take place on the molecular level. Besides their inherent genetic predisposition, cell behaviors like adhesion, growth, proliferation,

migration, differentiation, matrix production, protein/antigen/antibody expression and apoptosis entirely depend on the signals their receptors receive from the environment.

Polymer brushes can be created on a surface by either the “grafting to” or the “grafting from” approach. In either case, it involves two steps, surface activation followed by polymer chain grafting. Since chemically reactive functional groups are typically absent on many biomaterial surfaces, surface activation is needed to create such groups on the surface to continue the grafting process. Such reactive groups can be generated on the surface by chemical reactions (acid, alkali, etc), plasma treatment, ozone treatment, ion or election bombardment, γ-irradiation and SAM formation. In a “grafting to” approach, pre-formed end-functionalized polymer molecules react with reactive groups on the surface to form polymer brushes. On the other hand, the “grafting from” approach utilizes reactive species on the material surfaces to initiate the polymerization of monomers from the surface outwards. The bond formed between surface and polymer chain makes the polymer brushes resistant to common chemical and environmental conditions. In the next section, some important polymer grafting techniques and their use for surface modification in biomedical applications are discussed.

2.3.1 Surface Modification Using The “Grafting to” Approach

The main advantage of the “grafting to” technique is that the required preformed polymers can be synthesized with a narrow molecular weight distribution using living anionic, cationic, radical, group transfer and ring opening metathesis polymerizations. Surface modification via the “grafting to” approach has found some applications in the biomedical field. Surprisingly, studies using the “grafting to” technique for surface modification predominantly use PEG chains for grafting, which will be evident from the examples described below. There are two main reasons for this occurrence:

1. Numerous studies have demonstrated the excellent protein- and cell-resistant properties of PEG.
2. PEG chains of different molecular weights (MW) in unmodified form and with reactive functional end-groups are commercially available, thus eliminating the need to synthesize polymers for grafting.

The most commonly used "grafting to" techniques along with their biomedical applications are briefly discussed below.

2.3.1.1 Self-Assembled Monolayers

The technique to form polymer SAM is exactly as described earlier, the only difference being that the short-chain alkylthiol and alkoxysilane molecules are replaced by much larger polymer chains having the thiol or silane end-groups for attachment to the surface. The advantage is that the limitations associated with SAMs (like detachment, defects) described earlier can be easily compensated by neighboring polymer chains on the surface.[28] Just like short-chain SAMs, polymer-based SAMs can be used to not only prevent non-specific protein adsorption, but also to impart bioactivity to the surface by coupling specific biomolecules.

Xia et al. synthesized a novel copolymer containing methoxy-terminated PEG chains grafted onto a polysiloxane backbone.[29] This copolymer possessed dialkyl disulfide sidechains which allowed it to form a SAM on gold surfaces and was able to resist protein adsorption.[29] However, when the PEG methoxy groups were replaced with NHS groups, the copolymer was actually able to covalently bind significant amounts of protein.[29] Such protein-resistant and protein-binding PEG SAMs have potential applications in biosensor construction. In a similar study by Bearinger et al.. synthesized a special triblock copolymer PEG_{17}-b-PPS_{25}-b-PEG_9.[118] The disulfide groups in the poly(propylene sulphide) (PPS) block chemisorbed to gold surfaces to

form a SAM of the copolymer.[118] This copolymer layer reduced adsorption of serum proteins by as much as 95%, and resisted cell adhesion by >97%.[118] Emmenegger et al.. took a slightly different approach, wherein a –COOH terminated SAM was first deposited on gold surfaces.[119] These –COOH groups were then used to couple the $–NH_2$ groups on the PEG chain ends using a NHS-based crosslinker.[119] This PEG grafting to the SAMs was able to significantly reduce adsorption of plasma proteins.[119] However, an interesting observation was made that if the plasma solution contained a protein with MW greater than 350,000 Da, it itself adsorbed on the PEG surface or initiated deposition of other plasma proteins.[119]

The silane-based SAM formation route has been used to attach polymer chains to surfaces presenting –OH groups. Guo et al.. derivatized PEG chains of different molecular weights with alkoxysilane groups by reaction with 3-isocyanatopropyltriethoxysilane.[30] SAMs of these PEG-silane chains were then deposited on silicon and glass surfaces. These PEG-silane SAMs were very stable, and did not detach or show any change in surface contact angle for up to 4 weeks. They were able to significantly prolong the activated partial thromboplastin time (APTT), prothrombin time (PT), and thrombin time (TT), all of which are important measures of the blood coagulation pathway. Similarly, platelet adhesion was also significantly reduced for up to 3 hours, the time duration in this study.

In addition, some alternatives to PEG have been reported. For example, Wyszogrodzka and Haag created SAMs of polyglycerol dendrons on gold surfaces, with the understanding that a branched architecture will provide much better resistance to protein adsorption.[120] It was observed that dendrons with lesser branch generations (hence lower MWs), were best at resisting protein adsorption.[120] In fact, SAMs made from 426 g/mol MW dendrons were able to resist protein adsorption for 24 hours, the duration of this study.[120] Lower MW dendrons

with lesser generations formed better and more defined SAMs, while inconsistent coverage by higher generation dendrons allowed smaller proteins to penetrate and reach the gold surface.[120] These polyglycerol dendrons can be an excellent alternative to PEGylation of surfaces to prevent protein adsorption. Furthermore, each polyglycerol dendron provides multiple –OH groups for coupling of biomolecules to impart bioactivity to the surface.

2.3.1.2 Chemical Grafting

Typically in chemical grafting, a highly unstable reactive group is introduced either on the surface or on the polymer chains, which reacts with another stable functional group to form covalent linkages. For example, Archambault et al.. converted the hydrophobic nature of PU-urea (PUU) surfaces by covalently attaching PEG chains (550, 2000 and 5000MW) using a two-step coupling process.[31] A highly reactive crosslinker 4,4'-methylenebis(phenylisocyanate) (MDI) was used, due to the high reactivity of its isocyanate groups with primary and secondary amines. Accordingly, MDI was first covalent attached to free -N-H groups present on the PUU surfaces. This was followed by a reaction between amine groups on the PEG chains to the free isocyanate groups of MDI to form an extremely stable urethane bond. It was observed that adsorption of myoglobin, concanavalin A, albumin, fibrinogen and ferritin from single protein solutions was significantly reduced compared to unmodified PUU surfaces, with a maximum reduction of 90% seen with the PEG2000.[31] Similar results were obtained for fibrinogen adsorption from blood plasma, which is more significant because fibrinogen is one of the most important factors responsible for coagulation and thrombus formation on biomaterial surfaces. However, even with the PEG2000, adsorption of plasma proteins was not completely eliminated.[31] In fact, the concentration of all proteins was well above few ng/cm^2, which is the detection limit of most detection techniques like SPR.[28] This study clearly highlights the

limitations of the “grafting to” approach in creating sufficiently high surface densities of polymer chains to eliminate protein adsorption. In a similar chemical grafting procedure for an immediate clinical application, diisocyanate crosslinkers were reacted with –OH groups on the surface of commercially available poly(2-hydroxyethyl methacrylate-co-methyl methacrylate) (pHEMA-MMA) intraocular lenses.[32] The surface bound isocyanate groups were then used to covalently link PEG chains via their –OH end-groups to form stable urethane bonds. PEG grafting resulted in a decrease of the surface water contact angle from 66° for an unmodified lens to 47°, 44° and 40° for 1100, 2000 and 5000 MW PEG chains respectively. The transparence as well as refractive power of the lenses remained unchanged after PEG grafting. Non-specific adsorption of green fluorescent protein decreased with PEG MW, and was undetectable on lenses grafted with PEG 5000.[32] Culture of lens epithelial cells, which are the main cells involved in cataract formation, showed decreasing adhesion on the lenses with increasing PEG MW, and were completely absent on PEG 2000 and 5000.[32] While these results are indeed very promising, long-term tests need to be conducted because IOLs remain implanted in the patient’s eyes for years to decades. In another study by Harris et al., poly(acrylonitrile-co-vinyl chloride) (PAN/PVC) ultrafiltration membranes were derivatized with PEG by chemical grafting.[33] PAN/VC membranes are important because they are used for encapsulation of living cells which release bioactive products to treat serious diseases and/or disabilities like type 1 diabetes, Parkinson’s diseases and chronic pain.[33] First, the nitrile groups on the PAN/VC fibers were converted to -COOH by treatment with concentrated acid.[33] Finally PEG-NH_2 chains were covalently linked to the –COOH groups using the crosslinker N-3-dimethylaminopropyl carbodiimide to form stable amide bonds. In vitro tests showed that PEG grafting did not alter the permeability of the membrane, but did reduce non-specific BSA adsorption by up to

70%.[33] PEG grafting also lead to improvement of in vivo biocompatibility on implantation in rat brains for 4 weeks.[33]

Metallic biomaterials do not normally present functional groups on the surface, and need to be generated on the surface before chemical grafting. One way to achieve this is to first coat the metal surface with another polymer with functional side-groups, as was done by Caro et al.. to chemically grafted PEG chains on SS surfaces to prevent protein adsorption and bacterial biofilm formation.[121] The SS surfaces were first coated with a physically adsorbed layer of poly(ethyleneimine) which provided $–NH_2$ groups on the surface. PEG chains were then covalently coupled to these $–NH_2$ groups via reductive amination with reactive aldehyde groups present at the end of the PEG chains. This PEG grafting reduced BSA adsorption by 97%, while bacterial adhesion was reduced by 96% compared to bare SS.[121]

2.3.1.3 Plasma/Glow Discharge-Assisted Grafting

Physically coating the surface with another polymer that provides functional groups has long-term performance issues as the polymer can delaminate leading to loss of any surface modification that was carried out. As discussed earlier, plasma treatment can also be used to deposit polymer films on metal surfaces. These films tend to be much more robust because of possible covalent linkages created between the metal surface and the polymer film created the plasma treatment. For example, in a study by Gombotz et al.. amine groups were created on poly(ethylene terephthalate) (PET) films by depositing films of polyallylamine by exposing them to plasma glow discharge.[122] The amine groups were then activated with cyanuric chloride, followed by covalent conjugation of NH_2-PEG-NH_2. Even though gravimetric analysis indicated that the films grafted with the low-molecular weight PEG contained many more PEG molecules, the high-molecular weight PEG surfaces exhibited greater wettability (lower water contact

angles) and hence less protein adsorption than the low-molecular weight PEG surfaces.[122] In fact, adsorption of albumin and fibrinogen to the PEG surfaces decreased with increasing PEG molecular weight up to 3500.[122] These results shed light on how the interaction of water with the larger PEG molecules creates an excluded volume of the hydrated polymer coils, which may be an important factor in reducing protein adsorption.[122] A similar technique was used to graft PEGylated hyaluronan (PEG-HA) chains to Nitinol (NiTi) alloy surfaces.[123] Nitinol is a shape-memory alloy, which is under intense investigation for development of next generation of vascular stents. However, like any other stent material, it needs improvement in bio- and hemo-compatibility to prevent thrombus formation and intimal hyperplasia. Amine groups were introduced on the NiTi surface by depositing films of polyallylamine by exposing them to plasma glow discharge.[123] Finally, the carboxylic acid groups on the PEG-HA chains ends were covalently coupled to the surface primary amine groups using a solution of 1-ethyl-3-(3-dimethylaminopropyl) carbodiimide (EDC) and N-hydroxysuccinimide (NHS) to form stable amide bonds.[123] The advantage of this method is that using a PEG spacer improved HA surface binding and created smooth and highly hydrated surfaces. As a result, these surface reduced human blood platelet adhesion by as much as 62% compared to bare metal.[123] However, long-term studies are warranted for successful application on clinically relevant Nitinol stents.

Plasma treatment can also be used to create functional groups directly on the metal surface. In a study by Alcantar et al.., the concentration of hydroxyl (silanol) groups on the surface of silica was increased by water plasma treatment.[34] These silanol groups were reacted with hydroxyl groups on PEG chains to graft the PEG chains on the surface via stable Si-O-C linkages.[34] Water plasma treatment combined with PEG grafting improved the surface

wettability (lower water contact angle values) and decreased the surface roughness by 88%, compared to untreated silica.[34] This resulted in a significant reduction in BSA adsorption on the surface, as observed by negligible fluorescence on the PEG grafted surface.[34]

2.3.1.4 Radiation-Assisted Grafting

Instead of creating functional groups on the surface using plasma to tether polymer chains, electromagnetic radiation, like γ-rays and light, is typically used to directly trigger bond formation between polymer chains and the surface. For example, Kidane et al. covalently attached chains of the Pluronic PEG-poly(propylene oxide)-PEG (PEG-PPO-PEG) triblock copolymer to glass and Nitinol surfaces using γ-irradiation.[35] First, a SAM of vinylsilane was deposited on the glass and Nitinol surface to present acrylate groups on the surface. Next, PEG-PPO-PEG readily adsorbed on the surface due to the hydrophobic interactions between the vinylsilane and the PPO cbock of the copolymer. Upon γ-irradiation, the double bond converted to radicals and reacted with each other to covalently bond the copolymer to the glass and Nitinol surface.[35] In vitro studies revealed that copolymer grafting reduced fibrinogen adsorption by over 95% on glass surfaces and by 88% on Nitinol surface, compared to unmodified controls.[35] Similarly, platelet adhesion on glass and Nitinol surfaces was significantly reduced by copolymer grafting.[35]

Photochemical bonding, discussed earlier can be used to directly coupling a molecule to the surface via a photoactive group. This strategy has also been adapted to couple whole polymer chains to the surface by incorporating photoactive groups either in the polymer chains or on the surface. One important point to note here is that these polymers were attached to surfaces as flat films, and not brushes. However, since examples of brush formation via photochemical coupling could not be found, this discussion has been included to highlight the

possibility. It is very much possible to create brushes via photochemical coupling simply by having the photoactive group only at the polymer chain end, rather than throughout the polymer chain as was the case with the aforementioned examples. As an example of introducing photoactive groups on the surface, Adden et al. first deposited a SAM of the photoactive molecule 4-3'-chlorodimethylsilyl)propyloxybenzophenone on glass or silicon surfaces.[124] These surfaces were then spin coated with one of 22 different polymers, like pHEMA, PEG, pMAA, to name a few. Upon UV exposure, a biradical is created at the benzophenone moiety on the SAM, which reacts with any C–H group and binds polymers covalently to the surface.[124] The idea was to find the polymers which are most suitable for adhesion and differentiation of mesenchymal progenitor stem cells (MPSCs) to improve osseointegration of titanium-based orthopedic implants. Three polymers pMAA, poly(diethyl(p-vinylbenzyl) phosphonate) and poly(4-acetoxystyrene) were found to be as good as tissue culture polystyrene in promoting MPSCs adhesion and proliferation.[124] As the alternate approach, To et al. synthesized a novel PEG-based polymer with photoactive 4-azidobenzene side-groups.[125] This study also demonstrated the patterning advantage provided by using light to initiate reactions/polymerizations. Polyester, glass and titanium surfaces coated with the PEG-based photoreactive polymer were exposed to UV light with or without a patterned photomask.[125] Formation of patterns was confirmed by AFM scans, which indicated that the PEG layer was several hundred nanometers thick. Though the exact bond formation between the photoactivated azidobenzene groups and the surface was not elucidated, the authors proposed that the photolyzed aryl azide intermediates underwent ring expansion to create nucleophile-reactive dehydroazepines that reacted with functional groups on the surface to form covalent bonds.[125] Protein adsorption on PEG-grafted regions was significantly reduced down to

almost undetectable level.[125] This resulted in absence of any cell adhesion in the PEG-grafted regions, confining the cells only to the PEG-free regions of the grafted pattern.[125] Such a grafting technique can be potentially used to coat specific regions of polymeric and metallic implants to control cell adhesion and behavior.

In spite of the studies and applications of the "grafting to" approach discussed above, the "grafting to" approach does have its limitations. This approach is largely limited to the small number commercially available pre-synthesized polymers. If some specialized polymer is not available, an extra step of custom-synthesis is added before actual grafting to the surface. Furthermore, it has been experimentally proven that the "grafting to" approach allows only a small amount of polymer to be immobilized onto the surface.[28, 36] This is because the macromolecular chains must diffuse through the existing polymer chains to reach the reactive sites on the surface.[28, 36, 37] This barrier becomes more pronounced as the density of tethered polymer chains increases on the surface.[28, 36, 37] Thus, the polymer brush obtained has a low grafted-chain density and low thickness.[28, 36, 37]

2.3.2 Surface Modification Using The "Grafting from" Approach

The limitations faced by the "grafting to" approach do not exist in the "grafting from" approach, as the small monomer molecules are not as prone to diffusion barriers as the larger preformed polymer chains.[37] "Grafting from" results in polymer brushes with a much higher chain density and thickness.[37] Since the polymer chains are actually synthesized from the surface using monomers, there is no dependence on commercially available polymers and opportunities exist for using essentially any molecule that can be polymerized. Furthermore, the need to pre-synthesize them before grafting is completely eliminated as the polymer chains form directly on the surface to be modified. Expectedly, the biomedical applications of the

"grafting from" approach keep increasing at a phenomenal pace, with new polymers and new initiation techniques being rapidly developed. "Grafting from" requires the introduction of specific reactive groups called "initiators" on the surface which can initiate the polymerization of monomers from the surface. These techniques usually make use of cationic, anionic, ring-opening or radical initiators.[37] The most versatile and convenient method is radical initiated polymerization because it can be used to polymerize any of the thousands of available vinyl monomers. Complex procedures requiring matching of special initiators and monomers are not required. Additionally, grafting of copolymers is as easy as mixing two or more vinyl monomers together during the grafting process. For better organization and simplicity, the discussion about radical polymerization has been divided into two groups. In the first group, free radicals are generated on the surface to initiate "uncontrolled" polymerization of monomer on the surface. In this case, the polymerization continues until the monomer is consumed or removed, or the radicals are terminated by external means. The second group is where the radicals undergo repetitive and reversible initiation-termination so that polymerization progresses in a very "controlled" manner. In this case, polymerization can be terminated by simply removing the energy, like light, heat or chemical that triggers initiation.

2.3.2.1 Polymer Grafting From Surfaces via Uncontrolled Radical Polymerization

Surface-initiated uncontrolled radical polymerization (SIURP) depends on creation of free radicals on the surface to initiate the uncontrolled polymerization of monomers present near the surface. Such free radicals can be generated directly on the materials surface by methods like plasma treatment, ozone treatment, γ-irradiation and UV irradiation. In indirect methods, special "initiator" molecules are first attached to the surface followed by exposure to plasma, some form of radiation or heat. This triggers radical production by the initiator

molecules, which then initiates polymerization from the surface. A few examples highlighting the use of SIURP for polymer grafting from biomaterials are discussed below.

2.3.2.1.1 Plasma/Glow Discharge-Induced Uncontrolled Grafting From Surfaces

Since plasma contains highly energetic species like ions and radicals, it can transfer these radicals to pendent carbon, hydrogen, oxygen and other such atoms in the polymer chain. Plasma bombardment also leads to polymer chain scission, which also can create radicals on the surface. If such plasma treatment is done in the presence of oxygen, peroxide radicals can be created on the surface. As discussed earlier, plasma treatment is pervasive, so it can be used to treat samples with complex structures and porosity. For example, exposing medical grade silicone rubber to argon plasma followed by introduction of oxygen gas led to creation of peroxide radicals on the surface.[38] When this activated rubber was immersed in a solution of acrylic acid, polyacrylic (pAA) chains were grafted from the surface. The amount of pAA grafted on the surface was varied by changing the polymerization time. Surface wettability increased significantly as demonstrated by decrease in water contact angle from about 105° to about 45°. This increased wettability should have reduced protein adsorption and hence cell adhesion. Unfortunately, corneal epithelial cell adhesion was observed indicating significant protein adsorption. Collagen was also covalently linked to the –COOH groups on the pAA chains using the carbodiimide chemistry. Cell adhesion was obviously observed on the collagen conjugated surfaces, but it cannot be attributed only to conjugated collagen due to possible adsorption. Interestingly, the amount of collagen on the surface did increase with increase in amount of grafted pAA. However, this may have also resulted from increased protein adsorption. The authors did not include controls that were washed to remove such adsorbed protein, in which case cell growth would be only due to conjugated collagen. In a study closer to a potential

clinical application, ePTFE microporous membranes, often used as vascular grafts, were treated with hydrogen plasma to produce free radicals on the surface.[42] These radicals were used to graft PEG methacrylate (PEGMA) brushes from the surface, as a means to improve hemocompatibility. The amount of PEGMA grafted on the surface was controlled by changing the plasma intensity or treatment time, which was attributed to higher grafting densities on the surface.[42] Correspondingly, the surface wettability (measured by water contact angle) decreased with increasing amount of PEGMA on the surface. This increased wettability resulted in a decrease in non-specific protein adsorption from single production solutions of γ-globulin, human fibrinogen, and human albumin, with the amount of adsorbed fibrinogen and albumin going well below 10% of control membranes.[42] Protein adsorption from whole human plasma also decreased to 40% of controls.[42] All ePTFE membranes grafted with different amounts of PEGMA were able to completely resist platelet adhesion, which is an excellent result for reduced thrombogenicity.[42]

Similar to ePTFE, plasma/glow discharge induced grafting is very frequently used to modify the surface properties of PET, a polymer extensively used in various biomedical applications like sutures and vascular grafts due to its suitable mechanical properties. Surface modification is required as PET has poor hemocompatibility preventing endothelialization which leads to thrombus formation. In one study, pAA was grafted from PET surfaces via radicals created by argon plasma treatment. Next PEG-NH_2 chains were covalently attached to the -COOH groups on the pAA chains using the carbodiimide chemistry.[126] This was probably done as the pAA chains would provide far more sites for PEG chain attachment than directly grafting PEG chains from the surface. This would not only improve surface coverage, but also provide higher number of sites for conjugation of biomolecules compared to directly grafted

PEG. The PEG grafting led to a significant reduction in thrombus formation compared to unmodified PET films and pAA grafted PET films, which was attributed to the observed reduction in albumin and fibrinogen adsorption on PEG-grafted surfaces.[126] This protein adsorption was further reduced by covalently coupling heparin to the PEG chains.[126] Jingrun et al. went a step further and attempted to improve endothelialization of PET surfaces.[39] pAA was again grafted from PET films using plasma treatment, but in this case it was assisted with UV radiation to speed up the grafting process.[39] Finally, gelatin (Gel) was covalently conjugated to the –COOH groups on the pAA chains using the EDC-NHS chemistry.[39] It was observed that the PET-Gel surfaces promoted human umbilical vein endothelial cell (HUVEC) adhesion and proliferation, compared to unmodified PET.[39] HUVECs had in fact completely covered the Gel surface and had completely spread on the surface with cytoplasmic extensions.[39]

2.3.2.1.2 Ozone-Induced Uncontrolled Grafting From Surfaces

Besides creating radicals on the surface, plasma bombardment also results in unwanted etching and erosion of the surface. This changes the surface topography and/or increases the roughness in an uncontrolled manner, which can have undesired effects on both protein adsorption as well as cell adhesion. Ozone treatment is a very good alternative that is equally pervasive as plasma. Ozone, due to its inherent instability and extremely strong oxidizing ability, readily reacts with pendent hydrogen atoms on polymer chains to generate peroxide radicals. These radicals can be immediately used to initiate polymerization from any polymer surface. Ozone treatment does not alter the surface topography in any way and is emerging as a quick and simple procedure to modify polymer surfaces. The Sicong Lin group has conducted numerous studies using this technique to improve biocompatibility of various polymer types. It was shown that depending on the polymer that is subjected to ozone treatment, the peroxide

radical concentration reaches a plateau after exposure to ozone for a certain amount of time. For example, silicone and poly(ether urethane) reached a plateau after 30 minutes[45, 46], while light density polyethylene (LDPE) reached a plateau after 90 minutes. Silicone surfaces were grafted with two different polymers, a 2-methacryloyloxyethyl phosphorylcholine (MPC)-based polymer [44] and a N,N-dimethyl-N-methacryloyloxyethyl-N-(3-sulfopropyl) ammonium (DMMSA)-based polymer[45]. Grafting of these polymers on silicone surfaces reduced blood platelet adhesion and aggregation to extremely low levels even after immersion in platelet rich plasma (PRP) for 180 minutes.[44, 45] DMMSA is a zwitterionic polymer, which was also successfully grafted on PU and poly(ether urethane) (PEU) surfaces using ozone-induced polymerization.[46, 47] Yet again, platelet adhesion and aggregation was extremely low on zwitterionic polymer grafted PU and PEU surfaces. A similar zwitterionic polymer based on N,N-dimethyl(methacryloylethyl)ammonium propane sulfonate (DMAPS) was grafted on LDPE films to again obtain excellent platelet resistant surfaces.[49]

Moving away from zwitterionic polymers, Ko et al. grafted PEG monomethacrylate (PEGMA) and sulfonated PEG monomethacrylate (SO_3-PEGMA) from ozone activated PU, PMMA and PE surfaces, all of which are important biomaterials.[43] As with the previous studies, the concentration of peroxide groups on the surface increased with increasing ozonation. Blood platelet adhesion tests revealed that platelet adhesion decreased with increasing ozonation time, pointing towards increasing amount of PEG on the surface.[43] Specifically, sulfated PEG exhibited the lowest platelet adhesion, possibly due to its negative charge.[43]

2.3.2.1.3 Radiation-Induced Uncontrolled Grafting From Surfaces

UV and higher energy gamma (γ) radiation can also generate radicals on polymer surfaces to initiate grafting. Noh et al. described a novel though elaborate UV-induced polymer

grafting technique to improve the wettability of PTFE surfaces. On exposure to UV light, benzophenone (BP) and sodium hydride (NaH) produced reducing agents like diphenyl ketyl radical anions and benzhydrol anions, which rapidly reduced carbon-carbon bonds in the PTFE chains to produce unsaturated groups on the surface.[127] On re-exposure to UV radiation in the presence of the photoinitiator benzil dimethyl ketal (BDMK), the BDMK molecules converted to free radicals, which were transferred to the unsaturated bonds on the PTFE surface.[40, 127] These surface-bound radicals in turn caused grafting of pAA, poly(acrylamide) and PEG brushes from the PTFE surfaces.[40] Contact angle measurements reveals a significant improvement in hydrophilicity of the PTFE surfaces, with PEG grafting reducing the contact angle from 120° of unmodified PTFE to 11°.[40] Protein adsorption and cell adhesion tests are warranted to check if this increase in hydrophilicity can indeed improve biocompatibility of PTFE used in medical implants. Additionally, the functional groups provided by pAA, pHEMA and PEG grafting can be used to covalently conjugate specific biomolecules from the surface to control cell behavior. For example, endothelialization of ePTFE vascular grafts can be enhanced.

UV-induced grafting requires addition of a reducing agent and/or initiator to produce radicals on the surface, and these added chemicals can have toxic effects once the polymer is inside the body. γ-irradiation on the other hand, can produce radicals on the surface without addition of reactive chemicals, due to their highly energetic interactions with polymer bonds. In a recent study, pAA was grafted onto surfaces of biodegradable poly(L-lactide-co-ε-caprolactone) (PLCL) films as a means to later immobilize gelatin on PLCL surfaces.[41] PLCL-based materials are often used as scaffolds to repair bone defects by stimulating osteogenic activity, but the process usually takes months to years and is even slower in older patients. Attempts are being made to increase bone formation in and around such scaffolds. In one study,

PLCL films were immersed in AA monomer solution followed by γ-irradiation using a cobalt 60 (^{60}Co) source for 1-3 hours to graft pAA chains from the PLCL surface. The amount of pAA increased with increase in exposure time, which was confirmed by peak shifts in ATR-FTIR scans and increases in the amount of electrostatically attached toluidine blue. Gelatin (Gel) was then covalently attached to the pAA chains using EDC-NHS chemistry. Proliferation, spreading and cytoskeletal structure of human mesenchymal stem cells (HMSCs) was significantly better on PLCL-pAA-Gel films compared to unmodified PLCL and PLCL-pAA films, and approached that on tissue culture polystyrene.[41] Alkaline phosphatase activity, an indicator of osteogenic differentiation, of HMSC on PLCL-pAA-Gel films was more than twice that on PLCL-pAA films, and more than 7 times on unmodified PLCL films.[41] Such gelatin immobilized PLCL can help improve outcomes of PLCL-based bone grafts.[41]

One common side-effect of γ-irradiation is polymer chain scission on the surface and deeper layers which can significantly degrade mechanical properties of the scaffold. On the other hand, grafting via γ-irradiation is much slower requiring hours if not days, unlike UV which takes minutes. Therefore, depending on the specific biomaterial and application, either UV-induced grafting with added chemicals or γ-irradiation-induced grafting with potential change in mechanical properties will have to be selected for best physiological outcomes.

2.3.2.1.4 Chemical/Heat-Induced Uncontrolled Grafting From Surfaces

No published records of using plasma, ozone or radiation treatment for grafting polymer brushes from metal surfaces could be found. This is probably because neither can produce the required radicals on metal surfaces to initiate polymerization. A chemical treatment-based method has been recent described by Hélary et al. to graft poly(sodium styrene sulfonate) (pNaSS) from titanium surfaces.[50] The authors indicated that the charged nature of pNaSS can

improve osseointegration of titanium-based orthopedic implants by enhancing osteoblast activity. Titanium surfaces were first immersed in sulfuric acid followed by hydrogen peroxide to produce a thin film of titanium hydroxide and titanium peroxide on the surface. On heating, these groups produced peroxide radicals on the surface, which were used to initiate polymerization of NaSS monomer from the surface. The amount of polymer on the surface, measured by toluidine blue attachment, was found to be directly dependent on the temperature, polymerization time and monomer concentration. Adhesion strength and spreading of MG63 osteoblast-like cells was significantly better on Ti-pNaSS surfaces, compared to unmodified Ti.[50] ALP activity of cells on Ti-pNaSS was 19% higher compared to unmodified Ti.[50] Calcium deposition by osteoblasts, an important requirement of bone matrix formation, was also enhanced on Ti-pNaSS surfaces, compared to unmodified Ti.[50]

Chemical/Heat-induced grafting from polymer surfaces usually involves using heat to convert initiator molecules into free radicals, which in turn react with pendent atoms or unsaturated groups on the polymer surface to produce surface tethered macroradicals. For example, Jiang et al. first introduced acrylate groups on surface of PU films by covalently coupling unpolymerized AA or HEMA molecules using hexamethylene diisocyanate (HDI) as the crosslinker.[48] These films were then heated to 60°C in a solution of 2,2'-azobisisobutyronotrile (AIBN) and N,N'-dimethyl (methacryloylethyl) ammonium propanesulfonate (DMAPS) monomer.[48] On heating, AIBN molecules converted to free radicals, which were transferred to the acrylate groups of AA and HEMA on the surface. These surface tethered radical then initiated grafting of DMAPS from the PU surface.[48] Similar to DMAPS grafting using ozone discussed earlier, DMAPS grafting using heat reduced platelet adhesion and aggregation to extremely low levels compared to unmodified PU.[48]

There are two major limitations associated with the aforementioned SIURP techniques for biomedical applications:

1. The uncontrolled nature of radical generation, initiation, propagation and termination leads to large variations in the MW of the polymer chains grafted on the same surface. This may not be a major problem if simple coating of the surface is sufficient to prevent undesired cell responses by prevent protein adsorption and denaturation on the surface. However, as discussed earlier, better biocompatibility, integration and functioning of the implanted device can be achieved by eliciting specific responses from cells surrounding the implant. A high polydispersity (PD) on the surface will cause an uncontrolled variation in concentration of the biomolecule on the surface, which will cause uncontrolled variation in cell response on the same surface.

2. Most of the aforementioned techniques have been restricted to polymer surfaces, while many biomaterials fall into the metal and ceramic categories. With the exception of the acid treatment to generate peroxide on metals discussed above, there are no reports of easily modifying metals and ceramics for SIURP.

2.3.2.2 Polymer Grafting From Surfaces via Controlled Radical Polymerization

Surface-initiated controlled radical polymerization (SICRP) techniques have generated immense interest in the biomedical field. SICRP usually results in grafted-polymer chains with very low polydispersity ($M_w/M_n<1.3$)[128], which provides excellent control over the concentration of functional groups on the surface. Several SICRP techniques such as atom transfer radical polymerization (ATRP)[51, 52], nitroxide-mediated polymerization (NMP)[53, 54], reversible addition-fragmentation chain transfer polymerization (RAFT), and photoiniferter-mediated polymerization (PMP)[55-57] provide excellent control over the MW of the grafted

polymer chains using various polymerization parameters. Additionally, initiators used for these techniques are easily modified to contain reactive groups (like alkoxysilane, acid bromides and acid chlorides) that can covalently couple to functional groups on the surface. Fortunately, biomaterials either already have functional groups on the surface (like polymers), or can be easily modified (metals, ceramics and polymers) by various techniques (like plasma, ion, ozone, acid and alkali) to create functional groups on the surface. Of these SICRP techniques, ATRP and PMP are the predominant ones used to modify surfaces of biomaterials and therefore are the focus of the following discussion.

2.3.2.2.1 Polymer Grafting From Surfaces via Atom Transfer Radical Polymerization

An ATRP system consists of an organic alkylhalide initiator (R-X), a catalyst (L-M-X) made of a transition metal (M) halide (X) complexed with some organic ligand (L), and vinyl monomer (P).[129, 130] Figure 2.1 depicts the typical polymerization mechanism. Briefly, first the catalyst L-M-X abstracts the halogen atom X from the organic halide R-X, to form the oxidized species L-M-X_2, and the carbon radical R' (' = radical). This radical R' initiates polymerization by reacting with vinyl monomer P, with the formation of the intermediate radical species, R-P'. The reaction between L-M-X_2 and R-P reversibly terminates R-P' to form R-P-X, and regenerates the catalyst L-M-X. The catalyst L-M-X can again abstract the halogen X from R-P-X to form the propagation species R-P' which can react with another vinyl monomer P to extend the chain R-P-P'. This

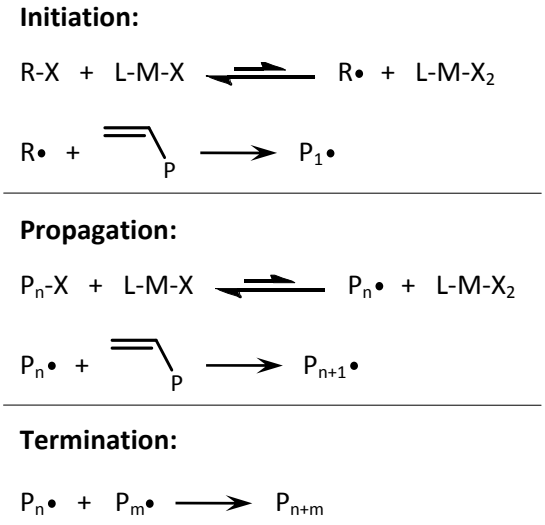

Figure 2.1 The ATRP mechanism.

reversible transfer of the halogen atom X between the catalyst and polymer chain continues till the monomer is consumed/removed or the radicals are artificially terminated. Copper-based halides (Cl or Br) are most commonly used as catalysts, but Ni, Pd, Ru, Fe and other transition metal halides have also been used.[129, 130] Ligands are mostly organic bases and derivates of 2,2'-bipyridine and 2-iminopyridine.[129] To graft polymer brushes from surface, the initiator needs to be covalently linked to functional groups on the surface. From the biomedical perspective, ATRP carries the following advantages in addition to its ability to graft polymer chains with low PD values.

1. ATRP initiators with different reactive groups can be synthesized to facilitate attachment to any biomaterial surface.
2. The length of the polymer chains (degree of polymerization or number of repeat units) grafted from the surface can be easily controlled by adding a sacrificial initiator into the monomer solution along with the catalyst and ligand. Depending on the concentration of the sacrificial initiator, it consumes part of the catalyst and ligand molecules available to propagate the chains in solution. As a result, higher the concentration of sacrificial initiator in the solution, slower will be the propagation on the surface, resulting in lower chain lengths.
3. Since ATRP does not depend on an external energy source like light, but uses chemical interactions in solution to initiate and propagate polymerization, ATRP can potentially graft polymer wherever the solution can reach. This can be very useful to modify surfaces of scaffolds with complex 3D structures and porosity.

ATRP has been used to modify surfaces of a wide variety of biomaterials, to graft protein-resistant polymers like PEG and pHEMA to prevent cell adhesion, as well as for covalent

conjugation of biomolecules via the grafted polymer chains to control cell behavior. Jin et al. subjected PU surfaces to oxygen plasma to generate peroxide and hyperoxide groups on the surface.[51] The ATRP initiator 2-bromoisobutyryl bromide (BIBB) was then covalent reacted with these species via its acid bromide group. The initiator-immobilized PU surfaces were immersed in a solution of copper bromide (CuBr, catalyst), 2,2'-bipyridyl (bpy, ligand) and PEGMA (MW 300, 475 or 1000) to initiate grafting of PEG from the surface by ATRP.[51] The length of grafted PEG chains on the surface was varied by changing the sacrificial initiator concentration. The water contact angle values reduced from about 85° to about 60°-30° depending on the PEG chain length. Fibrinogen and lysozyme adsorption on PEG-grated surfaces reduced by 84-98% and 67-91% respectively, compared to the unmodified PU surface.[51] An interesting observation was made that lysozyme adsorption increased as the MW of the PEG monomer used increased.[51] This was possibly due to decreasing graft density as monomer size and footprint on the surface increase.[51] Hoshi et al. covalently conjugated the same ATRP initiator BIBB to -OH groups on the surface of a polyethylene-poly(vinyl alcohol) (PE/PVA) composite plates.[131] The plates were then immersed in a solution of methacryloyloxyethyl phosphorylcholine (MPC) in the presence of CuBr and bpy for 24 hours to graft polyMPC brushes from the PE/PVA surface. The surface hydrophilicity (measured by contact angle) increased with increase in the grafted pMPC chain length.[131] It was argued that the shorter poly(MPC)-grafted chains did not cover the hydrophobic domains, while the longer grafted chains did. As a proof of principle study, non-specific adsorption of BSA was tested. pMPC grafted surfaces reduced protein adsorption by over 80% compared to unmodified PE/PVA surfaces.[131]

ATRP has also been used to graft polymer chains from metal surfaces. This has been very useful for titanium surfaces since Ti-based implants, though widely used, suffer from poor

osseointegration and implant-associated infections. Polymer brushes have been grafted from titanium surfaces using ATRP followed by biomolecule conjugation to prevent bacterial infections as well as promote osteoblast adhesion and bioactivity. To achieve this, a SAM of a specially synthesized ATRP initiator is deposited on the surface. For example, Zhang et al. converted the titanium oxide groups present on titanium films to hydroxyl groups by heating at 120°C overnight.[132] These hydroxyl groups were then used to deposit a covalently attached SAM of the ATRP initiator trichloro(4-(chloromethyl)phenyl)silane on the surface. This was followed by grafting of pHEMA chains from the surface in the presence of ligand and copper-based catalyst. The hydroxyl groups on these pHEMA chains were converted into carboxyl or amine groups to allow the coupling of gentamicin, penicillin, or collagen via carbodiimide chemistry. The covalently immobilized antibiotics almost completely inhibited growth of the bacteria *Staphylococcus aureus*. On the other hand, collagen immobilization significantly enhanced osteoblast adhesion. Centrifugation of unmodified TI surfaces covered will a monolayer of osteoblasts resulted in detachment of most cells. However, no cell detachment was observed from collagen conjugated Ti surfaces.[132] In another such study by Raynor et al., a SAM of α-bromo ester terminated dimethylchlorosilane was deposited on titanium films via surface –OH groups.[37] This ATRP initiator was used to graft PEGMA chains form the surface. These PEGMA grafted Ti surfaces resisted MC3T3-E1 osteoblast-like cell adhesion for up to 56 days.[37] However, when a polypeptide containing the collagen sequence GFOGER was covalently coupled to the terminal –OH groups on PEG, cell were now able to adhere, spread and proliferate on the surface. Similar results were obtained when a RGD containing peptide sequence or a recombinant fragment of fibronectin $FNIII_{7-10}$ was covalently coupled to the PEG chains.[37] The authors also tested for levels of focal adhesion kinase (FAK) Y397 and Y567

phosphorylation, which are indicators of osteoblast differentiation. Increased level of phosphorylated FAKs were observed on cells growing on $FNIII_{7-10}$ conjugated surfaces indicating increased osteoblast differentiation.[37] These excellent in vitro results were then translated to in vivo studies by the same group. Instead of films, ATRP grafting of PEGMA was conducted on clinical grade Ti cylinders.[37] These PEGMA grafted cylinders, with and without covalent conjugation of $FNIII_{7-10}$, were implanted into the proximal tibial metaphyses of mature Sprague-Dawley rats. Ti cylinders with $FNIII_{7-10}$ had 70% more bone tissue around their surface compared to unmodified Ti, the current clinical standard orthopedic implant material.[37] Improved osseointegration was further confirmed by the significantly higher force required to pull out $FNIII_{7-10}$ conjugated cylinders, compared to unmodified Ti or PEGMA-grafted Ti without $FNIII_{7-10}$.[37]

Studies have shown that pHEMA does not promote cell adhesion due to its highly protein resistant nature. Due to its excellent biocompatibility, it is being used to fabricate tissue engineering scaffolds to support tissue regeneration. However, due to its bioinert nature, it is unable to elicit any response from desired cells. In a very interesting study by Zainuddin et al., ATRP was used to graft polymer chains from surface or pHEMA hydrogels to improve their cell adhesion properties.[133] In the study, the ATRP initiator BIBB was covalently coupled to the –OH groups on the pHEMA hydrogel surface. Next, poly(mono(2-methacryloyloxyethyl) phosphate) (pMMEP) chains were grafted from the surface using the standard ATRP procedure. It was observed that the charged phosphate groups of pMMEP promoted attachment, spreading and growth of human corneal limbal epithelial cells, to a level comparable to tissue culture polystyrene.[133] However, it should be noted that this is uncontrolled growth of cells, and

most tissue engineering applications will require specific control over cell behavior. This is where controlling the presentation of specific biomolecules becomes significant.

The solution dependent nature of ATRP does have the advantage of being able to graft on surfaces with complex 3D structures and porosity. At the same time, the only way to control the thickness of polymer chains grafted by ATRP is by varying the temperature, solution composition and polymerization time. Thus, its use in creating surfaces with complex spatial distributions such as gradients, thickness patterns with different levels of minima and maxima, and even simple striped patterns is limited. Simple linear gradients may be achieved by slowly increasing the immersion level of the surface into the ATRP solution. Li et al. were able to graft thickness gradients of the thermoresponsive polymer poly(N-isopropylacrylamide) using an elaborate experimental set up involving fluid pumps.[59] Creation of patterns requires even more complex methods to be devised, like prior patterning of the initiator via μCP, photolithography, or restricted polymerization using microfluidics. As an example of procedural complexity, Chen et al. first deposited a SAM of hexamethyldisilazane (HMDS) on silicon wafers.[58] Next a layer of photoresist was spin coated on the HMDS SAM. Then UV lithography involving photomask was used to remove the photoresist in specific spatial patterns exposing parts of the HMDS layer. The sample was then subjected to oxygen plasma treatment to convert the methyl groups of exposed HDMS to hydroxyl groups. These –OH groups were then used to immobilize the ATRP initiator (4-chloromethyl)phenyltrichlorosilane, which assembled selectively onto the exposed regions of the silicon wafer. This elaborate procedure resulted in a surface patterned with regions of initiator ATRP and regions of photoresist.[58] Finally, PMMA brushes were grafted from the surface using a standard ATRP procedure, followed by removal of the leftover photoresist from the surface.[58] A microfluidics-based patterning procedure, as

developed by Sun et al., is equally complex.[134] Furthermore, as with any microfluidic device, only certain patterns are possible and the dimensions have to be very small, usually microns to millimeters. ATRP also suffers from extremely slow polymerization kinetics, thus requiring hours to days to obtain polymer layer thickness of a few hundred nanometers. ATRP procedures have to be performed in a solvent system, and require the catalyst/ligand, which in most cases is organic in nature. This can be very detrimental for biomaterials, especially polymer substrates, as these chemicals can leach out and produce toxic and/or inflammatory reactions in the body.

2.3.2.2.2 Polymer Grafting From Surfaces via Photoiniferter-Mediated Polymerization

Photoinifeter-mediated polymerization (PMP) to graft polymer chains from the surface offers a number of advantages, especially for biomedical applications. Spatial patterns can be easily achieved by simply controlling the location of light exposure across the surface. In fact, PMP allows grafting with the same spatial micropatterning resolution as achievable with traditional photolithographic techniques. It also allows creation of gradients with nanometer scale resolution in polymer layer thickness, simply by varying the light intensity or exposure time across the surface. Grafting via PMP is much faster, usually providing thicknesses of hundreds of nanometers in few minutes. Additionally, PMP can be performed at room temperature with or without solvent (pure monomer), requires no catalyst/ligand system, and is compatible with a wide range of vinyl monomers.

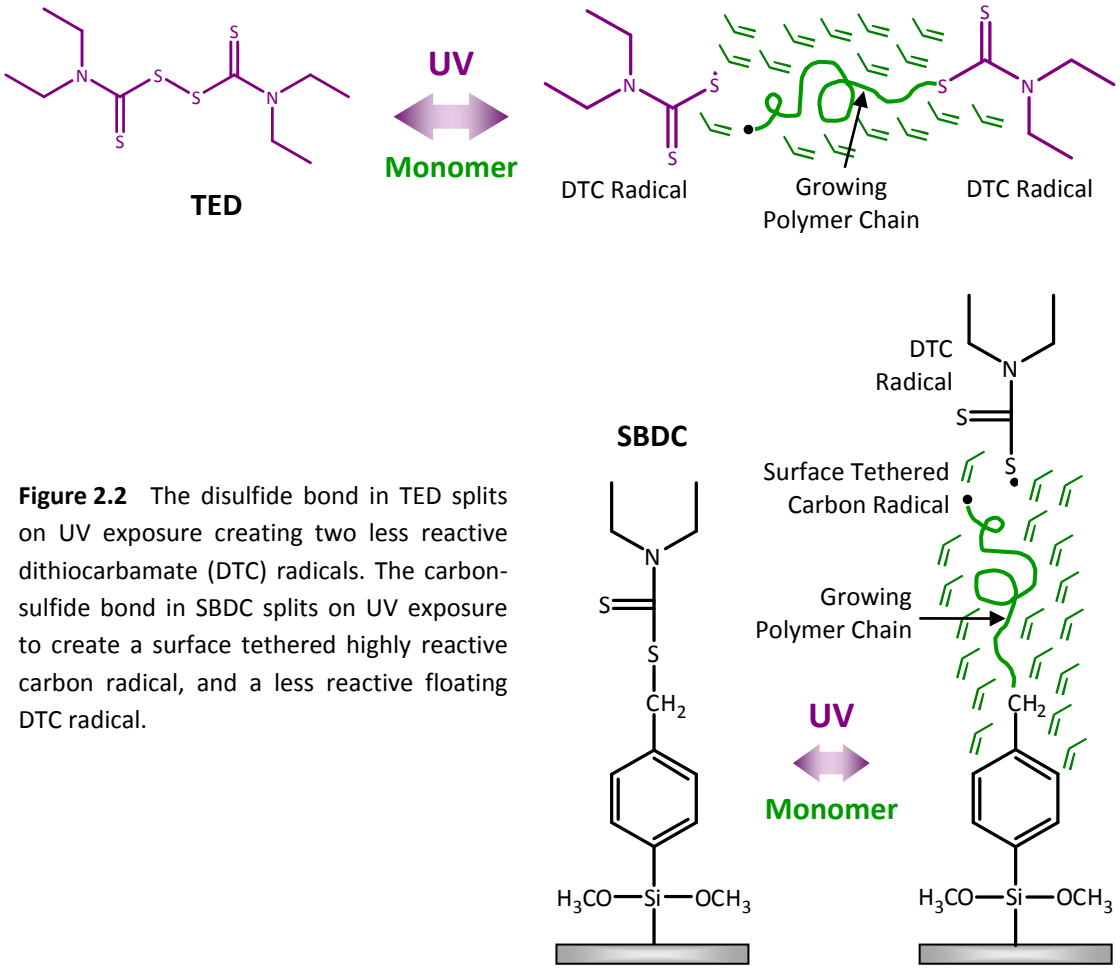

Figure 2.2 The disulfide bond in TED splits on UV exposure creating two less reactive dithiocarbamate (DTC) radicals. The carbon-sulfide bond in SBDC splits on UV exposure to create a surface tethered highly reactive carbon radical, and a less reactive floating DTC radical.

Surface-initiated PMP (SIPMP) depends on presence of special dithiocarbamate-derived iniferter (INItiator-transFER agent-TERminator) molecules on the surface. This iniferter molecule has a photo-labile carbon-sulfide or disulfide bond, which reversibly splits on UV exposure to create reactive radicals that initiate polymerization of vinyl monomers. Once the UV light is turned off, a carbon-sulfide bond is reformed to terminate the polymerization. However, just like the original iniferter molecule, this carbon-sulfide can be split again under UV light, to reinitiate polymerization and create block copolymers. Figure 2.2 shows two such iniferters, tetraethylthiuram disulfide (TED) and N,N-Diethylamino)-dithiocarbamoylbenzyl

(trimethyoxy)silane (SBDC), which can initiate controlled polymerization via a reversible termination process.

Controlled photopolymerization in solution using these iniferters was first developed by Otsu in the early 1980s. It was first adopted by the Matsuda group for grafting polymer brushes from surfaces. In the first study by Nakayama and Matsuda, the iniferter benzyl N,N-dithiocarbamate was used to synthesize polystyrene (PST) chains in solution using UV light.[135] The styrene chains were end-caped with a DTC group containing a carbon-sulfide bond which can split under UV to create a carbon radical. These DTC derivatized PST chains were either crosslinked to form films, or were cast onto PET films. PST or PET-PST films were then immersed in monomer solutions and exposed to UV light to graft either pMAA, poly(N,N-Dimethylacrylamide) (pDMAAm) or poly(N-[3-(Dimethylamino)propyl]acrylamide) (pDMAPAAm) chains from the surface. This study highlighted how exposure time and UV intensity can be used to very easily control the amount of polymer on the surface. For example, it was observed that contact angle of both PST and PET-PST films decreased with increasing UV exposure time, indicating that the amount of polymer can be controlled by simply controlling the exposure time. Metal photomasks were placed in the light path, to block certain regions from UV exposure. Dye staining was observed only on the exposed regions indicating that pMAA and pDMAPAAm was grafted only in the regions exposed to UV light. Patterns with a resolution of 60μm were created in this study, but their resolution is only limited by the resolution of the photomask. Next, metal photomasks were combined with a gradient neutral-density filter, to gradually increase the UV intensity from one end of the strip to the other. In this case, the dye staining intensity increased with UV intensity, indicating the amount of pMAA and pDMAPAAm grafted on the surface increase with intensity. AFM measurements further confirmed formation

of these patterns and gradients. The most important result came with cell culture experiments. When bovine aortic endothelial cell adhesion were seeded onto pDMAAm patterned PET-PST films, cells adhesion was restricted to the 60μm non-grafted hydrophobic regions, but were completely absent on pDMAAm grafted regions.[135] This was attributed to the hydrophilic nature of the pDMAAm regions which were very effective in preventing non-specific protein adsorption.

The versatility of SIPMP was further demonstrated by the same group, by grafting adjacent strips of 5 different polymers on the same PET-PST film.[136] First a small strip was exposed to UV for 10 minutes under the one monomer. Next, the film was washed and an adjacent strip was exposed to UV under the second monomer for 10 minutes. This process was repeated to graft strips of five different polymers, pMAA, pDMAAm, pHEMA, poly(N-[3-(dimethylamino)propyl]acrylamide methiodide) (DMAPAAmMeI), poly(3-sulfopropyl methacrylate) (pSMAK), adjacent to each other. Surface wettability significantly increased on all 5 regions compared to the hydrophobic ungrafted film. The polyDMAAm and polyHEMA caused significant reduction in bovine aortic endothelial cell (EC) adhesion, which can be attributed to their uncharged hydrophilic nature. The pDMAPAAmMeI and pMANa regions promoted EC adhesion and growth, which was most likely due to their ionic nature. Even though pSMAK regions are ionic as well, EC adhesion markedly decreased over time. The authors went a step further and created thickness gradients of pDMAAm, pDMAPAAmMeI and pMANa by slowly increasing the area under UV exposure. Interestingly, EC adhesion and proliferation gradually decreased with increasing polyDMAPAAmMeI and polyMANa grafted-layer thickness. In contrast, EC adhesion on the polyDMAAm gradient ceased abruptly above a certain graft thickness. While explanations for the observed cell behavior on different polymers and polymer

gradients were not provided, this study clearly demonstrated the high throughput nature of SIPMP to easily and very quickly compare cell response to different surface chemistries.

While the above studies used passive interaction of different polymers and different concentrations of a polymer, it is also possible to create patterns and concentration gradients of biomolecules on the surface by covalently attaching them to functional groups on the polymer. Such a study was conducted by Harris et al., where a concentration gradient of the cell adhesion peptide sequence RGD was created on silicon surfaces.[55] To achieve this, first a SAM of a silane-based DTC iniferter was deposited on the silicon surfaces. This iniferter SAM immersed in MAA monomer solution and the area of the surface exposed to UV was slowly reduced by moving an opaque photomask at a constant velocity over the surface. In essence, the exposure time gradually increased from one end of the surface to the other. This resulted in a thickness gradient of grafted pMAA chains on the surface, which was confirmed by ellipsometry measurements. The concentration of –COOH groups on the surface depends on the amount of pMAA on the surface, and in this case will follow the gradient profile. As a result, covalent coupling of RGD containing peptide sequence GRDGS to these –COOH groups should result in a concentration gradient of RGD across the surface. The increase in thickness post-RGD conjugation used to determine the RGD concentration across the gradient verified that it followed the polymer layer thickness. This gradually increasing RGD concentration translated into a gradual increase in the surface density of adhered NIH3T3 fibroblasts. In fact, it was possible to determine the absolute RGD concentration along the gradient and quantitatively correlate it to cell attachment behavior on the surface.

If such concentration gradients of biomolecules can be used to quantitatively analyze cell adhesion, it should also be possible to analyze other gradient dependent cell responses like

growth and migration. Furthermore, biomolecule concentration gradients with different baseline values and slopes can be created by simply adding a delay in mask movement and adjusting the mask velocity respectively. In an earlier study, Harris et al. have demonstrated the ability to graft pMAA gradients with different slope values.[56] Additionally, like studies by the Matsuda group, gradients can be also combined with patterned photomasks to create multiple sets of gradients with different slopes on the same surface. Such versatile surfaces can be used to study cell behavior on different gradient profiles in an extremely high throughput manner. For example, different gradient sets of neurotrophic factors can be used to determine the best gradient profile for axonal growth and guidance. Earlier it was discussed that successful spinal cord regeneration will require creation of concentration gradients of growth factors. Once the best gradient profile has been identified, 3D scaffolds can be fabricated that present such a gradient profile for in vivo testing in animal injury models. In short, the SIPMP technique can significantly accelerate the development of therapeutic regimes for tissue regeneration.

There are two main limitations associated with grafting via SICRP that need to be addressed. First, all radical polymerization are extremely sensitive to presence of atmospheric oxygen, which is a strong radical scavenger and can react in an uncontrolled manner with the radicals present on the surface. As a result, the polymerization process becomes uncontrolled, leading to PD in the grafted chains, or even preventing grafting from the surface. The first step to avoid this problem is degassing the monomer solution to remove all dissolved oxygen. Freeze-thawing the monomer solution under vacuum is the quickest methods to achieve this, and has become a standard procedure.[56, 57] To avoid dissolution of atmospheric oxygen during the polymerization procedure, samples are typically placed in custom-designed airtight chambers completely purged with an inert gas like nitrogen or argon. The above steps allow the

polymerization to proceed in the desired controlled manner. This added procedure does not pose a major hurdle for smaller samples, and is routinely done for most SICRP experiments. However, placing larger medical devices in such chambers is not always practically possible. An alternative is to add oxygen scavengers to the monomer solution, which rapidly react with and consume any oxygen that enters the monomer solution during the polymerization procedure.[137]

Second, the high surface grafting density and large size of some biomolecules like proteins can hamper covalent conjugation of the biomolecule to the polymer chains. Small biomolecules like RGD can diffuse deeper into the polymer brush layer for conjugation, even at relatively high polymer grafting densities. However, larger biomolecules like proteins will find it more and more difficult to diffuse deeper as the grafting density increases. It may so happen that the concentration of conjugated protein starts decreasing after a certain polymer layer thickness is reached due to excessively tight packing of polymer chains (extremely high grafting density). This limitation essentially puts a limit on the maximum allowable grafted polymer layer thickness, and gradients cannot have an upper value higher than this maximum allowable thickness. This limitation is not unique to SIPMP, but is valid for any surface initiated polymerization technique, and therefore needs to be addressed. Fortunately, SIPMP does provide a solution, as the biomolecules can themselves be acrylated and directly grafted from the surface like any other monomer. This is difficult to achieve with other techniques like ATRP, RAFT and NMP, because they involve use of organic solvents and chemicals which can easily denature and damage proteins. The highly reactive peroxide radical generated in plasma- and ozone-induced grafting techniques can easily cause oxidative damage to the protein.

One may argue that UV exposure during SIPMP can also damage the protein. Exposure time is not a problem as grafting via SIPMP is typically accomplished in a few minutes. Furthermore, UV intensity can also be reduced by increasing the monomer concentration up to saturation levels of the protein. Also, the radicals generated in the SIPMP technique are much less reactive, especially sulfide radicals generated from splitting of iniferter disulfide bonds. This approach has already been successfully attempted by Sebra et al., who grafted acrylated collagen from PU surfaces using SIPMP.[138] To achieve this, collagen was covalent coupled via its primary amine to NHS terminated PEG acrylate (NHS-PEG-Acy, PEG MW 3400). Since this coupling was carried out in an aqueous buffer, the protein bioactivity was preserved as verified by ELISA. DTC derivatized crosslinked PU substrates were synthesized by mixing TED into the PU precursor solution and exposing it to UV light for 500 seconds. Either PEG acrylate (MW 375), or collagen-PEG-Acy was grafted from these PU surfaces by exposure to 45 mW/cm^2 UV light for 900 seconds. Patterns of grafted PEG or PEG-collagen were created by placing a photomask in the light path. Successful collagen grafting was confirmed by ELISA. On seeding NIH3T3 fibroblasts on patterned PEG grafted surfaces, cells adhered only to the bare PU regions without PEG grafting. However, when cells were seeded on PEG-collagen grafted surfaces, cells adhered to the grafted regions as well. This clearly indicates that bioactivity of collagen needed for cell adhesion was preserved even after the acrylation and photografting procedure.[138]

To conclude this literature review, a myriad of techniques are available for surface modification of the plethora of biomaterials already under use clinically and under development for biomedical applications. It is possible that multiple techniques can achieve the desired surface modification, and the same surface modification technique can be used for different applications. In some cases, only one particular technique will be best suited for the targeted

surface modification. In yet other cases, the surface may have to be subjected to multiple techniques to yield the desired results. In short, careful consideration of the specific biomedical application as well as pros and cons of various surface modifications techniques will be required to select the most suitable one. Specifically from the bioengineering perspective, SIPMP seems to the most promising technique to quickly analyze cell behavior under a wide variety of conditions. This is required because unraveling how various extra-cellular factors affect cell behavior holds the key to developing successful long-term tissue regenerative therapies.

3. Systematic Variation of Surface Properties of Polyurethane Substrates Using Surface-Initiated Photoiniferter-Mediated Graft Polymerization

3.1 Introduction

Polymers have found widespread use in biomedical devices due to their low production cost, availability in high volume, ease of molding into any shape and size, ease of sterilization and considerable shelf life. A myriad of polymers such as poly(methylmethacrylate) (PMMA), Dacron polyester, poly(tetrafluoroethylene) (PTFE), high-density polyethylene (HDPE), polyurethanes (PU), poly(lactic acid) (PLA) and poly(glycolic acid) (PGA) have undergone testing and many have found extensive uses in biomedical applications including joints, artificial lenses, large diameter vascular grafts, heart valves, electrodes and catheters. Designing polymers with specific mechanical properties is relatively easy, with various polymer types and their blends possible to meet the requirements. However, selecting polymer(s) with the best mechanical properties does not always come with the best biocompatibility. Biocompatibility reflects the interaction of the material surface with the biological environment which will includes adsorbed blood proteins, the extra-cellular matrix (ECM), and most importantly cells.[72] As soon as a foreign material comes in contact with body tissue and fluids, proteins start adsorbing on its surface. Depending on which proteins have adsorbed, the amount of protein adsorbed, and the conformation of the adsorbed proteins, the cells may trigger a favorable or unfavorable response.[72] Since these interactions originate on the surface where proteins adsorb, several attempts have been made to alter the surface chemistry to either prevent protein adsorption altogether, or somehow control the state of the adsorbed protein to generate more favorable cellular responses such as bone tissue integration and endothelialization.[18] For example, devices made from PMMA such as contact lenses, intraocular lenses and biosensors suffer from

protein fouling, which adversely affects their functionality.[76-78] Surface modification that alters only surface properties, but not bulk properties can potentially address this issue.[76, 78] In other cases, certain biomolecules can be directly attached to the polymer surface to elicit specific responses, rather than relying on non-specific protein adsorption.[18, 139] For example, polyurethanes are extensively used in biomedical applications such as heart valves and catheters, due to their tunable mechanical properties. But they often suffer from calcification and thrombogenic biocompatibility issues, which lead to failure of the PU device in the long term.[79] Surface modification is being used to reduce these undesirable reactions by controlling non-specific protein adsorption as well as incorporation of anti-calcification and anti-thrombotic agents like 2-hydroxyethanebisphonic acid (HEBP), heparin and ε-lysine on the surface.[79, 80]

One approach to alter the surface chemistry is by changing the polymer type, structure and composition. For example, blending poly(ethylene glycol)-containing (PEG) copolymer into the polymer bulk, can potentially result in highly protein repellant surfaces due to diffusion of PEG chains to the surface.[88] Although this may be an easy method, there is a possibility of the PEG chains leaching out causing serious issues with long-term usability of this material. This can potentially be addressed by covalently linking the PEG chains to the bulk polymer backbone.[89] Although blending of bulk synthetic polymers with additive polymers can influence surface properties, they can adversely affect mechanical properties. Furthermore, blending is very specific, so the material to be added, the amount to be added, and the blending technique to use will change with the targeted bulk material and application. [92-94]

A better and easier approach would be to change the surface chemistry of the bulk polymer without altering the bulk properties. Such a technique can then be universally applied

to most if not all polymer types. The simplest of these approaches is physical coating of a protein resistant polymer, such as PEG, to the bulk material surface. Simple coating of PEG on PU, polysulfone, PMMA and PLA surfaces has been shown to be very effective in reducing non-specific protein adsorption.[76, 94, 117] However, long term stability is questionable as the physically coated polymer layer can be easily dislodged and lost permanently. One solution to this problem is to permanently attach the polymer chains to the surface. The two most commonly used techniques are “grafting to” and “grafting from”, both of which create polymer brushes on the surface. Besides changing the surface chemistry, the grafted polymer chains can be used to attach biomolecules to the surface as a means to control specific cell behaviors. For the “grafting to” technique, reactive groups are introduced on the material surface and used to attach polymer chains using appropriate conjugation chemistries. The covalent bond formed between surface and polymer chain makes the polymer brushes robust and prevents their removal. Reactive groups can be directly incorporated during the bulk polymer synthesis, as was done by Archambault et al. to attach PEO chains to PU substrates, which reduced protein adsorption by up to 70%.[31, 140] In another study by Shoichet et al., PEO chains were attached to poly(acrylonitrile-co-vinyl chloride) (PAN/VC) membranes, which reduced protein adsorption by up to 70%.[33] Plasma/Glow discharge treatment can also be used to introduce reactive groups on the surface followed by attachment of polymer chains.[34, 141] Attachment of PEG chains to silica surfaces activated by plasma treatment resulted in a significant decrease in adsorption of bovine serum albumin. However, it is difficult to achieve high grafting densities with “grafting to” approach because as chains attach to the surface, it becomes more and more difficult for subsequent chains to diffuse through the layer and reach the surface.[36] This may result in incomplete coverage of the surface and potentially allow protein molecules to diffuse

through and adsorb on the polymer surface.[122, 142] This limitation of the "grafting to" technique can be overcome with the "grafting from" approach to obtain higher grafting density, since monomer units that build individual polymer chains are less susceptible to steric hindrance than preformed polymer chains.[37] The most versatile "grafting from" approach is surface-initiated radical polymerization since a vast pool of vinyl monomers can be used to alter the surface properties as well as introduce reactive functional groups on the surface. This obviously requires introduction of initiator molecules on the polymer surface, which can be realized using plasma treatment, ozone oxidation, γ-irradiation, UV-irradiation, electron beam and laser treatment.[143-147]

At this stage, most of the problems associated with modifying the surface properties using polymer grafting have been addressed. However, there is an inherent limitation associated with the aforementioned free radical polymerization-based "grafting from" technique. Free radical polymerization produces grafted chains with high polydispersity.[128] As mentioned earlier, improvement in biocompatibility will also require eliciting specific responses from cells by attaching biomolecules to the surface. A high polydispersity on the surface will cause an uncontrolled variation in concentration of the biomolecule on the surface, which will cause uncontrolled variation in cell response on the same surface. This is why controlled surface-initiated polymerization (CSIP) techniques have generated immense interest in the biomedical field. Controlled surface-initiated polymerizations usually result in grafted-polymer chains with very low polydispersity ($M_w/M_n<1.3$)[128], which provides excellent control over the concentration of functional groups on the surface. Several CSIP techniques such as atom transfer radical polymerization (ATRP)[51, 52], nitroxide-mediated polymerization (NMP)[53, 54], reversible addition-fragmentation chain transfer polymerization (RAFT), and photoiniferter-

mediated polymerization (PMP)[55-57] provide excellent control over the amount of polymer grafted by changing parameters like polymerization time and monomer concentration. However, not all are amenable to creation of complex spatial patterns and thickness gradients of grafted polymer, especially on polymer substrates. The ability to create patterns and gradients of biomolecules is gaining importance as they can be used to direct cell behaviors beyond simple adhesion, like migration and growth. Since PMP uses UV light for graft polymerization, photomasks can be introduced to create spatial patterns[135, 148], while a gradual increase in exposure time can be used to create gradients[55, 56, 136]. Polymerization via PMP is also very quick, with relatively thick layers obtained in minutes. PMP requires the presence of photoiniferter on the material surface to initiate polymerization, which can be synthesized to allow modification of metallic, ceramic and polymeric surfaces. The iniferter molecules also have the unique ability to reinitiate (mechanism explained later), thus allowing block copolymers to be grafted from the surface.[149]

Polyurethane substrates (PU) were selected as a model surface to graft polymer chains using PMP since they are extensively used for biomedical applications, but suffer from biocompatibility issues as described above. The goal was to convert the hydrophobic nature of the PU surfaces to a more hydrophilic nature, and at the same time provide a way to control the degree of hydrophilicity of the surface. It would also be advantageous to demonstrate that small molecules can be attached to these surfaces with potential applications in drug delivery, antigen presentation, biosensing, antifouling, etc. To achieve these goals the iniferter tetraethylthiuram disulfide (TED) was incorporated into the crosslinked PU substrates as a means to graft polymer chains from the surface. Though this type of graft photopolymerization from PU substrates has already been demonstrated [148, 150, 151], a systematic variation of and control over the

amount of polymer grafted on PU surfaces using PMP has not. Four parameters were tested for this purpose, substrate iniferter concentration, UV intensity, monomer concentration and polymerization time. Methacrylic acid was selected as the monomer as it would provide carboxylic acid –COOH functional groups on the surface after grafting. The –COOH groups will not only increase the hydrophilicity of the surface, but should also allow electrostatic or covalent attachment of molecules on the surface. In this study, a positively charged dye, toluidine blue, was electrostatically attached to the negatively charged $–COO^-$ groups on pMAA chains [152]. The study demonstrates that by altering polymerization conditions, the hydrophilicity of PU substrates and the concentration of an attached molecule can be systematically and reproducibly altered as required.

3.2 Materials and Methods

3.2.1 Synthesis of Polyurethane Substrates

Hexafunctional urethane acrylate (CN975, Sartomer, PA), crosslinker triethylene glycol dimethacrylate (TGD, Sigma, MO), photoiniferter tetraethylthiuram disulfide (TED, Sigma, MO), and photoinitiator Irgacure 2959 (Ciba, NY), were mixed together in a weight ratio of either 49:49:1:1 or 48:48:3:1 to give either 1 w/w % or 3 w/w % of TED respectively in the mixture. This mixture was sonicated for about 30 minutes to obtain a homogeneous yellow colored precursor solution. This solution was injected between two clean and transparent glass slides separated by a 1mm thick Teflon spacer, taking care not to introduce any air bubbles. Each side of the glass slide sandwich was exposed to 365nm UV light at 25mW/cm^2 for 5 minutes to form a crosslinked PU substrate. The cured substrate was gently detached from the glass slides and washed with copious amounts of ethanol (≥99.5%, Fisher, PA) and acetone (≥99.5%, Fisher, PA)

to remove any debris and unreacted chemicals. These substrates were cut into 12mm x 10mm samples, which were used for graft photopolymerization.

3.2.2 Graft Photopolymerization of Methacrylic Acid

Graft photopolymerization was carried out under a Mask Aligner system (OAI, CO) which provided collimated 365nm UV light at a constant intensity of 25mW/cm^2. The cut 12mm x 10mm samples were attached to a glass plate using double-sided adhesive tape. A viton o-ring (AS568A #017, McMaster, GA) was placed on the glass plate around each substrate using a minimal amount of vacuum grease. The plate with the attached substrates was placed on the N_2 gas-based floating platform of the mask aligner.

Either a 15% v/v or 50% v/v solution of methacrylic acid (Sigma, MO) monomer in deionized (DI) nanopure water was degassed by subjecting it to three freeze-vacuum-thaw cycles in a glass Schlenk tube sealed with a rubber septum. A long steel needle attached to a 5ml glass syringe was introduced through the septum into the Schlenk tube to aspirate out monomer solution. Enough monomer solution was added inside the o-ring area so as to completely submerge the sample. The mask aligner hatch was immediately closed over the platform to form a chamber which was continuously purged with N_2 gas to prevent oxygen from entering the system. The platform was raised slowly until the o-rings completely contacted the transparent glass window of the hatch. This helped maintain a uniform spacing between the sample surface and the bottom surface of the window, and form an airtight seal to prevent oxygen from dissolving into the monomer solution. Substrates were exposed to UV light for 5, 10, 20, 30, 45, and 75 minutes to graft poly(methacrylic) acid (pMAA) chains from the surface. To study the effect of UV light intensity, samples were exposed at an intensity of either 25mW/cm^2 or 6.25mW/cm^2. The higher intensity was obtained by exposing the samples directly

to the mask aligner light, while the lower intensity was obtained by introducing a neutral density filter in the light path. After exposure the polymer grafted samples were rinsed with copious amounts of pure ethanol and sonicated in pure ethanol for 60 minutes to remove any unreacted monomer and untethered polymer chains. Samples were dried using a N_2 gas blowgun and stored at room temperature (RT) in sealed test tubes until further use. Table 3.1 summarizes the polymerization conditions and values that were tested.

Parameter Tested	Values	Exposure Times (min)	Other Constant Parameters
TED Concentration	1% and 3% w/w	5, 10, 20, 30, 45, 75	Monomer Concentration = 50% v/v; UV Intensity = 25 mW/cm2
Monomer Concentration	15% and 50% v/v		TED Concentration = 3% w/w; UV Intensity = 25 mW/cm2
UV Intensity	6.25 and 25 mW/cm^2		Monomer Concentration = 50% v/v; TED Concentration = 3% w/w

Table 3.1 Values of various parameters varied for graft photopolymerization of pMAA from PU surfaces.

3.2.3 Water Contact Angle Measurement of PMAA Grafted Surfaces

Static water contact angles of the pMAA grafted PU surfaces were measured via the sessile drop technique using a Kruss DSA10 goniometer equipped with a digital camera and drop shape analysis software. Control samples consisted of unmodified PU substrates without polymer grafting. A 3µl drop of HPLC grade water was placed onto the sample surface and allowed to equilibrate for about 15 seconds before the contact angle was measured using the drop shape analysis software. Three measurements were taken per sample at different locations and three samples were measured for every polymerization condition. Thus, nine contact angle values per polymerization condition were used to calculate a mean for data analysis.

3.2.4 Dye Adsorption Measurement of PMAA Grafted Surfaces

The amount of dye adsorbed to the pMAA grafted PU samples was determined by measuring the absorbance using a BioTek μQuant Microplate spectrophotometer. Controls consisted of PU substrates without polymer grafting. For dye binding, pMAA grafted and control samples were soaked in 0.1M pH 8.0 phosphate buffer for one minute. The buffer was quickly wicked off from the edges using Kimwipes and the samples were immediately placed in a 50mM solution of toluidine blue in pH 8.0 phosphate buffer for 15 minutes. The samples were then rinsed with 5ml of DI water three times to remove excess toluidene blue solution. Samples were dried under a N_2 gas flow and placed in a 24-well plate. The plate was placed in the spectrophotometer chamber and the absorbance was measured at 570nm. The absorbance value of the control samples was subtracted from that of the pMAA samples to give absorbance values of only the adsorbed dye. Dye absorbance of three samples polymerized under the same conditions was measured to give a mean for data analysis.

3.2.5 Statistical Data Analysis

For every polymerization condition tested, contact angle and dye absorbance values of three samples were measured for every exposure time value. These three values for every exposure time value were used to calculate the mean and standard deviation. In all the data figures, data points represent these mean values, while the error bars represent the corresponding ± one standard deviation.

3.3 Results and Discussion

3.3.1 Synthesis of Polyurethane Substrates

When the precursor mixture of CN975 (urethane), TGD (crosslinker), TED (photoiniferter) and Irgacure (photoinitiator) was exposed to UV light, the photoinitiator molecule initiated free radical polymerization and hence crosslinking of the CN975 and TGD (figure 3.1). While this was happening, the disulfide bond in the TED molecules added to the precursor solution split creating two diethylthiocarbamoyl disulfide (DTCS) groups with low reactive sulfide radicals (figure 3.1). When the UV light was turned off, these low reactive DTCS radicals reacted with the prorogating carbon radicals to terminate the crosslinked polymer

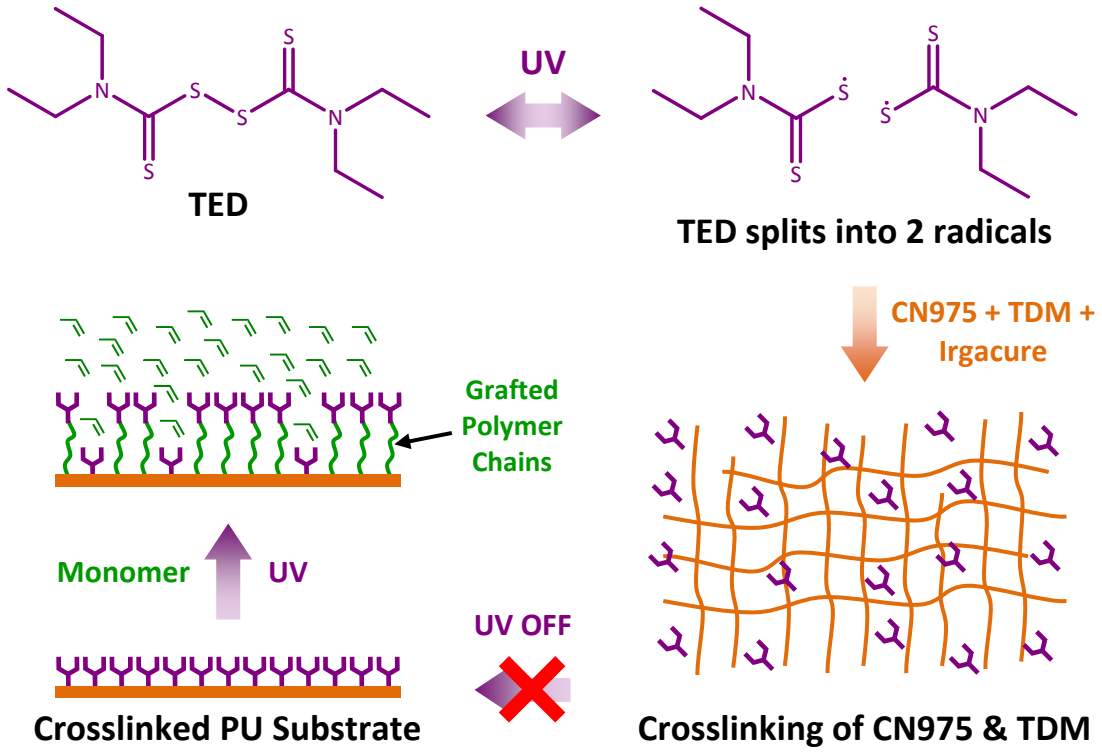

Figure 3.1 Crosslinking of CN975 and TDM under UV light using photoinitiator Irgacure in the presence of photoiniferter TED. TED molecules on the surface of PU substrates then initiate graft polymerization of monomer under UV light.

chains. The carbon-sulfide bonds thus formed at the chain ends can split again on exposure to UV light to initiate another polymerization reaction. Some of the diethylthiocarbamoyl disulfide groups capping the polymer chains will be present at the surface of the substrate (figure 3.1). The carbon-sulfide bond of these end-caps will split again on exposure to UV light and in the presence of any vinyl monomer will initiate grafting of polymer chains from the PU surface (figure 3.1). This method was used to graft poly(methacrylic acid) (pMAA) chains from PU surfaces.

3.3.2 Graft Photopolymerization of Methacrylic Acid

In this study, four parameters (exposure time, iniferter concentration, UV light intensity and monomer concentration) were used to control the amount of polymer grafted on the PU surface. To get a comprehensive picture of how exposure time will affect the amount of pMAA grafted, the exposure time was varied from 5 minutes to 75 minutes for every variation of the remaining three parameters. The amount of polymer grafted on a surface can increase in the form of MW of the polymer chains, or by an increase in the grafed-chain density.[56] Iniferter-based graft photopolymerization has been shown to be psuedo-living, which means the MW of the grafted polymer chains remains essentially constant with exposure time.[56] However the number of iniferter molecules initiated per unit area increases with time, resulting in more polymer chains per unit area or higher grafting densities at longer exposure times.[56] On the other hand, increasing the monomer concentration does increase the MW of the grafted chains with other polymerization conditions kept same.[56]

3.3.3 Contact Angle and Dye Absorbance Measurements of PMAA-Grafted PU Substrates

Since pMAA chains are hydrophilic due to presence of the carboxylic acid groups, grafting of pMAA should cause an increase in the hydrophilicity of the surface (figure 3.2A).[151]

This variation in hydrophilicity was measured using water contact angle measurements. At lower grafted-chain density and/or polymer chain MW, the PU surface will not be completely covered causing the water drop to interact with both the PU surface and polymer chains. As a result, the measured contact angle will be between that of unmodified PU and pure pMAA. As the amount of grafted pMAA on the surface increases, more and more of the PU surface will be covered causing the contact angle to shift from that of PU towards pure pMAA (<20°) (figure 3.2A) [149, 153].

Along similar lines, the carboxylic acid –COOH groups on the pMAA chains dissociate at acidic pH thus creating negative $–COO^-$ charges on the pMAA chains. The concentration of negative charges will obviously increase with an increase in the amount of polymer grafted on the surface. A positively charged molecule will electrostatically attach to these negative charges on the pMAA chains, the concentration of the molecule will follow the amount of polymer grafted. For this study, the positively charged dye toluidine blue was attached to the surfaces by electrostic binding with the negative charges on the pMAA chains[152] which resulted in a purple coloration of the PU substrates (figure 3.2B). The intensity of this color, which should follow the amount of dye attached,

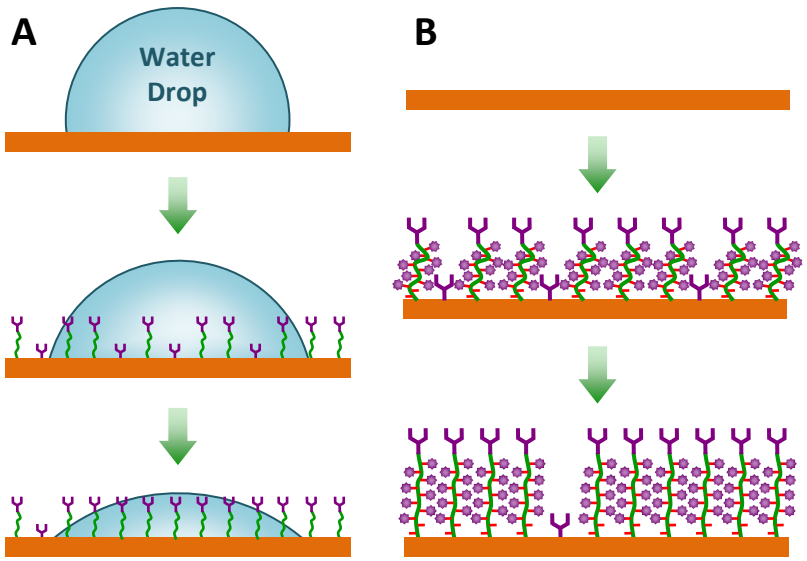

Figure 3.2 Effect of amount of polymer from PU surface on (A) hydrophilicity and contact angle, and (B) on dye attachment and corresponding light absorbance.

was determined by light absorbance measurements at 570nm using a spectrophotometer. Such electrostatic coupling can be used to attach and present small positively charged signaling molecules to cells. If long term presentation is required, drugs or other biomolecules such as peptides, proteins or antibodies can be covalently attached to the carboxylic acid groups using one of the well known conjugation chemistries such as N-hydroxysuccinimide and carbonyldiimmidazole. In short, this grafting technique will not only allow alteration of multiple surface properties (hydrophilicity and charge as in this study) but also provide a way to attach molecules to make the surface bioactive.

The first parameter tested was TED concentration, with pMAA grafted on substrates synthesized with either 1% w/w or 3% w/w TED. The UV light intensity was kept consant at 25mW/cm^2 while the monomer concentration was fixed at 50% v/v. As seen in figure 3.3A, the contact angle values on 3% TED substrates were lower than those of 1% TED. Similarly, figure 3.3B shows that dye absorbance values of 3% TED substrates were lower than those of 1% TED.

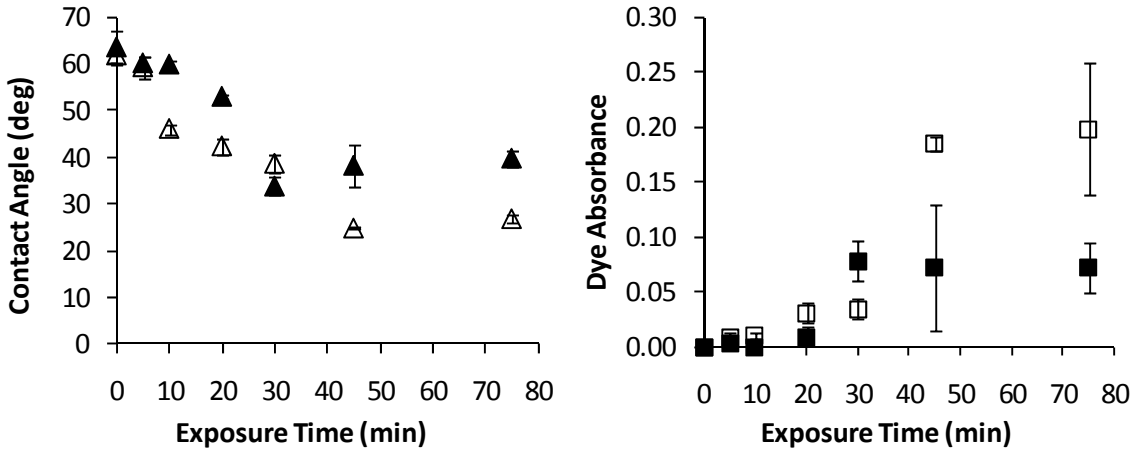

Figure 3.3 Effect of increasing TED concentration from 1% w/w to 3% w/w on surface properties. Contact angles values (A) are much lower, while dye absorbance values (B) are much higher for pMAA grafted surfaces with 1% w/w TED (△,□) than 3% w/w TED (▲,■). (UV intensity = 25mW/cm^2; Monomer concentration = 50% v/v; n = 3 for each time point; Error bars = ± Std. Dev.)

A higher TED concentration means a higher density of iniferter sites on the PU surface, which means more polymer chains grafted from 3% TED substrates compared to 1% TED substrates under the same conditions. Also seen in figures 2.3A and B is a decrease in contact angle values and increase in absorbance values respectively with exposure time. As explained earlier, longer exposure times resulted in higher chain grafting densitites thus lowering the contact angle and increasing the amount of attached dye.

The second parameter tested was monomer concentration, with pMAA grafting done with 15% v/v and 50% v/v monomer solutions. UV light intensity was kept consant at 25mW/cm^2 while the TED concentration was fixed at 3% w/w. As seen in figure 3.4A, the contact angle values on substrates grafted with 50% v/v monomer solution were lower than those grafted with 15% v/v monomer solution. Similarly, figure 3.4B shows that dye absorbance values of substrated grafted with 50% v/v monomer solution were higher than those grafted with 15% v/v monomer solution. Harris et al. have explained earlier that increasing the

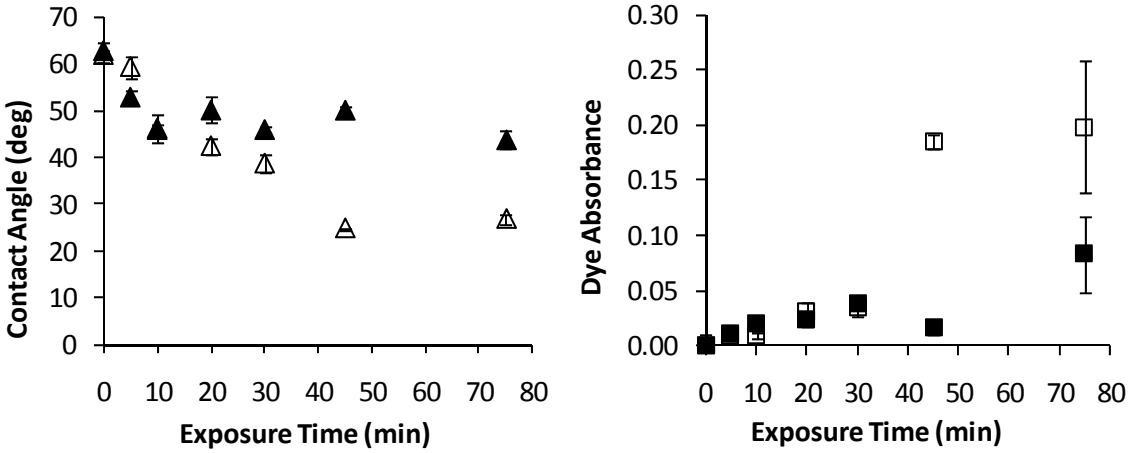

Figure 3.4 Effect of increasing monomer concentration from 15% v/v to 50% v/v on surface properties. Contact angles values (A) are much lower, while dye absorbance values (B) are much higher for pMAA grafted surfaces with 50% v/v monomer (△,□) than 15% v/v monomer (▲,■). (TED concentration = 3% w/w; UV intensity = 25mW/cm^2; n = 3 for each time point; Error bars = ± Std. Dev.).

monomer concentration causes the MW of the grafted polymer chains to increase but keeps the chain grafting density constant with other conditions kept the same.[56] This is what most likely happened, wherein higher monomer concentration of 50% v/v caused grafting of higher MW pMAA chains on the PU surfaces compared to 15% v/v monomer solution. Figures 2.4A and B also show a decrease in contact angle and increae in dye absorbance values with exposure time. As explained earlier, longer exposure times resulted in higher chain grafting densitites thus lowering the contact angle and increasing the amount of attached dye.

The third and final parameter tested was the UV light intensity with pMAA grafted on PU surfaces at either 6.25mW/cm^2 and 25mW/cm^2. The TED concentration was kept constant at 3% w/w while the monomer concentration was fixed at 50% v/v. As seen in figure 3.5A, the contact angle values on substrates exposed at 25mW/cm^2 were lower than those exposed with 6.25mW/cm^2. Similarly, figure 3.5B shows that dye absorbance values of 3% TED substrates was lower than those of with 1% TED. Increasing the UV intensity from 6.25mW/cm^2 to 25mW/cm^2

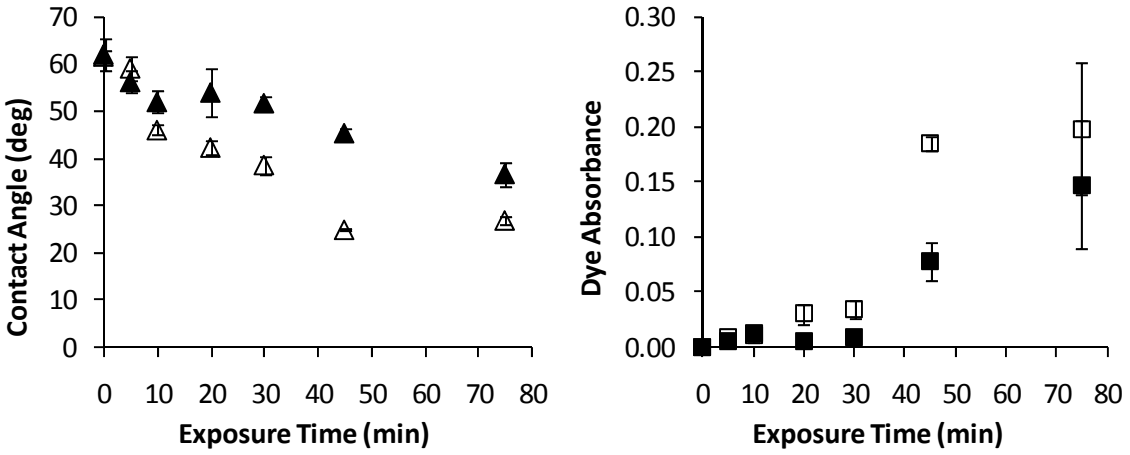

Figure 3.5 Effect of increasing the UV intensity from 6.25mW/cm^2 to 25 mW/cm^2 on surface properties. Contact angles values (A) are much lower, while dye absorbance values (B) are much higher for pMAA grafted surfaces with 25mW/cm^2 (△,□) than 6.25 mW/cm^2 (▲,■). (TED concentration = 3% w/w; Monomer concentration = 50% v/v; n = 3 for each time point; Error bars = ± Std. Dev.).

increased the rate at which iniferter molcules are initiated, resulting in higher grafting densities under same conditions. Figures 2.5A and B also show a decrease in contact angle and increae in dye absorbance values with exposure time. As explained earlier, longer exposure times resulted in higher chain grafting densitites thus lowering the contact angle and increasing the amount of attached dye.

Contact angle and dye absorbance values of samples containing 3% TED grafted with an intensity of 25mW/cm^2 and monomer concentration of 50% v/v were further used to compare contact angle and dye absorbance values of samples grafted under different conditions. Interestingly, contact angle and dye absorbance values reached a plateau beyond an exposure time of 45 minutes for samples containing 3% TED grafted using an intensity of 25mW/cm^2 and monomer concentration of 50% v/v (△ and □ in figures 3.3, 3.4 and 3.5). This mostly likely happened because by 45 minutes all the iniferter sites on the surface had been consumed to initiate chain growth, with none available to graft more polymer chains. Expectedly, since 1% TED surfaces contain less amount of iniferter molecules, the plateau was reached much earlier at 30 minutes (▲ and ■ in figure 3.3), compared to 45 minutes for the 3% TED samples. On the contrary, for samples grafted at a lower UV intensity of 6.25mW/cm^2 no such plateau in the contact angle and dye absorbance values was observed (▲ and ■ in figure 3.5). The most plausible explanation is that the lower UV intensity reduced the initiation rate of iniferter molecules on the surface. As a result, even at the maximum exposure time of 75 minutes used in this study, all the iniferter sites had not been consumed to initate chain growth. It is likely that a plateau could be eventually reached at a longer exposure time. Finally, no specific trend could be concluded from the results of samples grafted at a lower monomer concentration of 15% v/v.

3.4 Conclusions

In conclusion, by grafting pMAA to PU substrates its hydrophobic nature was converted to hydrophilic. Additionally, the degree of hydrophilicity can be varied by controlling the amount of polymer grafted from the surface. This study demonstrates that this can be achieved using one or more of the four parameters tested, exposure time, photoiniferter concentration, monomer concentration and UV light intensity, showing the tremendous flexibility of the grafting technique. While this study involved the use of PU substrates with one set of mechanical properties, the same grafting technique can be used for substrates made with other precursor materials, urethanes or otherwise [154-156], having the desired mechanical properties. TED can be either incorporated during synthesis of these substrates, as demonstrated by this study and those by other researchers [150, 155-157], or different kinds of photoiniferter can be attached to the surface [56, 57, 151]. A positively charged dye was also electrostatically attached to the polymer chains in this study, but covalent coupling is very much possible, as other studies have demonstrated.[55] Such coupling can be used for drug delivery applications or to render the surface of a PU based biomedical device bioactive. Covalent tethering of the polymer chains to the surface provides durability, and will prevent loss of the altered surface properties and attached biomolecules for long term usage. Furthermore, the flexibility of the polymer chains, especially in biological liquids, can provide suitable mechanical properties and better accessibility of attached biomolecules to probing cells. Though beyond the scope of this study, polymers with functional groups other than –COOH can be grafted to facilitate the use of other conjugation chemistries.[158] Just like the degree of hydrophilicity can be controlled, the amount of biomolecule attached to the surface can be varied by controlling the amount of polymer grafted from the surface. Furthermore, since light was used for

polymerization, spatial patterns and gradients of grafted polymer chains can be created. All together, it is possible to create spatial patterns or concentration gradients of biomolecules on the surface. Spatial patterns can be used to promote or prevent cell adhesion in certain areas, while concentration gradients can find applications in cell guidance, such as neuron guidance for spinal cord regeneration.

4. Noradrenalin Conjugated Grafted-Polymer Surfaces As A Novel Anti-Biofouling Strategy

4.1 Introduction

Ships have long been coated with special marine paints to prevent corrosion from the elements.[159] At the same time, these paints keep the surface smooth by preventing biofouling, which is the unwanted accumulation of bacteria, algae, plants and marine animals on submerged structures in marine environments [60]. Besides negatively impacting aesthetics, biofouling increases the ships' surface roughness[159]. This translates into higher frictional resistance, which combined with the increased weight reduces the ships' speed and maneuverability.[160] This has been estimated to increase fuel consumption by 40% resulting in an increase in the cost of the voyage by up to 77%.[60] Biofouling can also degrade the existing protective coating leading to corrosion. As a result, ships need to be dry-docked to remove the biofouling and recoat the ships' surface with the protective layer. This leads to unnecessary service time and monetary loss as well as the need to dispose of the hazardous waste generated by the cleaning and re-painting process.[60] On the ecological front, biofouling can introduce non-native species to new geographical regions leading to unfavorable and unbalanced competition, and even extinction of native species.

The history of combating marine biofouling is as old as ships themselves. Covering hulls with copper and lead sheathing or coating them with wax, asphalt, pitch, tar, brimstone and tallow, have all been attempted as antifouling coatings since a millennium.[60, 159] Prior to the 1960s, organometallic paints containing toxic pigments based on copper, mercury, tin, arsenic and others were used to kills and dislodge attaching marine organisms.[159] This ultimately led to extensive use of triorganotin-based paints as antifoulants (AF). In the absence of any better

antifouling agent, the use of tributyltin (TBT) incorporated in marine coatings as an effective and broad spectrum antifouling agent became widespread since the 1960s. Besides research on the effectiveness of TBT itself, considerable progress was made in developing paint materials which incorporated TBT. The most commonly used technique became self-polishing coats (SPC) which contain special acrylic copolymers that slowly degrade in seawater. The TBT groups were bonded to the main polymer chains via ester bonds, and were released slowly upon contact with seawater.[159] After immersion, the polymer itself starts degrading and dissolving leaving a fresh area of the coat containing TBT.[159] This SPC technology extended dry-docking intervals up to 5 years, saving the shipping industry billions of dollars every year. In fact, in 1999 it was estimated that 70% of all commercial ships were protected by them, leading to direct savings of close to US$ 2400 million a year.[60, 159] Unfortunately, TBT-SPC paints were found to have disastrous effects on the marine ecosystem, especially around docks and ports. TBT leaching out of paints caused deformities in marine organisms, weakened fish immune systems and accumulated in mammals that consumed marine biota. Consequently, manufacturing of TBT containing antifouling coats was banned in January of 2003, with complete removal from all ship surfaces to be completed by January of 2008.[60, 159]

Since the ban on TBT, copper and other organometallic co-biocides are now incorporated into most currently used antifouling paints.[60, 159] The application methods have remained largely the same, SPCs being the most effective. However, the total release rate of copper from all such coated ships has been estimated to be around 3000 tons per year.[159] The ever-increasing global trade combined with increased ship sizes is only going to increase the amount of copper released, and is an impending environmental disaster. For example, copper-

coated vessels can aid the transport and establishments of copper tolerant non-indigenous species to new habitats.[161]

Environmental regulations worldwide are becoming increasingly stringent, forcing paint manufacturers to intensify research in the development of environmentally friendly antifouling coatings. This has shifted the focus to investigating fouling-release (FR) coatings, which reduce the adhesive strength of organisms to the ship's hull. These coatings do not prevent fouling, but facilitate easy removal of the organisms by washing or movement of the ship in the sea. The FR characteristics of these coatings have been attributed to three properties, viz. surface energy, elastic modulus and coating thickness.[160] Fluoropolymers and silicones seem to best fulfill these requirements and are foci of intense research to tailor their properties for the best FR effect. Even though silicones have been demonstrated to have good FR properties, widespread use is limited due to the high speed (>22 knots) required to achieve complete FR, restricting their use to high speed vessels.[159] Furthermore, these FR coating are sensitive to mechanical damage, and are not as effective as biocidal paints in spite of being 2 to 7 times more expensive than biocidal paints.[159]

More recently, research efforts are focusing on altering the settlement and attachment mechanisms used by fouling organisms as an environmentally friendly antifouling strategy.[60, 162] Studies are being conducted to identify and isolate secondary metabolites in marine organisms and bacterial extracts that can disrupt the settlement process.[60, 163] Specific to the focus of this study, catecholamines, adrenoreceptor agonists and antagonists have been shown to inhibit larval settlement in a wide variety of marine organisms. [164-171] The well known hormone noradrenaline (NA), which is an adrenoreceptor agonist, was selected for this study. For a more detailed explanation about selection of NA and its effect on the settlement process

of marine organisms, please refer to “Development Of A Novel Fouling Deterrence Strategy By Understanding The Effect Of Noradrenaline On The Cells Of Eastern Oyster, *Crassostrea Virginica* And Cypris Larvae Of The Striped Barnacle, *Balanus Amphitrite*”, Gohad NV, 2008, Ph.D. dissertation.[172]

The goal of this study was to present unfavorable bioactive signals to the invertebrate larvae exploring the surface as a means to deter their settlement on the surfaces. To achieve this goal, NA needed to be immobilized on the surface while fulfilling the following requirements:

1. immobilization needs to be covalent so that surface bioactivity is retained,
2. immobilized NA needs to be accessible to the larvae,
3. immobilized NA needs to retain its bioactivity to deter larval settlement, and
4. concentration of NA on the surface needs to be high enough for AF effect.

Loss of NA from the surface, either due to dissolution or internalization by cells, needed to be prevented, so physical adsorption as an immobilization technique was ruled out. Self-assembled monolayers (SAMs) presenting reactive groups for coupling are a common method to immobilize biomolecules.[37, 173] However, the concentration of NA on the surface would be extremely low [37] and accessibility would be a concern, especially for larvae, because of the stiffness and high packing density of the short SAM chains. Attaching molecules to polymer chains grafted on surfaces is another prominent method to render a surface bioactive.[37] Flexibility of such grafted polymer chains will aid in maintaining accessibility. Various “grafting to” and “grafting from” techniques are available to graft polymer chains with reactive functional groups on surfaces, and covalently attach biomolecules to these chains.[37] The “grafting from” approach was selected as it can provide much higher grafting densities, and hence, complete

surface coverage to prevent access of untreated surface area to cells.[122, 142] Within the various "grafting from" approaches, surface-initiated photoiniferter-mediated polymerization (SIPMP) is an extensively studied and versatile technique, which provides excellent control over the amount of polymer grafted on the surface.[55-57] Studies have also demonstrated the ability to covalently attach small peptides like RGD to poly(methacrylic acid) (pMAA) chains grafted from silicon surfaces.[55] The accessibility as well as bioactivity of the immobilized RGD peptide was maintained and a high enough surface concentration was obtained to promote fibroblast adhesion on the surface.[55] Therefore, this technique was selected to graft pMAA or poly(hydroxyethylmethacrylate) (pHEMA) chains from glass surfaces, which provide –COOH and –OH functional groups respectively for covalent conjugation of NA. NA was conjugated using two chemistries suitable for linking the –COOH or –OH groups to the primary amine $–NH_2$ group on NA molecules. As a preliminary study, the accessibility and bioactivity of such immobilized NA molecules was tested using adhering hemocytes of the Eastern Oyster *Crassostrea virginica*. Oysters constitute a major portion of the biofouling fauna, and studies have already demonstrated that NA added to seawater triggers apoptosis in oyster hemocytes [171, 174-176].

4.2 Materials and Methods

4.2.1 Synthesis of Photoiniferter N,N-(Diethylamino)dithiocarbamoylbenzyl(trimethyoxy) silane (SBDC)

SBDC was synthesized by adapting the protocol as described by de Boer *et al.*.[177] The synthesis step was done in a glove-box to eliminate moisture which will react with and degrade the silane groups. All glassware used for synthesis was dried in a vacuum oven at 100°C overnight. 3.123 grams of sodium diethyldithiocarbamate trihydrate (NaDTC, Sigma) was

dissolved in about 30ml of anhydrous tetrahydrofuran (aTHF, 99.9%, Acros) in a 100ml round bottom flask, and stirred on a magnetic stir plate. In a separate pear flask, 3ml of p-chloromethylphenyltrimethoxy silane (pCPTS, Gelest Inc., 95%) was dissolved in about 5ml of aTHF. The silane solution was added dropwise to the NaDTC solution using a Pasteur pipette while being stirred. The reaction flask was sealed with a rubber septum, and a 25 gauge needle was introduced through the septum to prevent pressure buildup due to evaporation of aTHF. After overnight reaction, the solution as filtered through 0.2µm Teflon syringe filters to remove the sodium choride salt, and obtain a clear yellow colored SBDC solution in aTHF. The SBDC solution was transferred to a dry 25ml round bottom flask and the aTHF was evaporated using a Kugelrohr distillation apparatus under vacuum, and by slowly raising the temperature to 160°C. The purified SBDC, a highly viscous and amber-colored liquid, was diluted with appropriate amounts of anhydrous toluene (aTol, Acros, 99.9%) to facilitate removal using a microliter syringe. The SBDC solution was transferred to a dry 5ml round bottom flask, sealed with a rubber septum and parafilm, and stored in a dessicator to prevent exposure to moisture.

4.2.2 Formation of SBDC Photoiniferter Monolayers on Glass Substrates

Borosilicate glass substrates (1cm x 1cm) were cleaned by treatment with freshly prepared piranha solution (3:1 volume ratio of sulfuric acid (96%, Acros) and hydrogen peroxide (30%, Fisher)) for 1.5 hours. The substrates were then rinsed with copious amounts of deionized (DI) water, followed by pure ethanol (99.9%, Fisher) and finally dried with a N_2 gas blowgun. The substrates were individually placed in clean, dry test tubes and sealed with rubber septa. Each test tube containing the cleaned substrate was flame dried under vacuum to eliminate moisture which can degrade the SBDC silane groups and prevent monolayer formation. Two hundred microliters of SBDC solution was aspirated out using a gastight microsyringe and dissolved in

56ml of aTol in another clean and dry pear flask. 3ml of this final SBDC solution in aTol was added to each test tube containing the flame dried glass substrates. The monolayer deposition was allowed to continue at RT under N_2 gas purging for 16-18 hours. After monolayer formation, the substrates were rinsed with copious amount of pure toluene and sonicated in pure toluene for 40 minutes to remove unreacted SBDC and reaction byproducts. After sonication, substrates were again rinsed with pure toluene, dried using a N_2 gas blowgun and placed in clean and dry test tubes. The samples were baked in a vacuum oven at 100°C for 1 hour to complete the SBDC silane linking to the glass surface. Finally, test tubes were cooled and sealed with rubber septa and stored at RT until polymer grafting.

4.2.3 Graft Photopolymerization of Poly(Methacrylic acid) and Poly(2-Hydroxyethyl methacrylate)

A 100% v/v solution of either methacrylic acid (MAA, Sigma) or 2-hydroxyethylmethacrylate (HEMA, Sigma) was degassed by subjecting it to three freeze-vacuum-thaw cycles in a glass Schlenk tube sealed with a rubber septum. Four SBDC monolayer-deposited glass substrates were placed in a custom designed Teflon exposure cell. A viton o-ring (McMaster, GA) was placed around the samples, followed by a round soda lime glass window. The glass window was sealed against the o-ring by clamping down using steel plates with screws and nuts. The degassed monomer solution was then injected into the sealed reaction cell using a glass syringe. The assembly of the exposure cell and injection of monomer solution was carried out in a N_2 environment glovebox to prevent introduction of oxygen into the system. The prepared exposure cell was removed from the glovebox and placed under a Mask Aligner system (OAI, CO). Substrates were exposed to collimated 365nm UV light at a constant intensity of 25mW/cm^2 UV light for 5-15 minutes to graft poly(methacrylic) acid

(pMAA) or poly(2-hydroxyethylmethacrylate) (pHEMA) chains from the surface. After exposure the polymer-grafted samples were rinsed with copious amounts of pure ethanol and sonicated in pure ethanol for 40 minutes to remove any unreacted monomer and untethered polymer chains. Samples were dried under N_2 gas flow and stored in clean, dry test tubes sealed with septa until further use.

4.2.4 Conjugation of Noradrenalin to Grafted PMAA and PHEMA Chains

NA was covalently conjugated to –COOH groups of pMAA using carbonylimidazole (CDI) chemistry, while it was covalently conjugated to –OH groups of pHEMA using the CDI or disuccinimidylcarbonate (DSC) chemistry. A 10mg/ml solution of 1,1'-carbonyldiimidazole (CDI, 97%, Acros) or N,N-disuccinimidyl carbonate (DSC, ≥95%, Sigma) in anhydrous dimethylsulfoxide (aDMSO, 99.9%, Fisher) or anhydrous dimethylformamide (aDMF, 99.9%, Fisher) respectively, was prepared in an oven dried round bottom flask. Specifically for the DSC chemistry, an equimolar quantity of 4-(dimethylamino)pyridine (DMAP, ≥99%, Sigma) was added to the solution. Polymer samples were individually placed in oven-dried scintillation vials and 3ml of the CDI or DSC solution was added to each vial. The vials were sealed with caps and parafilm to prevent entry of moisture. The activation was allowed to proceed on an orbital shaker at 250rpm, for 16 hours for the CDI chemistry, and 7 hours for the DSC chemistry. After activation, the samples were rinsed with 60ml of DI water and placed in wells of a 24-well tissue culture plate. One milliliter of 1mg/ml NA solution in pH 7.4 phosphate buffer was added to each well. The plate was sealed with parafilm and the conjugation was allowed to proceed at RT on an orbital shaker at 250rpm for 16-18 hours. After conjugation, the samples were rinsed with copious amounts of DI water and sonicated in pH 7.4 phosphate buffer for 30 minutes to remove unconjugated NA and reaction byproducts. Samples were rinsed again with DI water,

dried using a N_2 gas blowgun and stored in sealed test tubes at 4°C in dark until further use. NA conjugated pMAA samples and NA conjugated pHEMA samples will hereafter be referred to as pMAA-NA and pHEMA-NA, respectively.

4.2.5 Measurement of Polymer Layer Thickness Pre- and Post-NA Conjugation

The thickness of the polymer layer was measured using a Veeco Instruments Dimension 3100 Atomic Force Microscope (AFM). Measurements were performed in air, in contact mode using a silicon nitride cantilever (DNP, Veeco Probes). Before AFM scanning, a narrow strip (about 200µm wide) of grafted polymer was mechanically removed to expose the glass surface (see figure 4.1). For the AFM scans, the cantilever was moved perpendicular to the strip from the bare glass onto the polymer layer (see figure 4.1). Since the sample surface and AFM platform were not perfectly flat on the nanometer scale, the raw height data was processed using a flattening algorithm to compensate for such errors. The difference between the raw height values of the glass and polymer surface was used to calculate the absolute thickness of the polymer layer. Three measurements taken at different locations on each sample (figure 4.1) were used to calculate a mean for data analysis. All polymer grafted samples were scanned before NA conjugation to eliminate samples with excessively thin or thick polymer layers. Three pMAA and pHEMA samples were re-scanned after NA conjugation to determine the increase in thickness post-conjugation.

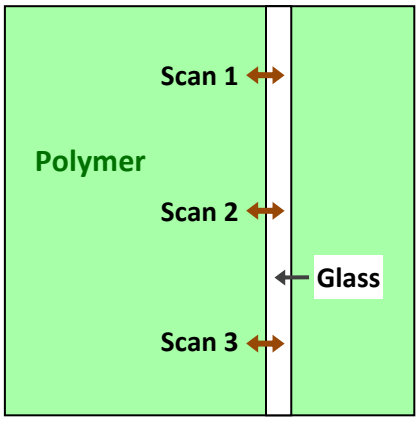

Figure 4.1 Location and direction (brown arrows) of AFM scans on polymer grafted (green) glass surfaces. White band depicts the strip where polymer was mechanically removed.

4.2.6 XPS Characterization of NA-Conjugated PHEMA Grafted Surfaces

Two experimental sample groups were used for X-ray photoelectron spectroscopy (XPS) characterization, A) pHEMA-NA samples conjugated using DSC chemistry, and B) pHEMA-NA conjugated using CDI chemistry. Control samples consisted of pHEMA surfaces subjected to the entire DSC or CDI conjugation procedure but without addition of NA. XPS characterization was performed by Dr. Joan Hudson at the Clemson University Electron Microscopy Laboratory.

4.2.7 Oyster Hemocyte Seeding on Polymer Grafted Surfaces

Experimental samples consisted of pMAA-NA and pHEMA-NA. Control samples consisted of unmodified pMAA and pHEMA grafted surfaces, as well as pMAA and pHEMA grafted surfaces taken through the entire conjugation procedure without addition of NA. All the above samples were tested for their effect on oyster hemocytes by Dr. Neeraj Gohad in Dr. Andrew Mount's laboratory in the department of the Biological Sciences at Clemson University. Hemocytes obtained from the eastern oyster *Crassostrea virginica* were added on the aforementioned surfaces and analyzed using various cell biology assays, optical microscopy and scanning electron microscopy. For detailed cell culture procedures and results please refer to "Development Of A Novel Fouling Deterrence Strategy By Understanding The Effect Of Noradrenaline On The Cells Of Eastern Oyster, *Crassostrea Virginica* And Cypris Larvae Of The Striped Barnacle, *Balanus Amphitrite*", Gohad NV, 2008, Ph.D. dissertation.[172] The procedures are briefly discussed below with permission from Dr. Neeraj V. Gohad and Dr. Andrew Mount.

4.2.8 Viability Assay

Oyster hemocytes seeded on polymer samples were treated with calcein-AM (Invitrogen) and counter stained with 4′-6-diamidino-2-phenylindole dihydrochloride (DAPI, Invitrogen). Calcein-AM is a fluorophore coupled with an acetoxymethyl (AM) ester and is not fluorescent in the calcein-AM form. However, living cells possessing esterase enzymes take up

the dye and cleave the AM moiety rendering the dye fluorescent [178]. Samples were analyzed using a Carl Zeiss Axiovert-135 (Carl Zeiss, Inc.) inverted microscope and a Nikon Eclipse TiE microscope with appropriate filter sets for Calcein-AM and DAPI, and equipped with a 40X oil immersion objective. Images were taken using a CoolSnap HQ2 (Roper Scientific) camera for the Nikon TiE microscope, and a Carl Zeiss Axiocam MRC-5 camera for the Zeiss Axiovert-135 Microscope.

4.2.9 Cytoskeletal Assay

Oyster hemocytes seeded on experimental and control samples were fixed with a 4% paraformaldehyde solution. Cells were permeabilized with a 0.1% Triton-X 100 solution followed by treatment with FITC-phalloidin (Sigma-Aldrich). Cells were counterstained with DAPI, and fluorescence microscopy was performed as described in the viability assay.

4.2.10 Apoptosis Assay

Samples were prepared as described in the cytoskeletal assay. Samples were analyzed using the Vybrant Apoptosis Assay Kit #11 (Invitrogen). Cells were first treated with the mitochondrial dye MitoTracker Red followed by incubation with Alexa Fluor 488 Annexin-V in a annexin binding buffer. Fluorescence microscopy was performed as described previously.

4.2.11 Analysis of Cell Structure by Scanning Electron Microscopy

Hemocytes seeded on experimental and control samples were prepared for SEM analysis and imaged using Hitachi Field Emission S4800 and Hitachi S3400 scanning electron microscopes.

4.2.12 Anti-Noradrenalin Antibody Treatment

To determine if the covalently conjugated NA molecules are indeed responsible for inducing apoptosis in adhering hemocytes, pHEMA-NA substrates were incubated with anti-

noradrenalin antibody (Advanced Targeting Systems). This was followed by seeding oyster hemocytes and analysis using the viability assay described previously. Control samples consisted of unmodified pHEMA substrates, and pHEMA substrates taken through both the CDI and DSC conjugation procedure without addition of NA.

4.3 Results

4.3.1 Formation of SBDC Monolayer on Glass

Instead of physisorption, the SBDC iniferter was covalently attached to the glass surface using silane chemistry. Polymer chains that are initiated by these iniferter molecules will also be covalently tethered to the surface, thus facilitating sonication to remove unreacted monomer and untethered chains. More importantly, this allowed sonication after the NA conjugation procedure to remove unconjugated NA molecules, which could produce false positive results during cell culture.

4.3.2 Graft Photopolymerization of PMAA and PHEMA

Oxygen is a very powerful radical scavenger, which can drastically slow down or even halt radical polymerization reactions.[179] To prevent this from occurring, dissolved oxygen was removed from the monomer by subjecting it to four freeze-vacuum-thaw cycles, a very effective method to remove gases dissolved in liquids.[180] Furthermore, assembly of the airtight Teflon exposure cell and monomer injection was carried out in a glovebox where the oxygen concentration was maintained at less than 30ppm.

On exposure to UV light the disulfide bond of the SBDC iniferter molecules tethered to the glass surface split to create a reactive carbon radical on the surface and a less reactive floating dithiocarbamate (DTC) radical.[57] In the presence of acrylated monomer the surface tethered carbon radical initiates free radical polymerization to graft polymer chains from the

surface.[55-57, 149] Figure 4.2 shows a schematic of this grafting process, with a large number of such chains simultaneously growing from the surface to form the polymer layer.[57] For this study, the acrylated monomers used were MAA and HEMA which resulted in grafting of pMAA and pHEMA chains respectively from glass surfaces. Crosslinking and ensuing gel formation on the surface was never observed at the exposure times used for grafting. This most likely happened because both MAA and HEMA have limited susceptibility to chain transfer. In contrast, preliminary studies with acrylated poly(ethylene glycol) (PEG) consistently resulted in crosslinking and gelation (data not shown).[154, 181]

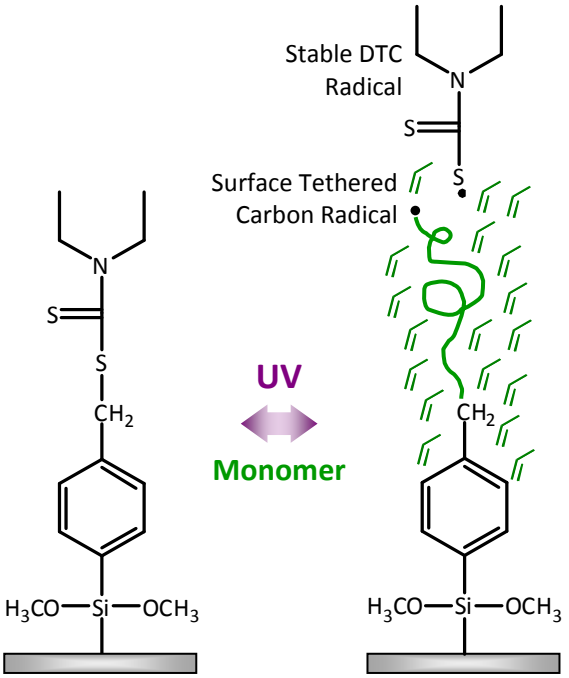

Figure 4.2 Growth of polymer chains from glass surface initiated by a surface tethered carbon radical generated on exposure of SBDC to UV.

4.3.3 Measurement of Grafted Polymer Layer Thickness Using AFM

Previous studies have shown that polymer layer thickness can be controlled by changing several parameters including exposure time and monomer concentration.[55, 56] Even though photopolymerization was carried out under controlled conditions keeping all variables constant, initial studies revealed that inconsistencies in the polymer thickness were introduced due to human and experimental errors. Therefore, thickness measurements needed to be carried out to screen samples and discard ones with inconsistent thickness values. The upper and lower limits for usable polymer layer thickness were set to 30nm and 100nm respectively. Ellipsometry

is the most commonly used technique to measure surface layer thickness in the nanometer range because of its non-destructive nature. Unfortunately, the transparent and non-reflective nature of glass prevented use of ellipsometry for thickness measurement. Therefore, AFM was chosen, as it provides equal, if not better, accuracy in measurement of surface layer thickness in the nanometer scale. For determination of absolute thickness of any surface layer using AFM, the difference between the raw height values of the upper and lower surface level is required. Since glass surfaces were completely covered with polymer chains, it was necessary to remove polymer from a small region to facilitate measurement of raw height values of the lower glass level and the higher polymer level. Removal of polymer was restricted to a thin strip of about 200μm to preserve the remaining area covered with polymer chains for further processing and/or cell culture.

4.3.4 Conjugation of NA to Grafted PMAA and PHEMA Chains

MAA and HEMA were selected as the monomers for graft photopolymerization as they provided carboxylic acid (–COOH) and hydroxyl (–OH) functional groups for covalent conjugation of the primary amine $–NH_2$ on NA molecules using suitable chemistries. Other studies have successfully demonstrated covalent conjugation of small molecules to functional groups of polymer chains grafted from a surface.[55, 158] Accordingly, NA was conjugated to pMAA using CDI chemistry (figure 4.3A), and to pHEMA using either the CDI (figure 4.3B) or the DSC chemistry (figure 4.3C).[182]

It should be noted that CDI and DSC molecules themselves, as well as the activated states of –COOH and –OH groups are prone to hydrolysis.[182] Exposure to moisture was minimized by using anhydrous organic solvents for the activation step, and drying all glassware and tools in a vacuum oven at 100°C prior to use. Coupling of –COOH to $–NH_2$ using CDI lead to

formation of the very stable amide bond, while coupling of –OH to $–NH_2$ using either CDI or DSC lead to formation of the very stable urethane bond.[182] Before further characterization or oyster hemocyte experiments, all samples were sonicated for 30 minutes to ensure removal of any unconjugated NA molecules from the surface.

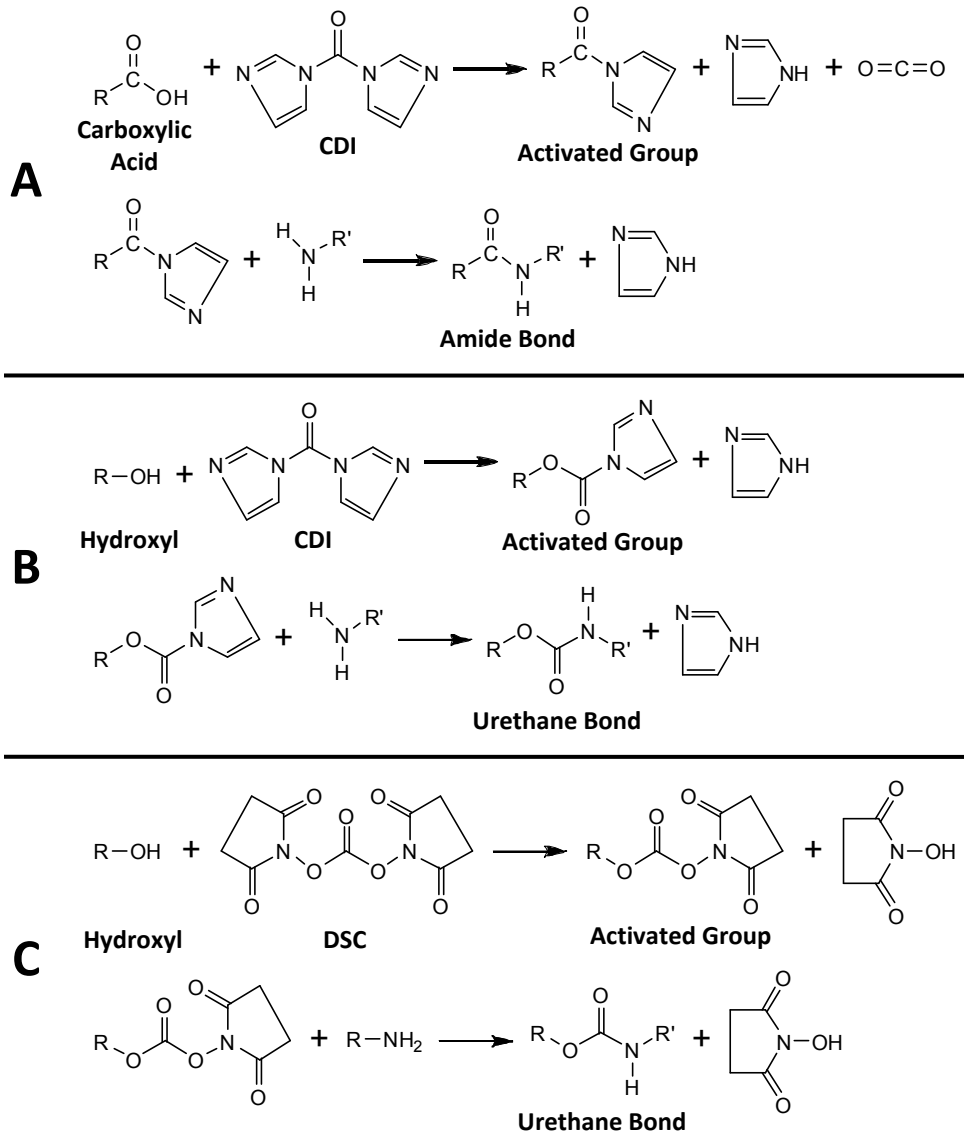

Figure 4.3 Covalent coupling of primary amine $–NH_2$ on NA molecules to (A) Carboxylic acid groups –COOH using CDI, (B) Hydroxyl groups –OH using CDI, and (C) Hydroxyl groups –OH using DSC.

4.3.5 Measurement of Polymer Layer Thickness After NA Conjugation Using AFM

As has been demonstrated previously, conjugation of small molecules to grafted polymer chains leads to an increase in thickness of the polymer layer due to added steric hindrance.[55, 158] A similar effect was seen on conjugation of NA to grafted pHEMA chains using the DSC and the CDI conjugation chemistry (figure 4.4). However, when NA was not added during the DSC conjugation procedure, a very small increase in thickness was observed (figure 4.4). A similar result was obtained for the CDI conjugation procedure without addition of NA (data not shown). Ideally, this increase in thickness would be absent since nothing was added to couple to the polymer chains activated by DSC. It is possible contaminants were introduced during the conjugation procedure, which caused the slight increase in thickness. However, this contamination did not seem to have any effect on the oyster hemocytes, and was evident from the cell culture results on control samples discussed below. This was the first piece of evidence that NA had been successfully conjugated to the grafted pHEMA chains.

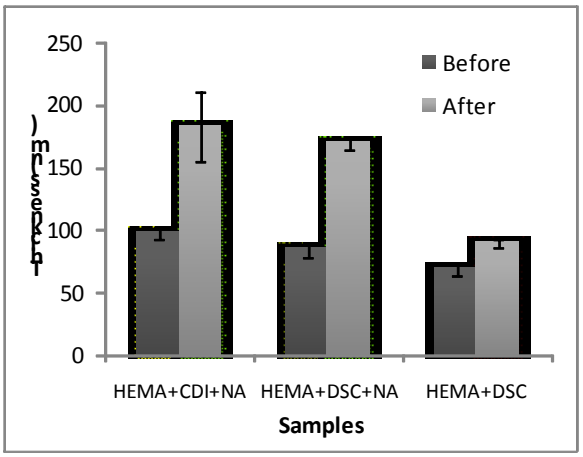

Figure 4.4 AFM thickness measurements of pHEMA layers before and after NA conjugation using CDI and DSC.

4.3.6 XPS Characterization of PHEMA-NA Surfaces

Conjugation of NA to polymer was further confirmed by XPS analysis, which provided elemental analysis of the sample surface. A nitrogen peak was observed in the XPS spectra of only pHEMA-NA surfaces using either the CDI (figure 4.5A) or DSC (figure 4.5B) chemistry. This nitrogen peak was absent in XPS spectra of control surfaces from both CDI (figure 4.5A) and DSC

(figure 4.5A) sample groups. The polymer backbone of pHEMA does not contain any nitrogen atoms, only carbon, oxygen and hydrogen which was confirmed by their peaks in the XPS spectra of all samples (figure 4.5). The only way nitrogen could have been introduced into the polymer chains was via successful coupling of the $-NH_2$ group of NA molecules to functional groups on pHEMA (figure 4.3).

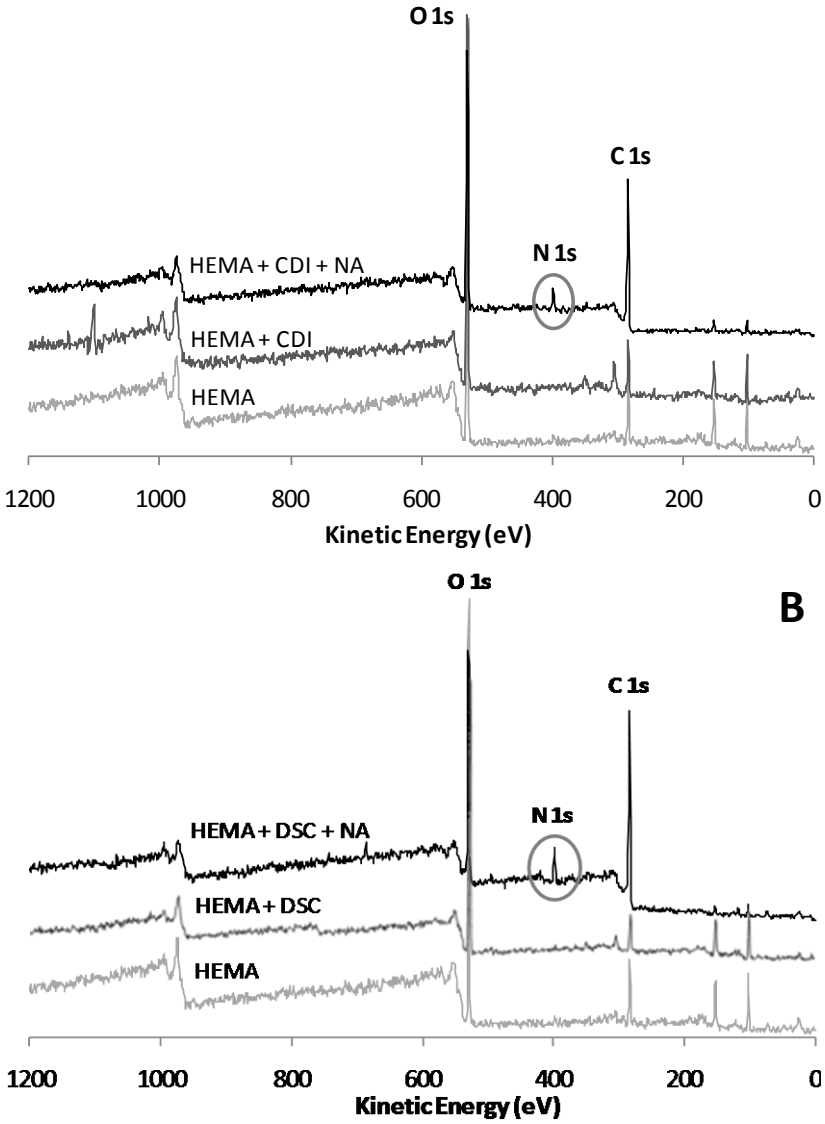

Figure 4.5 XPS characterization of NA conjugated substrates. Comparison between XPS spectra of the samples from the (A) CDI chemistry group, and (B) DSC chemistry group. In both cases, nitrogen peak (inset oval) was only observed on the NA-conjugated surfaces and was absent from all the control surfaces.

The AFM and XPS measurements above verified conjugation of NA to pMAA and pHEMA chains. However, verification was required that the conjugated NA molecules were accessible and bioactive to produce a response from cells. To test this, NA conjugated and control samples were given to Dr. Neeraj Gohad in Dr. Andrew Mount's laboratory. The obtained results are described in brief

below with permission from Dr. Neeraj Gohad and Dr. Andrew Mount. For an in-depth analysis of the effect of NA-conjugated surfaces on oyster hemocytes please refer to "Development Of A Novel Fouling Deterrence Strategy By Understanding The Effect Of Noradrenaline On The Cells Of Eastern Oyster, *Crassostrea Virginica* And Cypris Larvae Of The Striped Barnacle, *Balanus Amphitrite*", Gohad NV, 2008, Ph.D. dissertation.[172]

4.3.7 Viability Assay of Hemocytes on NA-Conjugated Polymer Surfaces

DAPI can only enter and label nuclei of cells with compromised membranes. On the other hand, only live cells with active esterases can cleave calcein-AM into its fluorescent form after internalization. Since hemocytes adhering to the control surfaces labeled positive for calcein-AM and failed to label for DAPI (figure 4.6A), unmodified polymer did not exert any deleterious effects on the adhering cells. Hemocytes adhering to pMAA-NA and pHEMA-NA did not exhibit any fluorescence from calcein-AM, but labeled positive for DAPI indicating NA-conjugated surfaces negatively affect the viability of hemocytes.[172]

4.3.8 Cytoskeletal Assay of Hemocytes no NA-Conjugated Polymer Surfaces

Structure of the cytoskeleton is a very good indicator of the cell's health and viability. A very diffuse pattern of actin filaments without fragmentation was observed in hemocytes seeded on control samples (figure 4.6B). On the other hand, fragmentation of actin filaments and disruption of the cell structure was observed in hemocytes seeded on pMAA-NA and pHEMA-NA surfaces (figure 4.6C). Loss of nuclei from some hemocytes was also observed indicating an advanced degree of cytoskeleton degradation.[172] These results show that pHEMA-NA and pMAA-NA polymer surfaces induce significant cytoskeletal degradation in adhering hemocytes.

4.3.9 Apoptosis Assay of Hemocytes on NA-Conjugated Polymer Surfaces

The calcein-AM and DAPI results above indicated that NA-conjugated surface have destructive effects on hemocyte viability, but it was necessary to confirm the trigger of apoptosis in these cells. MitoTracker red stains mitochondria in live cells and is an indicator of

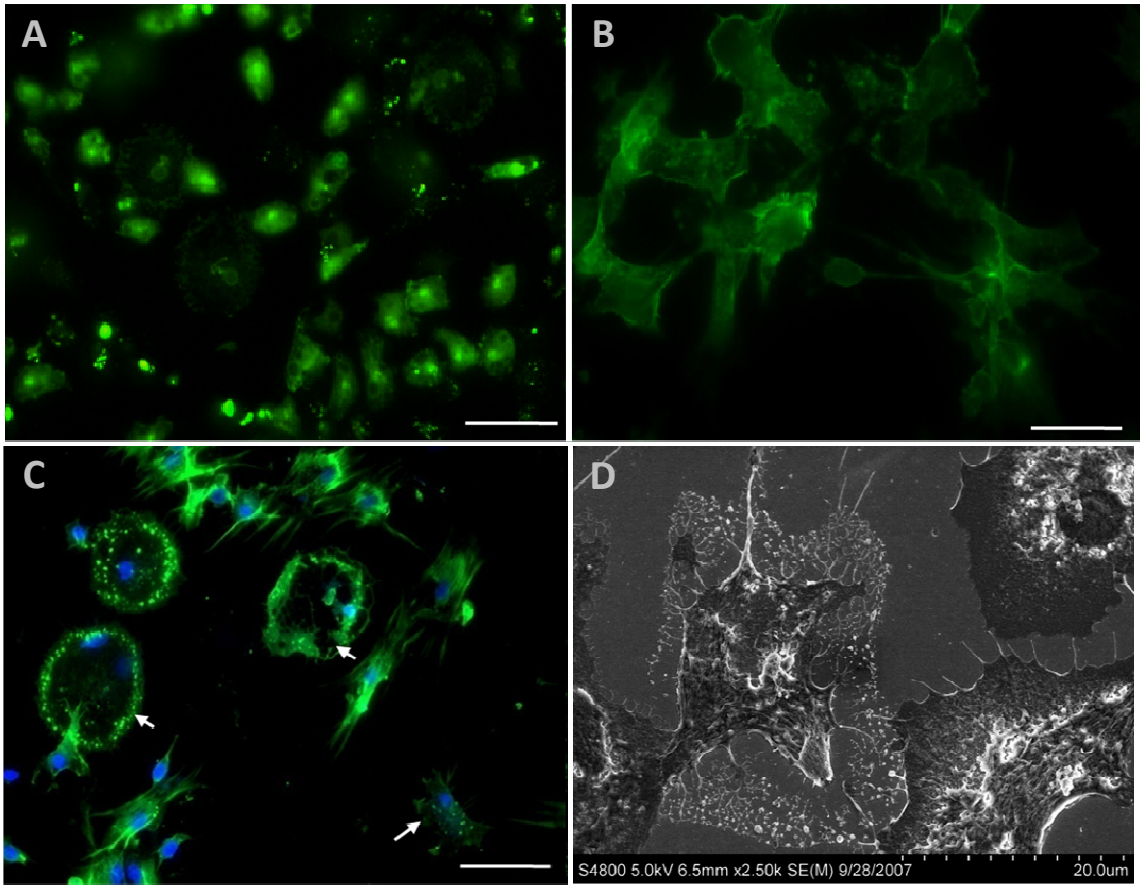

Figure 4.6 Representative micrographs of the effects of NA-conjugated polymer surface on the viability and cytoskeletal structure of hemocytes. A) Hemocytes incubated on control surfaces labeled with calcein-AM (green fluorescence) but not DAPI indicating they are healthy and viable. B) Hemocytes incubated on control surfaces and labeled with FITC-phalloidin (green fluorescence) show a very diffused cytoskeletal structure. C) Hemocytes incubated on pHEMA-NA polymer surfaces and labeled with FITC-phalloidin and DAPI (blue fluorescence) showed pronounced cytoskeletal fragmentation with abnormal morphologies (arrows). D) SEM micrograph of hemocytes incubated on pMAA-NA surfaces showing pronounced structural disintegration. Scale bars: A and C = 15µm; B = 10µm. Images reproduced with permission from Dr. Neeraj Gohad and Dr. Andrew Mount in the department of Biological Sciences at Clemson University.

mitochondrial activity, which would be absent in apoptotic cells. On the other hand, apoptosis results in the translocation of the membrane phospholipid phosphatidylserine (PS) from the inner to the outer leaflet of the plasma membrane. This exposed PS can bind Annexin V with a high affinity. Similar to the calcein-AM results, intense red staining was observed in hemocytes seeded on control surfaces indicating mitochondrial activity.[172] These cells further failed to label for Annexin-V indicating an absence of apoptosis. MitoTracker labeling was absent, while intense Annexin-V labeling was observed in hemocytes seeded on pMAA-NA surfaces indicating that the cells had undergone apoptosis.[172] Since cells were healthy and viable on unmodified polymer surfaces, the observed apoptosis can only be attributed to interaction of hemocytes with NA-conjugated to the polymer chains. Similar results were obtained for hemocytes incubated on pHEMA-NA surfaces (data not shown).

4.3.10 Analysis of Cell Structure by Scanning Electron Microscopy

Just like fragmentation of the actin cytoskeleton, the cell membrane will also undergo structural disintegration in apoptotic cells. To visualize and verify this disruption of cell membranes and cell structure, hemocytes seeded on NA-conjugated and control samples were analyzed using scanning electron microscopy. Hemocytes incubated on pMAA-NA surfaces exhibited abnormal morphology, with disintegration or blebbing of the cell membranes towards the periphery of the cells (figure 4.6D). Cells incubated on pHEMA-NA surfaces exhibited similar effects.[172] Conversely, hemocytes seeded on control surfaces exhibited a normal morphology, with intact cell membranes and cells spreading over the surface. [172]

4.3.11 Effect of Anti-Noradrenalin Antibody Treatment on Hemocyte Viability

All the above results have indicated a direct and extremely adverse effect of NA-conjugated polymer surfaces on hemocytes. It was required to verify that the bioactivity of

conjugated NA was the only factor responsible for the observed effects on hemocytes. If NA-conjugated surfaces are treated with an anti-NA antibody, the antibody should bind to the NA molecules thus blocking their bioactivity. When pHEMA-NA surfaces were treated with an anti-NA antibody, adhering hemocytes displayed calcein-AM staining but lack of DAPI staining, indicating they were viable.[172] These cells did not show fragmentation of the actin cytoskeleton and had intact cell membranes.[172] These results were similar to those obtained on control surfaces with unmodified polymer, but exactly opposite of the results on NA-conjugated surfaces. Conversely, pHEMA-NA surfaces not treated with the anti-NA antibody resulted in absence of calcein-AM labeling but presence of DAPI labeling, indicating that the cells were not viable and had compromised cell membranes.[172] These cells also exhibited an abnormal morphology with fragmentation of the actin cytoskeleton as well as disintegration and blebbing of the cell membrane.[172]

4.4 Conclusions

The conjugation chemistries used in this study were very effective in immobilizing NA to pMAA and pHEMA chains grafted from glass surfaces. The significant increase in height measured using AFM and detection of the nitrogen peak in XPS scans for NA-conjugated samples, but not control samples clearly indicated successful conjugation of NA. When oyster hemocytes were seeded onto NA-conjugated surfaces, they underwent apoptosis as observed by absence of calcein-AM staining and the apoptosis assay. The apoptosis was further associated with significant cytoskeletal degradation as observed by phalloidin staining and SEM analysis. None of the control surfaces without NA were able to produce such destruction, with the cells remaining healthy and viable. These cell-based assays demonstrate that the accessibility and bioactivity of immobilized NA was retained, and the surface concentration was

high enough to produce such pronounced results. Furthermore, all NA-conjugated samples were sonicated and extensively washed before cell culture. This proved the robustness of the grafted polymer layer, excellent stability of covalent conjugation bonds, and absence of nonspecifically bound NA that could have produced false positive results. Studies are currently in progress to assess the effect of these NA conjugated polymer surfaces on oyster and barnacle larvae as the next step to develop a non-toxic and environmentally friendly antifouling strategy.

5. Controlling Cell Behavior Using Bioactive Polymer-Grafted Surfaces

5.1 Introduction

One of the goals of biomedical engineering is to restore functioning of or regenerate biological tissues and organs to alleviate debilitating and/or deadly disease conditions such as myocardial infarction, spinal cord injury, osteoarthritis, osteoporosis, diabetes, liver cirrhosis and retinopathy. In some cases, implantation of a device inside the body can completely or partially restores the tissue or organ function. For example, coronary stents have been used since the 1980s to open arteries occluded by plaque formation to restore blood supply to the heart and prevent infarction. Unfortunately, the stainless steel stents used in this strategy have long encountered problems with thrombotic vascular occlusion and intimal hyperplasia (IH) leading to long-term failure of the device.[80] Coating the stent material with antiproliferative agents has yielded limited success.[80] The focus has therefore shifted to promote endothelialization, since the native endothelium actively functions to prevent thrombosis inside healthy blood vessels.[81, 82] Endothelialization however, requires attaching certain signaling molecules to the stent's surface, which can recruit neighboring endothelial cells to migrate, adhere, proliferate and form a healthy endothelium over the stent's surface, which will last the patient's lifespan.[81, 82] For example, a recent study reported enhanced attachment, adhesion and growth of endothelial cells on 316 stainless steel surfaces grafted with a synthesized mussel adhesive polypeptide via PEG spacer chains, compared to unmodified steel surfaces.[81]

However, some complex tissue functions cannot be restored by simple means like the one mentioned above, requiring regeneration of the diseased organ, an elaborate process commonly known as tissue engineering (TE). One current area of focus is the implantation of a biomaterial scaffold which provides the appropriate physical structure and incorporates

mechanical and biochemical cues to recruit endogenous cells. These cells can then deposit the required extra-cellular matrix, express the required proteins and assume the desired phenotype to regenerate the diseased tissue. The desired structure and mechanical properties can be obtained by selecting the appropriate material and fabrication technique. In fact, in some cases appropriate design of these two aspects is sufficient for successful tissue regeneration. The success story of Smith & Nephew's TRUREPAIR line of bioabsorbable bone graft substitutes (BGS) is one such example.[183] The BGS are made with poly(lactic acid) subjected to a special fabrication process and achieve excellent bone and cartilage tissue integration without addition of any bioactive agent.[183] Another regenerative pathway being aggressively pursued is recruiting resident stem and progenitor cells, which due to their multipotent nature can differentiate into multiple phenotypes and regenerate the diseased tissue. For example, injecting alginate or hyaluronic acid gels into a space between the tibia and the periosteum, stimulated bone and cartilage formation from resident progenitor cells in the inner layer of the periosteum.[184] In this case, the stem cells obtained all the required physical and biochemical cues from the surrounding tissue to convert into the regenerative phenotype.

Unfortunately, such simple strategies are not universal, especially in case of tissues with intrinsically low regeneration potential such as cardiac myocytes, blood vessels and central nervous system neurons. Even stem cells directly injected into infarcted heart muscle of mice did not differentiate into myocytes.[185] In these cases, a scaffold incorporating specific signaling molecules which can stimulate the desired regenerative response from native cells needs to be provided. The simplest approach is to mix biomolecules with the biomaterial during fabrication.[90] Some of these biomolecules will be present on the scaffold's surface, which the cells will recognize and produce desired responses. This strategy has met with considerable

success and many commercial products are currently available.[91] However, this technique is largely restricted to polymeric materials, and nearly impossible to achieve with ceramics and metals. Additionally, such bulk modification can adversely affect the mechanical properties of the scaffold, and has the potential to denature or degrade the biomolecule during the fabrication process.[90] An alternative approach is to attach the biomolecules to the scaffold's surface after fabrication. Since this approach will be restricted to the surface, the scaffold's bulk properties will be preserved. Furthermore, bioactivity of the biomolecules can be preserved by using well established protein conjugation techniques. In fact, some growth factors function better when covalently tethered compared to their soluble form.[91] A potential application is treatment of expanded polytetrafluoroethylene (ePTFE) and polyethylene terephathalate (Dacron) commercially used to make large diameter vascular grafts since they match the mechanical properties of native blood vessels. Unfortunately, their thrombogenic surface shortens their lifespan and prevents their usage as grafts for small diameter (<5mm) blood vessels.[82] Similar to the stent problem discussed above, efforts are under way to incorporate signaling molecules on the graft's surface which can trigger successful endothelialization after it has been implanted in the body. Some studies have been able to show increased endothelial cell (EC) adhesion and proliferation when vascular grafts are coated with specific peptide sequences like RGD and YIGSR, or whole ECM proteins like laminin.[82]

Before such strategies can yield clinical success, effects of various parameters like which biomolecule, its concentration, and its spatial and temporal distribution on the behavior of target cells need to be thoroughly studied. Axonal guidance for spinal cord regeneration exemplifies this need. A considerable amount of evidence points towards the need to control the spatial distribution of trophic factors presented to stimulate axonal regrowth.[83] This idea

stems from the fact that axonal growth cones can be guided by concentration gradients of growth factors.[84, 85] Therefore, it has become imperative to study how gradients of different trophic factors and different concentration profiles will affect axonal guidance and growth. Diffusion gradients have been attempted to stimulate axon growth, both in vitro and in vivo, but they suffer from procedural complexities and potential to cause systemic effects.[86] A number of immobilization approaches have also been tested to create concentration gradients, such as differential evaporation and microfluidics to overcome limitations of the diffusion technique.[85, 87] However, evaporation methods are very crude with little control over the gradient profile, while microfluidics techniques are restricted by small dimensions and require at least two proteins to obtain the gradient.

Development of such versatile bioactive surfaces will first require making the surface bioinert, so that the observed cell response can be attributed to only the attached biomolecules. This requires prevention of non-specific adsorption of biomolecules on the surface that have the potential to affect cell behavior and alter the results. Various polymers like poly(ethylene glycol) (PEG) and poly(hydroethyl methacrylate) (pHEMA) when coated on surfaces, have demonstrated excellent resistance to protein adsorption. Furthermore, they themselves do not possess any bioactivity, and in fact prevent any form of cell adhesion. Therefore, it will be advantageous to first create a layer of such bioinert polymers on the surface. Next, the functional groups on the polymer chains can be used to covalently couple biomolecules for analyzing cell behavior. Additionally, some procedure will have to be adopted to control the location and amount of polymer on the surface and in turn that of the covalent coupled biomolecule.

Taking all the aforementioned factors into consideration, a technique is required that,

1. facilitates modification of surface properties to prevent non-specific interactions,
2. facilitates surface modification of polymers, ceramics as well as metals,
3. facilitates covalent attachment of any biomolecule to elicit specific responses,
4. maintains accessibility and bioactivity of the attached biomolecule, and
5. facilitates creation of concentration gradients where required.

A very important point to note is that all cellular behaviors including adhesion, proliferation, differentiation, migration, protein expression, extra-cellular matrix (ECM) production and even apoptosis depend on the interaction of receptors on the cells surface with biochemical cues present in the environment. Since these interactions take place on the molecular level, the surface modification technique should also allow precise control over the concentration of any biomolecule attached on the surface.

For reasons explained previously in sections 2.1 and 3.1, surface-initiated photoiniferter-mediated polymerization (SIPMP) was selected as the surface modification technique for this study. Besides being able to create homogeneous polymer layers, thickness gradients can be easily created by varying the exposure time along the surface area.[55, 56] The goal of this study was to graft polymer layers on glass surfaces with homogeneous and gradient thickness profiles. Two polymers, pMAA and pHEMA were grafted from glass surfaces, and their thickness profiles were analyzed using atomic force microscopy (AFM). The hydrophilic nature of the pMAA and pHEMA chains will help reduce non-specific protein adsorption, as well as provide carboxylic acid –COOH and the hydroxyl –OH functional groups respectively for covalent attachment of molecules. In this study, covalent conjugation of a fluorescent dye allowed visualization of polymer thickness profile on the surface. NIH3T3 and B35 cell culture was carried out on unmodified pHEMA surfaces to test their ability to block nonspecific cellular interactions.

Preliminary attempts were also made to covalently conjugate the ECM protein fibronectin (Fn) and the neural cell adhesion protein L1 to homogeneous pHEMA layers. Fn was selected as it is a ubiquitous ECM protein containing several peptide sequences such as RGD, which can modulate cell behavior, and is extensively used for tissue regenerative applications.[186, 187] L1 was selected to eventually develop L1 gradients to guide axonal growth in scaffolds designed for spinal cord regeneration. L1 has some unique advantages over other biomolecules capable of guiding axonal growth. L1 is expressed on axons and growth cones, and stimulates axon growth and provides guidance via homophilic binding to L1 expressed on other cells.[188, 189] L1 also prevents adhesion and proliferation of non-neuronal cells such as astrocytes, meningeal cells and fibroblasts, all of which are present in at any spinal cord injury site and are associated with inhibition.[190, 191] Bioactivity and accessibility of Fn was tested by NIH3T3 fibroblast and B35 neuroblastoma cell culture, while that of L1 was tested by B35 and primary chick forebrain neuron culture. The results, limitations encountered, and alternate approaches are also discussed.

5.2 Materials and Methods

5.2.1 Synthesis Of Photoiniferter SBDC

SBDC was synthesized by adapting the protocol previously developed and tested by de Boer *et al*.[177] and is already described in detail in section 4.2.1. Briefly, the synthesis step was done in a glovebox to eliminate moisture which will react with and degrade the silane groups. Three milliliters of p-chloromethylphenyltrimethoxy silane (pCPTS, Gelest Inc., 95%) was dissolved in 5ml of anhydrous tetrahydrofuran (aTHF, 99.9%, Acros) and added drop wise to a solution containing 3.123g of sodium diethyldithiocarbamate trihydrate (NaDTC, Sigma) dissolved in 30ml of aTHF in a 100ml round bottom flask. After overnight stirring, the solution

was filtered through 0.2μm Teflon syringe filters to remove the sodium chloride salt and obtain a clear yellow colored SBDC solution in aTHF. The SBDC was purified by evaporating the aTHF using a Kugelrohr distillation apparatus under vacuum and by slowly raising the temperature to 160°C. The highly viscous amber colored SBDC was diluted with appropriate amounts of anhydrous toluene (aTol, Acros, 99.9%), and stored in a dessicator to prevent exposure to moisture that would degrade the methoxysilane groups.

5.2.2 Formation Of SBDC Photoiniferter Monolayers on Glass Substrates

A monolayer of SBDC photoiniferter was deposited on glass substrates as described previously in section 4.2.2. Briefly, 1cm x 1cm borosilicate glass substrates were cleaned with freshly prepared piranha solution for 1.5 hours. After washing with DI water and pure ethanol, substrates were dried and individually placed in clean and dry test tubes and sealed with rubber septa. The test tubes were flame dried under vacuum to eliminate moisture. Three milliliters of the SBDC solution made by dissolving 200μl of SBDC stock solution in 56 ml of aTol was added to each test tube. After monolayer deposition for 16-18 hours, the substrates were rinsed in pure toluene followed by sonication in pure toluene for 40 minutes. The washed and dried substrates were baked in a vacuum oven at 100°C for 1 hour to complete the SBDC silane linking to the glass surface. After cooling, samples were stored in clean, dry and sealed test tubes at RT until polymer grafting.

5.2.3 Graft Photopolymerization of PMAA and PHEMA

Assembly of the exposure cell, injection of the degassed monomer solution, and use of the mask aligner system has already been described in detailed in section 4.2.3. Homogenously grafted polymer surface were created as described previously. For creation of polymer thickness gradients, prior to UV exposure an opaque photomask attached to a syringe pump was aligned

to one of the substrate's edges. The syringe pump movement and UV exposure were started simultaneously so that the mask slowly moved over the substrate gradually covering more and more of the substrate's surface. The speed of the syringe pump was set so that the mask moving over the sample would completely cover it at the end of the desired exposure time of 5-15 minutes. After exposure, the polymer-grafted samples were rinsed with copious amounts of ethanol and sonicated in ethanol for 40 minutes to remove any unreacted monomer and untethered polymer chains. Samples were dried under N_2 gas flow and stored in clean, dry test tubes until further use.

5.2.4 Characterization of Grafted PMAA and PHEMA Layers Using AFM

The thickness was the polymer layer was measured using a Veeco Instruments Dimension 3100 Atomic Force Microscope (AFM). Measurements were done in air in contact mode using a silicon nitride cantilever (DNP, Veeco Probes). The sample preparation, scanning and data analysis procedure has been described previously in section 3.2. Figure 5.1 shows the scan locations for homogeneous and gradient polymer samples. In case of gradients, the first scan was done 1mm from the lower end of the gradient, followed by scans at intervals of 2 mm thereafter till the opposite edge of the sample was reached (figure 5.1). All polymer grafted samples were scanned before conjugation to eliminate samples with excessively thin or thick polymer layers.

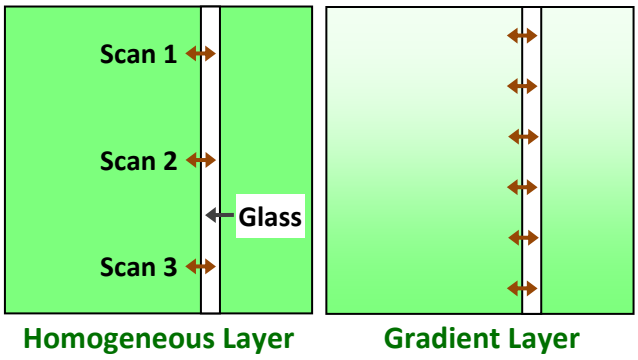

Figure 5.1 Location and direction (brown arrows) of AFM scans on homogeneous and gradient polymer grafted glass surfaces. White band depicts the strip where polymer was mechanically removed.

The mean thickness values of several homogeneous samples grafted under identical conditions were subjected to a one-way ANOVA with the significance cutoff set to $p < 0.05$. This was done to determine the reproducibility of the SIPMP technique. Similarly, mean thickness values at each exposure time obtained from several gradient samples grafted under identical conditions were subjected to a one-way ANOVA with the significance cutoff set to $p < 0.05$. This verified if polymer thickness gradients were indeed created on the surface.

5.2.5 Covalent Conjugation of Dansylcadavarine to Visualize Homogeneous and Gradient PMAA Layers

The fluorescent dye dansylcadavarine (DCAD) was conjugated to the carboxylic acid -COOH groups on the pMAA chains using acyl-halide chemistry, illustrated in figure 5.2. Homogeneous or gradient pMAA grafted samples were individually placed in oven dried test tubes, sealed with rubber septa and kept under N_2 gas purging. A 3% w/v solution of phosphorus pentachloride (PCl_5, ≥98%, Sigma) was prepared in anhydrous dichloromethane (aDCM, 99.5%, Acros) and 3ml of this solution was added to each test tube containing the sample. The conversion of carboxylic acid groups of pMAA to acid chloride was allowed to continue for 3 hours at RT. The samples were then rinsed with copious amounts of pure DCM and sonicated in aDCM for 15 minutes to remove unused PCl_5 and reaction

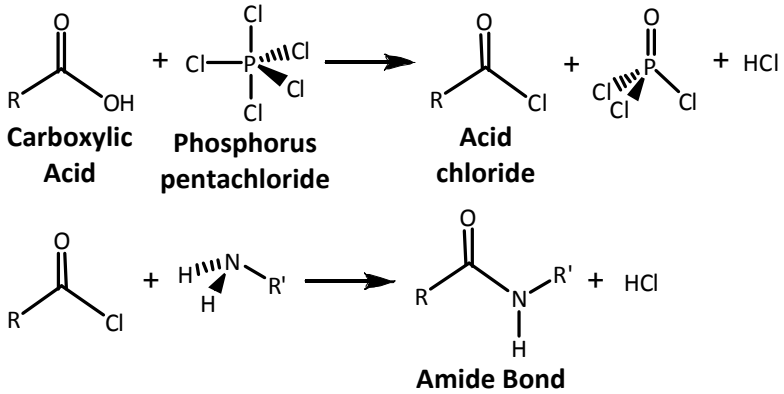

Figure 5.2 Covalent coupling of primary amine $–NH_2$ on DCAD molecules to carboxylic acid –COOH groups using the acid-halide chemistry.

byproducts. Samples were then individually placed in clean oven dried test tubes, sealed with rubber septa and purged with N_2 gas. Three milliliters of 1mg/ml DCAD solution in aDCM was added to each test tube and allowed to react for 16-18 hours in dark. The samples were then rinsed with copious amounts of pure DCM and sonicated in pure DCM for 30 minutes in dark to remove reaction byproducts, and DCAD molecules physically adsorbed on the surface. The samples were dried with a N_2 blow gun and stored in dark to prevent photobleaching of the conjugated DCAD molecules.

DCAD conjugated homogeneous and gradient pMAA grafted samples were observed using a Nikon SMZ-1500 dissection microscope equipped with a suitable filter for excitation (λ_{ex} = 335nm) of DCAD and visualizing the emitted light (λ_{em} = 508nm). Images were taken using a digital color camera attached to the microscope.

5.2.6 Covalent Conjugation of Proteins to PHEMA-Grafted Surfaces

One of two proteins, fibronectin (from bovine plasma, 1mg/ml, in 0.5 M NaCl, 0.05 M Tris, pH 7.5, Sigma) or recombinant human L1 (expressed and purified in our lab as described by Cribb et al., 2008 [192]) was covalently conjugated to grafted pHEMA using two different chemistries. The first one was the DSC chemistry, which couples primary amines $–NH_2$ on the protein molecules to the hydroxyl –OH functional groups on the pHEMA chains (figure 5.3A). The second one was thiol-acrylate chemistry, which couples thiol –SH groups on reduced protein molecules to acrylate groups created on the pHEMA chains (figure 5.3B). Prior to use, all glassware and equipment used for the conjugation procedure, like scintillation vials, caps, 10ml glass syringe, steel needle and spatula were sterilized by autoclaving at 121°C for 60 minutes. After the sterilization procedure, the autoclaved packet was placed in a vacuum oven at 100°C

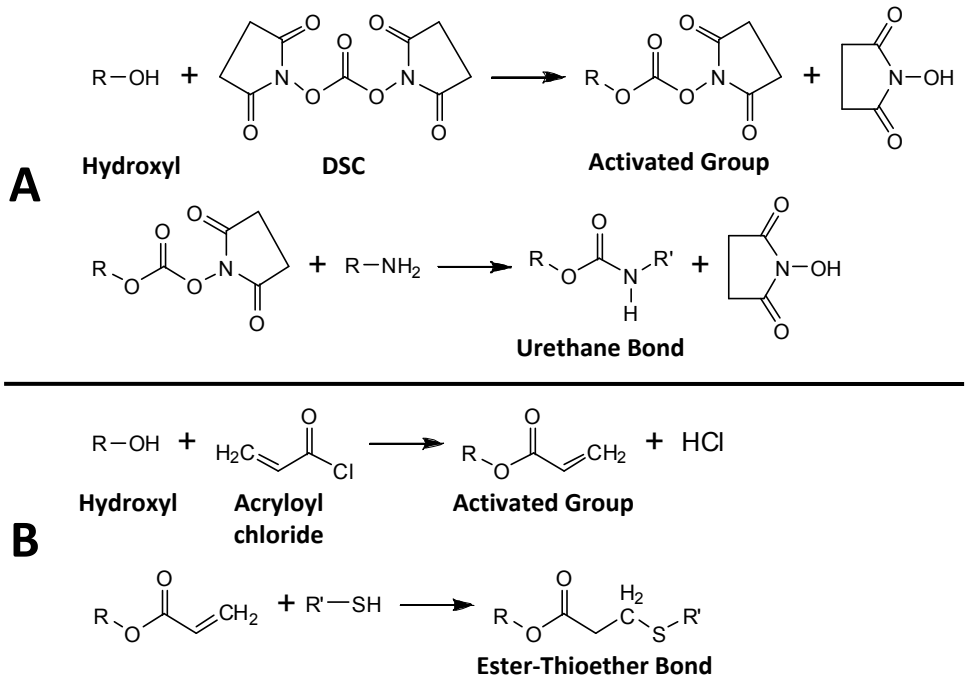

Figure 5.3 Conjugation chemistries used to covalently attach proteins to grafted pHEMA chains. Hydroxyl –OH groups were coupled to (A) primary amine $–NH_2$ groups on protein molecules using the DSC, and (B) Thiol –SH groups on reduced protein molecules using the thiol-acrylate chemistry.

for at least 1 hour, taking care not to damage the packet which would have resulted in loss of sterility.

The following procedure was carried out under aseptic conditions in a biological safety cabinet right until the vials were sealed and placed on the orbital shaker, which was outside the hood. For DSC conjugation, a 10mg/ml solution of N,N'-disuccinimidyl carbonate (DSC, ≥95%, Sigma) in anhydrous dimethylformamide (aDMF, 99.9%, Fisher) was prepared in an oven dried round bottom flask. An equimolar quantity of 4-(dimethylamino)pyridine (DMAP, ≥99%, Sigma) was also added to the solution. For acrylate-thiol conjugation, a 5µl/ml solution of acryloyl chloride (AC, 97%, Sigma) in aDMF was prepared in an oven dried round bottom flask. An equimolar quantity of triethylamine (TEA, 99.7%, Acros) was also added to the solution. pHEMA

samples were individually placed in oven dried scintillation vials and 3ml of the DSC or AC solution was added to each vial. The vials were sealed with caps and parafilm to prevent entry of moisture. The activation was allowed to proceed on an orbital shaker at 250rpm at room temperature (RT) for 6 hours for DSC activation, and for 4 hours for AC activation. After activation, the vials were again taken into the biological safety cabinet to maintain aseptic conditions. The samples were removed from the vials and rinsed with 60ml of deionized (DI) nanopure water to wash away the organic solvent, excess reagents and reaction byproducts. The samples were placed in wells of a 24-well .

For DSC conjugation the proteins were used in their normal condition. Fibronectin or L1 was dissolved in sterile pH 7.4 50mM phosphate buffer (PB) at a concentration of 25µg/ml. Six hundred microliters of the protein solution was added to each well containing the sample. The lid was placed on the plate and it was sealed with parafilm. The reaction was allowed to proceed on an orbital shaker at 230rpm at RT for 16-18 hours. For acrylate-thiol conjugation, the disulfide bonds in the protein molecules needed to be reduced to obtain free thiol –SH groups, which could react to the acrylate groups present on the pHEMA chains after activation. First, a solution of D,L-1,4-dithiothreitol (DTT, ≥99%, Acros) was prepared at a concentration of 3.9mg/ml in sterile PB. About 4µl of the DTT solution was added for every 100µl of protein solution to be reduced. The reduction was allowed to proceed at RT on an orbital shaker for 1 hour. The reduced protein solution was then purified by passing it through a spin desalt column (for <130µl, ZEBA 0.5ml column, Pierce; for >130µl, PD-10 column, GE) in a centrifuge at 1000g for 1-2 minutes and collected in a 1.5ml microcentrifuge tube. 75µl of this reduced protein solution was transferred to a UV transparent 96-well plate. Light absorbance of the solution was measured at 280nm using a spectrophotometer. The obtained absorbance value was compared

to a pre-determined standard concentration curve to determine the concentration of the purified reduced protein solution. Finally, the protein was diluted in sterile PB to a final concentration of 25µg/ml. 600µl of the protein solution was added to each well containing the sample. The lid was placed on the plate and it was sealed with parafilm. The reaction was allowed to proceed on an orbital shaker at 230rpm at RT for 16-18 hours.

After conjugation, the protein solution was removed and each sample was rinsed three times with 1ml of sterile PB. The samples were then washed in 1ml of sterile PB on an orbital shaker at 230rpm for 10 minutes. The above rinsing and washing procedure was repeated one more time. Finally, the samples were stored in sterile 1x PBS until further use.

5.2.7 Control Samples

To verify that only the protein conjugated to pHEMA was responsible for any observed cell adhesion, a set of controls were prepared with both the DSC and the acrylate-thiol chemistry. Table 5.1 shows all the control samples prepared and used for cell culture analysis (Detailed description of the samples is provided in Results and Discussion below).

Table 5.1 List of control samples that were prepared for cell culture analysis by subjecting pHEMA grafted surfaces to DSC or thiol-acrylate conjugation procedure under various conditions.

Sample Label	Details	Activation[1]	Conjugation[2]	Challenge[3]	Washing[4]
HaF/HaL	pHEMA+a[5]Fn/aL1	-	-	Fn or L1	-
HD	pHEMA+DSC	DSC	PB	-	-
HDaF/HDaL	pHEMA+DSC+aFn/aL1	DSC	PB	Fn or L1	-
HDaFT	pHEMA+DSC+aFn+Triton	DSC	PB	Fn or L1	Yes
HA	pHEMA+AC	AC	PB	-	-
HAaF	pHEMA+AC+aFn	AC	-	Unreduced Fn[6]	-
HAaFT	pHEMA+AC+aFn+Triton	AC	-	Unreduced Fn	Yes
HAM	pHEMA+AC+ME[7]	AC	ME	-	-
HAMaF	pHEMA+AC+ME+aFn	AC	ME	Unreduced Fn	-
HAMaFT	pHEMA+AC+ME+aFn+Triton	AC	ME	Unreduced Fn	Yes

1 Activation was done as described in previously;
2 Conjugation step was done for 16-18 in PB as described previously, with or without addition of ME;
3 Non-specific protein adsorption test. Samples treated with protein solution for 6 hours;
4 Samples washed in 0.1% triton-X 100 solution on an orbital shaker at 230 rpm for 2 hours;
5 a: Polymer surface challenged with protein adsorption;
6 Fn was not reduced, so –SH groups were absent;
7 ME: Mercaptoethanol, which couples to acrylate groups via its –SH group

5.2.8 Seeding of NIH3T3 Fibroblasts and B35 Neuroblastoma Cells

All cell culture procedures were carried out under aseptic conditions in a biological safety cabinet to prevent contamination. Experimental and control samples were already sterile after treatment with aDMF during the conjugation procedures. Any samples used for cell culture but not subjected to the conjugation procedure were sterilized by immersing in 70% ethanol for 1 hour followed by rinsing with sterile DI water three times. The samples were transferred to wells of a sterile 24-well tissue culture polystyrene (TPS) plate for cell seeding.

NIH3T3 fibroblasts or B35 cells used for seeding were grown in 75cm^2 TPS T-flasks in Dubelco's Modified Eagle Medium-Ham's F-12 Mixture (DMEM/F12, Mediatech) with L-glutamine, and supplemented with 10% v/v of bovine growth serum (BGS, HyClone) and 1% v/v of penicillin-streptomycin solution (50x, Mediatech). Cells were passaged once a week, and used prior to the 16th passage. The cells were detached using 4ml of trypsin solution (0.05% with 0.53mM EDTA in HBSS without sodium bicarbonate, calcium and magnesium, Mediatech) and the trypsin-cell suspension was centrifuged at 1000rpm for 5 minutes to obtain a cell pellet. The supernatant trypsin solution was slowly aspirated out taking care the cell pellet was not removed as well. The cell pellet was disassociated and cells were resuspended in 10ml of fresh media. The cell concentration was determined using a hemocytometer and cells were seeded at

a concentration of 15,000 cells per sample per ml. The plate was placed in a sterile CO_2 incubator at 37°C to allow cells to adhere to the sample surface.

For fixation, the samples were carefully removed using sterilized forceps and gently placed in another well containing 4% paraformaldehyde solution in 1x PBS. Cells were fixed for 1 hour and then rinsed thrice with staining media (1x PBS with 5% BGS and 1% sodium azide). Samples were incubated in 0.1% triton X-100 (Sigma) solution in 1x PBS for 3 minutes followed by washing thrice with staining media. Samples were then placed in a rhodamine phalloidin (Invitrogen) solution for 60 minutes in the dark to label the actin filaments in the cell cytoskeleton. Samples were washed trice with staining media and placed in DAPI (Invitrogen) solution for 3 minutes to stain the cell nuclei. Samples were finally rinsed thrice with staining media and stored under staining media. Cells were observed using a Nikon AZ-100 microscope and a Nikon LV-UDM upright microscope, both equipped with filters suitable for visualizing rhodamine phalloidin and DAPI. Imaged were obtained using a Nikon DS-Ri1 digital color camera attached to the microscopes.

5.2.9 Seeding of Chick Forebrain Neurons

Forebrain neurons were isolated from day 8 white leghorn chicken embryos as previously described[193] and seeded on unmodified pHEMA surfaces, and pHEMA surfaces conjugated with L1 using the DSC and the thiol-acrylate chemistry. The neurons were seeded at a density of 120,000 cells per sample in Basal Medium Eagle (BME, Gibco) supplemented with 6 mg/mL glucose (Sigma), 1% of antibiotic/antimycotic 100x stock solution (Gibco), 10% of fetal bovine serum (FBS, Invitrogen), and 2mM L-glutamine (Hyclone). Cells were fixed at 24 or 48 hours in 4% paraformaldehyde for 1 hour. Presence of neuron adhesion and neurite outgrowth was analyzed using a Zeiss Axiovert optical microscope in phase contrast mode.

5.3 Results and Discussion

5.3.1 Grafting of Homogeneous and Gradient PMAA and PHEMA Layers

Oxygen is a very powerful radical scavenger which can drastically slow down or even halt radical polymerization reactions.[179] To prevent this from occurring, dissolved oxygen was removed from the monomer by subjecting it to four freeze-vacuum-thaw cycles, a very effective method to remove gases dissolved in liquids.[180] Furthermore, assembly of the airtight Teflon exposure cell and monomer injection was carried out in a glovebox where the oxygen concentration was maintained at less than 30ppm. The mechanism of polymer grafting via SBDC on UV exposure has already been described in section 4.3.2. For this study, the acrylated monomers were MAA and HEMA which resulted in grafting of pMAA and pHEMA chains, respectively, from glass surfaces. Crosslinking and ensuing gel formation on the surface was never observed at the exposure times used for grafting. This most likely happened because both MAA and HEMA have limited susceptibility to chain transfer, which is a major cause of unwanted crosslinking and gelation. In contrast, preliminary grafting studies with acrylated PEG consistently resulted in crosslinking and gelation (data not shown).[154, 181]

By exposing entire substrates uniformly with UV light, a homogeneous layer of pMAA or pHEMA was grafted on the glass surface. Figures 5.5A and B show AFM thickness measurements of homogeneously grafted pMAA and pHEMA samples respectively. Every sample grafted with one particular polymer was photopolymerized under the same conditions. One-way ANOVA revealed no significant difference ($p>0.05$) between the homogeneously grafted samples of each polymer type, demonstrating the reproducibility of SIPMP.

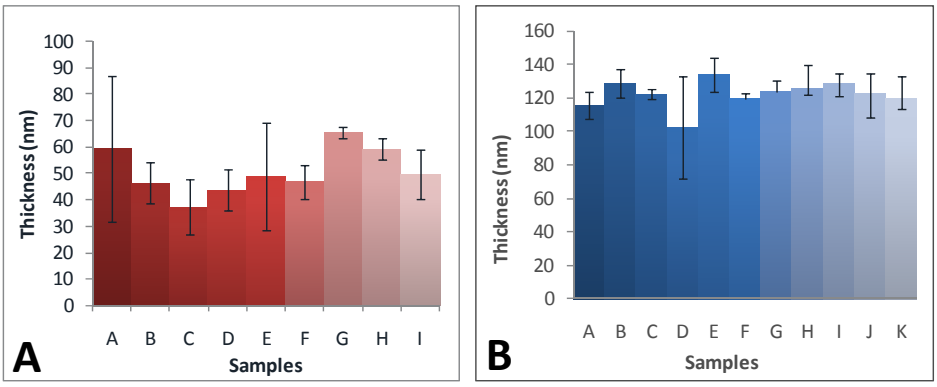

Figure 5.5 AFM thickness measurements of homogeneously grafted (A) pMAA, and (B) pHEMA on glass surfaces. No significant difference between samples of each polymer type ($p<0.05$).

To create polymer thickness gradients an opaque photomask was moved over the sample surface at a constant velocity. In other words, the polymerization time increased from one edge of the sample to the opposite, resulting in a polymer thickness gradient in the direction of photomask movement. Figures 5.6A and B show AFM thickness measurements of pMAA and pHEMA gradients respectively, again the conditions were kept constant for all samples grafted with a particular polymer. In this case a one-way ANOVA indicated a significant difference ($p<0.05$) between thickness values at successive positions (or exposure times) measured along the surface, verifying creation of a thickness gradient. As described in section

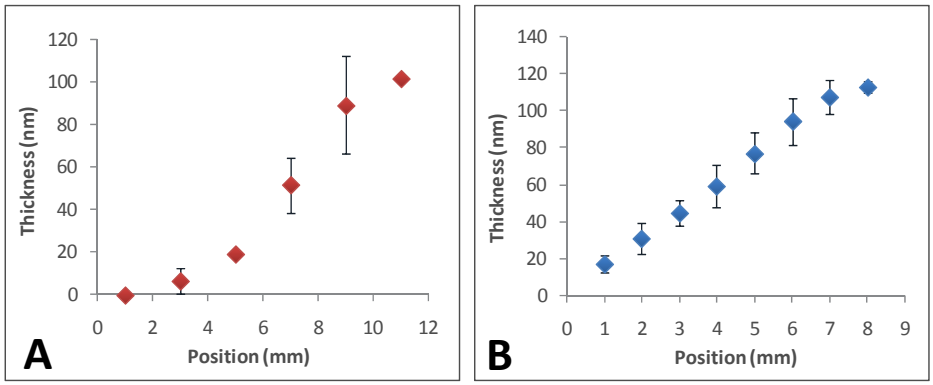

Figure 5.6 AFM measurements of thickness gradients of (A) pMAA, and (B) pHEMA on glass surfaces. There was a significant difference between successive measurements along gradient for both polymer samples ($p<0.05$).

3.2.2, increasing exposure time results in an increase in the grafted-chain density on the surface, and not MW. Thus, the thickness gradients created in this study resulted from such an increase in grafted-chain density from the lower to higher exposure time edge of the sample. At lower grafting densities, the polymer chains have more room to coil and collapse resulting in lower measured thickness values. As the grafting density increases, individual polymer chains begin to stretch out providing more space to accommodate more and more chains in the same unit area. These stretched chains result in higher measured thickness values.

pMAA and pHEMA grafted surfaces provided –COOH and –OH groups respectively for covalent conjugation of various biomolecules. While AFM measurements provided physical proof of the polymer thickness on the glass surfaces, it was imperative to show that that concentration of available functional groups follows the amount of polymer on the surface. Therefore, a small fluorescent dye, dansylcadavarine (DCAD) was covalently conjugated to the -COOH groups of pMAA chains grafted from the glass surface. DCAD was conjugated using the highly efficient acid-halide chemistry using phosphorus pentachloride (PCl_5) to activate the -COOH groups. On homogeneously grafted pMAA samples, the concentration of –COOH groups on the entire sample surface should also be homogeneous. This was demonstrated by the uniform fluorescent intensity observed

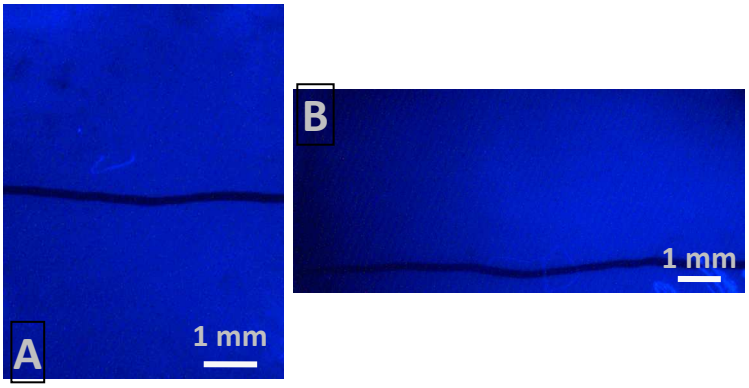

Figure 5.7 Fluorescence microscopy images of dye dansylcadaverine conjugated to (A) homogeneous, and (B) gradient pMAA layers. Black line in center of A and B is the strip with polymer removed for AFM measurements. The fluorescent intensity remains constant for homogeneous pMAA sample (A), while increases with thickness for the gradient sample (B).

on the surface (figure 5.7A). On the other hand, on gradient pMAA samples, the concentration of –COOH groups on the sample surface should increase from lower polymer thickness to higher polymer thickness. This was demonstrated by the increase in fluorescent intensity observed on the surface (figure 4.7B). The black line seen in the center of figure 4.7A and B is the strip where polymer was removed for AFM measurements. Lack of any fluorescence in this region demonstrates that DCAD was covalently conjugated to the polymer chains, and not covalently attached or physically adsorbed to the glass surface. These results verify that SIPMP can be used to create surfaces with precise control over the location and concentration of a covalently conjugated molecule on the surface. Patterns and/or concentration gradients of a specific protein can be created on the surface which in turn can modulate cell behavior.

5.3.2 Protein Conjugation and Cell Culture

pHEMA grafted surfaces were selected for protein conjugation studies since pHEMA has been shown to very effectively prevent non-specific protein adsorption and hence cell attachment.[194] For this study only homogeneously grafted pHEMA samples were used. As expected, unmodified pHEMA surfaces prevented non-specific protein adsorption and hence adhesion of fibroblasts (figure 5.8A) and B35 cells (figure 5.8B) on the surface. On bare glass, represented by the AFM measurement strip, protein adsorbed freely resulting in uncontrolled cell adhesion and proliferation (figure 5.8A & B). Next, Fn or L1 was conjugated to pHEMA using the DSC chemistry as described above. Fibroblasts and B35 cells were observed to adhere to pHEMA surfaces conjugated with Fn (figure 5.9A) and L1 (figure 5.9B) respectively.

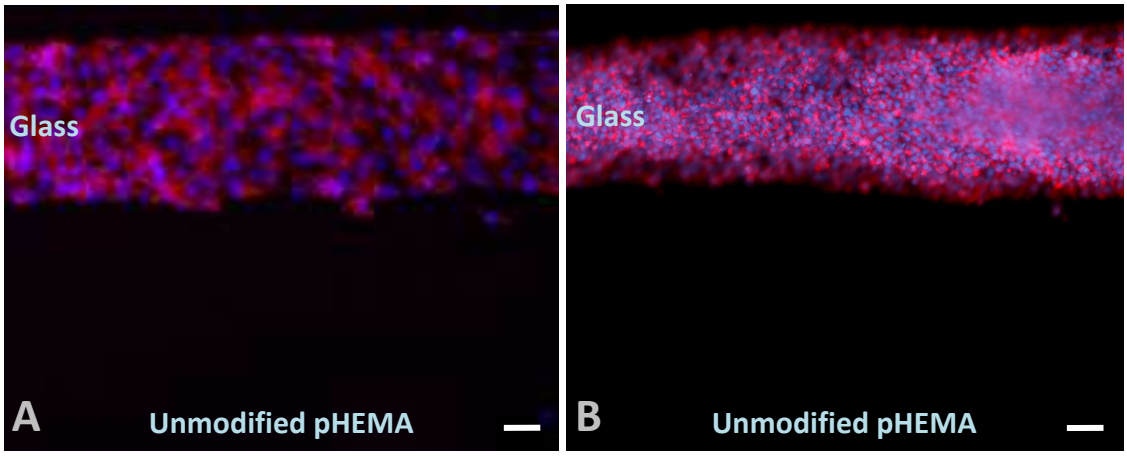

Figure 5.8 Fluorescent micrographs of (A) NIH3T3 fibroblast and (B) B35 cell culture on unmodified homogeneous pHEMA surfaces. (Cell density = 15,000 cells per sample; Fixed on day 4; Cell cytoskeleton is stained with rhodamine phalloidin and nucleus with DAPI; Scale bar = 500µm)

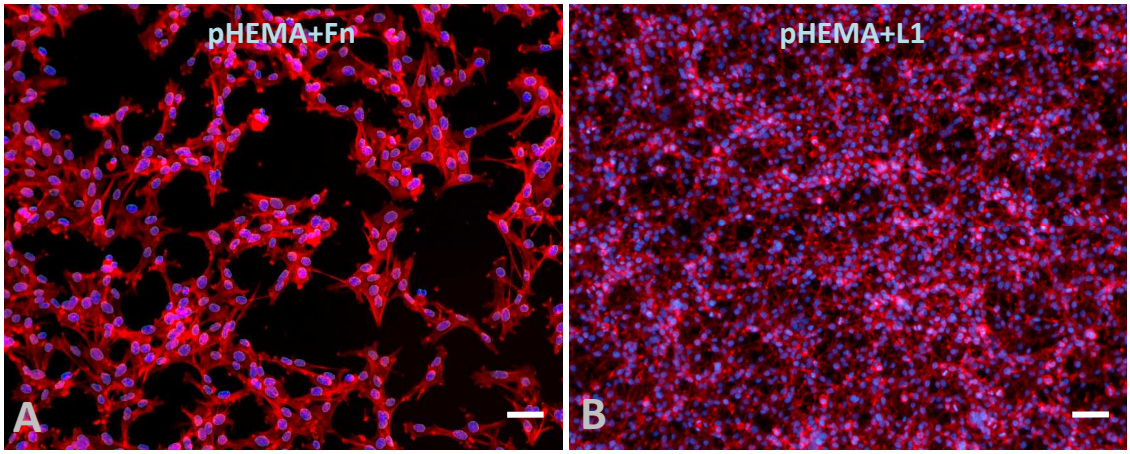

Figure 5.9 Fluorescent micrographs of (A) NIH3T3 fibroblast on Fn conjugated, and (B) B35 cells on L1 conjugated to homogeneous pHEMA surfaces. (A) is also a representative image for NIH3T3 culture on control samples HAM, HAMaF and HAMaFT. (B) is also a representative image for B35 culture on control samples HD, HDaF, HDaFT, HA, HAaF and HAaFT. (Cell seeding density = 15,000 cells per sample; Fixed on day 4; Cell cytoskeleton is stained with rhodamine phalloidin and nucleus with DAPI; Scale bar = 500µm)

It was important to verify that conjugated protein was the only factor responsible for cell attachment, and the conjugation procedure did not alter the surface chemistry and permitted non-specific protein adsorption resulting in cell adhesion. In case of the DSC chemistry, under ideal circumstances all pHEMA control samples subjected to the DSC conjugation procedure without addition of Fn, should revert back to the original hydroxyl groups due to hydrolysis of

the hydroxysuccinimide groups.[182] As a result, these surfaces should again resist non-specific protein adsorption, and hence cell adhesion. To verify this, controls were prepared by subjecting them to the entire DSC conjugation procedure, but without addition of Fn. One set (HD) was used as is for B35 culture, while another set (HDaF) was challenged with Fn adsorption followed by B35 culture. In case protein adsorption did take place, another set (HDaFT) was challenged with Fn adsorption and washed in a 0.1% triton X-100 solution in PBS for 2 hours to remove the adsorbed protein via surfactant action. Unexpectedly, seeded B35 cells adhered to all the control samples tested (figure 5.9B represents these results). One possibility is that contaminants were introduced into the solution during the conjugation procedure, which covalently attached to the activated –OH groups thus changing the surface chemistry. This change in surface chemistry possibly resulted in the failure to prevent protein adsorption, either from cell culture medium or the direct Fn adsorption challenge, resulting in cell adhesion and proliferation. It is also possible that not all of the activated pHEMA –OH groups were hydrolyzed in 24 hours, the time for which control samples were immersed in protein-free buffer solution. Serum protein could have conjugation to the pHEMA chains via these leftover activated groups, resulting in cell adhesion. It will be worthwhile to allow the hydrolysis to proceed to completion by leaving the samples in buffer for 48 hours or longer, and re-testing cell adhesion.

On the other hand, –OH groups converted to acrylate groups by acryloyl chloride for the thiol-acrylate chemistry will not revert back to –OH as this activation is not prone to hydrolysis. The hydrophobic acrylate groups will allow protein adsorption and hence cell adhesion and proliferation. To test this, one sample set (HA) was used as is for B35 culture. Similar to DSC control samples, one set (HAaF) was challenged with Fn adsorption. In case protein adsorption did take place, another set (HAaFT) was challenged with Fn adsorption and washed in a 0.1%

triton X-100 solution in PBS for 2 hours to remove the adsorbed protein via surfactant action. Again, seeded B35 cells adhered to all the control samples tested (figure 5.9B represents these results). To prevent protein adsorption, control samples (HAaFM) were therefore treated with mercaptoethanol (ME) to covert the acrylate groups back to hydrophilic –OH groups. Another set was treated with ME as well as washing with triton (HAaFMT). NIH3T3 fibroblasts adhered to both these sample sets (figure 5.9A represents these results) indicating that ME treatment was not able to restore the non-fouling property similar to unmodified pHEMA surfaces. These cell culture results on control samples indicate that any deviation from the original pHEMA surface changes the surface chemistry in such a way that the surface is no longer prevents protein adsorption. Thus, it is impossible to conclude from these results if conjugated protein was indeed responsible for cell adhesion and proliferation.

When chick forebrain neurons were seeded on unmodified homogeneous pHEMA surfaces no cell adhesion was observed, similar to the results with NIH3T3 fibroblasts and B35 cells mentioned above. Since L1 is known to promote neural adhesion and neurite outgrowth via homophilic binding, chick forebrain neurons were also seeded on homogeneous pHEMA surfaces conjugated with L1 using either the DSC or thiol-acrylate chemistry. However, neurons did not adhere and survive on these L1-conjugated surfaces. The bioactivity of L1 would be in question, but neurons did adhere and extended neurites on the exposed glass surface (strip for AFM) where non-specific L1 adsorption had occurred. It is possible that L1 did conjugate to the pHEMA chains, but underwent conformational and structural changes making it unrecognizable by the neurons. Further tests, such as ELISA, are required to prove that L1 was indeed present on the pHEMA surface, either conjugated or adsorbed as described earlier.

5.4 Conclusions

SIPMP is a very versatile technique to graft homogeneous as well as gradient polymer layers from a surface. The successful grafting of pMAA and pHEMA from glass surfaces and covalent conjugation of NA demonstrated in the previous study, was used as the basis to develop protein concentration gradients to control cell behavior for tissue engineering applications. SIPMP allowed grafting of pMAA and pHEMA layers from the surface with homogeneous and gradient thickness profiles, which was verified by AFM thickness measurements. Since the concentration of functional groups should follow the polymer thickness, covalent conjugation of dansylcadavarine yielded homogeneous and gradient fluorescent intensity profiles for the corresponding polymer layers. NIH3T3 fibroblasts failed to adhere on unmodified pHEMA-grafted surfaces, but attached on bare glass, verifying the protein-resistant nature of pHEMA.

It seemed that covalent conjugation of Fn to pHEMA using the DSC chemistry promoted NIH3T3 and B35 cell adhesion. Similar results were obtained with B35 cells on L1-conjugated surfaces. Unfortunately, cell culture on control samples also promoted cell adhesion and proliferation, making it impossible to attribute cell adhesion to successful protein conjugation. This indicated protein adsorption due to deviation from the original pHEMA surface chemistry. Even if it were assumed that protein conjugation did occur, non-specific protein adsorption due to a change in surface chemistry after DSC treatment would negate the gradient effect. Taking extra care to eliminate impurities during DSC conjugation, and hydrolyzing leftover activated groups may help partly alleviate this problem. Retesting by seeding cells will be required to verify if this procedure is enough to prevent the undesired protein attachment to the pHEMA chains. The thiol-acrylate chemistry used as an alternative to the DSC also suffered from non-

specific protein adsorption due to the hydrophobic nature of the acrylate groups. Furthermore, since the acrylate groups cannot be cleaved quickly enough, regaining the original pHEMA surface chemistry is not a possibility with the thiol-acrylate procedure. Changing the acrylate groups to –OH by conjugating mercaptoethanol was not able to restore the protein resistant properties exhibited by unmodified pHEMA surfaces, resulting in cell adhesion and proliferation. Finally, primary chick forebrain neurons seeded on L1 conjugated pHEMA surfaces failed to adhere and survive. The bioactivity of L1 would be in question, but neurons did adhere and extended neurites on the exposed glass surface (strip for AFM) where non-specific L1 adsorption had occurred. It is possible that L1 did conjugate to the pHEMA chains, but underwent conformational and structural changes making it unrecognizable by the neurons.

The delicate nature of proteins prevents usage of sonication, a very effective technique to remove adsorbed molecules. An alternative approach would be to use peptides sequences which can have the same or similar effects on cells behavior, but can be subjected to sonication without the fear of denaturation. If use of whole proteins cannot be bypassed, acrylate groups can be attached to the protein molecules via polymer spacers. The proteins can then be directly grafted from the surface via these acrylate groups eliminating the need for post-functionalization of the grafted polymer chains. However, this entails exposing the protein to UV radiation, which may damage its structure and adversely affect its bioactivity. Some recent studies show successful grafting of acrylated antibodies from polymer surfaces without loss of bioactivity[150], so a possibility does exists to extend this technique to other proteins of interest. Irrespective of whether acrylated proteins are grafted or peptides are used for functionalization post-polymer grafting, SIPMP still remains an excellent technique to modify surface properties. Non-specific protein adsorption can be prevented and specific bioactivity can

be imparted to the surface as a homogeneous or a gradient layer and anything in between. In summary, with improvements in the protein immobilization procedure this technique carries tremendous potential for biomedical applications.

6. Conclusions, Limitations and Recommendations

The overall goal of this project was to develop a technique that,

1. facilitates modification of surface properties to prevent non-specific interactions,
2. facilitates surface modification of polymers, ceramics as well as metals,
3. facilitates covalent attachment of any biomolecule to elicit specific responses,
4. maintains accessibility and bioactivity of the attached biomolecule, and
5. facilitates creation of concentration gradients where required.

To achieve this goal, the well documented SIPMP technique was selected for surface modification. SIPMP allows usage of virtually any vinyl monomer for grafting, and it was exemplified in these studies by grafting of poly(methacrylic acid) (pMAA) and poly(hydroxyethyl methacrylate) (pHEMA) from surfaces. Additionally, selection of an appropriate iniferter will allow modification of polymer, ceramic and metal substrates. This was successfully demonstrated by grafting polymer chains from polyurethane (PU) (chapter 3) and glass surfaces (chapter 4 and 5) by using iniferter molecules suitable for each substrate type. Besides homogeneous polymer layers (chapters 3, 4 and 5), it also facilitates creation of patterned and gradient (chapter 5) polymer layers by using appropriate photomasks. An easy method to create polymer thickness gradients was developed and successfully used to create gradients of both pMAA and pHEMA on glass surfaces (chapter 5).

Polymers with hydrophilic functional groups were selected for this study because they facilitate attachment of biomolecules and have the potential to protect the surface from non-specific protein adsorption. The ability to attach molecules to the grafted polymer chains was successfully verified by electrostatic coupling of a colored dye toluidine blue (chapter 3) and covalent coupling of a fluorescent dye dansyl cadavarine (chapter 5), both to –COOH groups on

pMAA. The ability to attach a bioactive molecule was also demonstrated (chapter 4) by covalent conjugation of noradrenalin (NA) to –COOH groups on pMAA and –OH groups on pHEMA chains. Oyster hemocyte culture further verified that the accessibility and bioactivity of the conjugated NA was preserved (chapter 4). However, results from protein conjugation and subsequent cell culture experiments (chapter 5) remain inconclusive. From the biomedical perspective, pMAA grafting from PU surface was able to significantly improve its hydrophilicity, but protein adsorption and cell adhesion tests were not performed in this preliminary study. However, preliminary experiments with pMAA grafted on glass surfaces revealed that it was not able to resist protein adsorption (chapter 5, data not shown), which is why pHEMA grafted samples were used for all the protein conjugation and cell culture experiments in chapter 5. Unmodified pHEMA surfaces demonstrated an excellent ability to prevent protein adsorption and hence attachment of both NIH3T3 mouse fibroblasts and B35 neuroblastoma cells. However, activation of pHEMA –OH groups for covalent conjugation appears to facilitated nonspecific interactions, making it difficult to validate that cell adhesion and growth on the substrates was solely attributable to covalently conjugated biomolecules.

6.1 Translational Limitations of SIPMP

The preceding discussions in the literature review and the last three research chapters highlight the versatility and control SIPMP provides to easily and rapidly modify surface properties of a wide variety of materials. Additionally, it facilitates creation of spatial patterns, concentration gradients and their combinations, of biomolecules on surfaces to study their effect on cell behavior in a high-throughput manner. These aforementioned advantages can greatly speed up testing and validation of new technologies for a variety of bioengineering

applications like biocompatibility, tissue regeneration and anti-biofouling, exemplified in the previous chapters.

However, SIPMP has some limitations that can make it unsuitable for specific applications. Two such limitations have already been discussed at the end of Chapter 2. Preventing exposure to atmospheric oxygen is going to be a challenge for surfaces with large areas typically found in real life applications like biomedical implants and ship hulls. Degassing the monomer solution and using airtight chambers is possible, but can become cumbersome and expensive. Therefore, alternative approaches like adding oxygen scavengers (like carbohydrazide) may be more suitable for large surface areas and large-scale manufacturing operations. Another limitation highlighted earlier was the diffusion problem faced by larger biomolecules at high polymer chain grafting densities, preventing conjugation at greater depths in the polymer layer. This will require keeping the grafting density below a certain level, which in turn will require restricting the maximum polymer layer thickness. This thickness limit will put restrictions on the number of biomolecule concentration slopes that can be created on the surfaces to study cell behavior. However, as cells are able to probe depths of only few tens of nanometers even with the flexible nature of the polymer chains, conjugation at greater depths will carry limited practical value. Nevertheless, as suggested earlier, biomolecules can be acrylated and grafted directly from the surface to overcome the diffusion limitation.

Since SIPMP uses UV light, the pathlength can affect the light intensity and in turn polymerization kinetics. Therefore, all studies done using SIPMP, including the ones discussed in this dissertation, use flat surfaces to keep the thickness of the monomer solution layer and thus the pathlength uniform across the surface. However, most if not all surfaces used in real-life applications, like biomedical implants and ship hulls, are not flat. Therefore, special transparent

windows that conform to the curvature of the surface will have to be fabricated and used to keep the thickness of the monomer layer uniform. Fabricating such windows, albeit complex and expensive, is possible for surfaces with simple topographies, like ship hulls, ocular lenses and pacemaker casings, but will become difficult for surfaces with complex topographies like artificial joint implants. In fact, grafting using SIPMP will be impossible from surfaces with 3D topographies like porous joint surfaces, thus requiring use of alterative grafting techniques like ATRP.

The polymer chains covalently attached to the surface via SIPMP do have limitations on their mechanical and chemical stability. The grafted chains can be easily damaged or removed by an external mechanical force. Similarly, harsh chemical environments involving extreme temperatures, pH values and ionic strength can potentially damage, degrade or cleave the grafted polymer chains. Therefore, usability of surfaces with grafted polymer via SIPMP needs to be thoroughly tested by simulating the conditions of their real-life application. For example, even though SIPMP is aiding development of novel bioactive anti-fouling strategies, such grafted polymer will not survive the extreme marine environment. However, the knowledge gained from the anti-fouling experiments involving biomolecule conjugation using SIPMP can be utilized to develop more robust surface modification techniques that can survive the extreme marine environment. Similarly, the mechanical forces involved with artificial joint implants can quickly erode any grafted polymer chains on their surface. Even if SIPMP becomes the technique of choice for certain biomedical implants, careful handling will be required by the surgeon to prevent inadvertent damage to the grafted polymer chains. Additionally, appropriate sterilization procedures will have to be adapted that do not damage the polymer grafted

surfaces. Sterilization by immersing in 70% ethanol solutions will be a much safer alternative to autoclaving, ethylene oxide treatment or gamma exposure.

Finally, the financial costs involved in using SIPMP to modify surfaces needs to be taken into consideration. Costs will be relatively low when common monomers (like HEMA and PEG), and surfaces with small areas and simple topographies are involved. Any deviation involving use of special monomer types, and/or developing contoured windows and UV light sources, can quickly escalate the costs. Conjugating biomolecules will further add to the costs, since the custom synthesis and purification procedures involved make most biomolecules very expensive. For example, NA currently used for developing anti-fouling surfaces is purified from animals, making it very difficult and expensive to obtain in large quantities. Therefore, synthetic analogs that can be economically synthesized in large quantities need to be developed for application on ships. Similar steps may need to be taken for biomolecules like peptides, proteins, hormones, growth factors and enzymes required to modify surfaces of biomedical implants.

The three applications discussed in this dissertation, surface modification of PU surfaces, development of anti-fouling surfaces, and development of protein gradients, face specific limitations along with many of those mentioned above. These limitations, ways to overcome them, and possible future experiments to improve outcomes, are briefly discussed below.

6.2 Conclusions, Limitations and Recommendations for Surface Modification of PU

Polyurethane substrates were chosen as the model polymer for surface modification using SIPMP. In this case, the goal was to convert the hydrophobic nature of PU surfaces to hydrophilic and provide a means to couple a biomolecule to the surface. TED was easily incorporated into the PU substrates during their synthesis, and used to graft pMAA chains from

the surface. Furthermore, SIPMP being a controlled polymerization technique, provided tremendous flexibility in controlling the amount of pMAA grafted on the surface. In this study, good control over PU hydrophilicity was obtained by systematically varying four parameters, PU TED concentration, monomer concentration, UV light intensity and UV exposure. Increase in the value of any of these parameters resulted in decrease of the water contact angle. Increase in amount of polymer on the surface resulted in better coverage of the exposed hydrophobic PU surface, resulting in increased surface hydrophilicity. Control over the amount of pMAA grafted was further corroborated by the increase in absorbance values of electrostatically attached toluidine blue with increase in values of any of the four variables. Such fine control over hydrophilicity and biomolecule concentration can be very useful to control cell interactions with biomedical implants synthesized from PUs.

TED is just one of the many possible iniferter molecules that can be used for polymer grafting. TED or another iniferter type can be used to expand this grafting technique to other polymers commonly used as biomaterials, as has been demonstrated by studies from the Peppas[195], Anseth[196, 197] and Matsuda groups[135, 136]. PUs themselves can provide a wide variety of materials with tunable mechanical properties. Sometimes, iniferter molecules cannot be incorporated into the polymer matrix as they can change the mechanical properties. In such a scenario, silane-based iniferters can be attached to –OH groups created on the bulk polymer surface by plasma treatment. While pMAA was selected for this proof of concept study, other vinyl monomers like acrylic acid, HEMA, PEG, and N-isopropylmethacrylamide, (NIPAM) can be as easily grafted from polymer surfaces. Polymers like pMAA, which responds to pH changes, and polyNIPAM, which responds to temperature changes, can be grafted to develop stimuli sensitive surfaces for tissue engineering, anti-fouling or drug delivery applications.[149]

A very important limitation encountered in this study was the inability to accurately quantify the amount of polymer grafted and the molecule attached to on the bulk polymer surface. Ellipsometry was ruled out because polymer surfaces are not reflective, while AFM was not possible due to the micron scale surface roughness. FTIR-based chemical analysis was not possible as signals from the bulk polymer would overshadow those from the grafted polymer. Other surface specific analytical techniques like XPS and Auger electron microscopy are a possibility, especially to verify successful conjugation of a molecule, but they come with their specific limitations. For example, XPS cannot probe deeper than 10nm, which Auger required the sample to be made conductive, and both are destructive and only semi-quantitative at best. Cleaving of the polymer chains from the surface for any type of analysis was impractical as a very large sample area would be required to collect enough grafted polymer chains for reliable analysis. Therefore, getting accurate quantification is going to be a major challenge. Nevertheless, direct surface modification of polymeric medical devices by this technique can be used to generate empirical cell culture data and develop a clinically relevant modification procedure.

Based on the conclusions and limitations discussed above, there is tremendous scope for development on this technique for surface modification of polymeric biomaterials. Here are a few recommendations for possible future studies.

1. Dye absorbance measurements only provided semi-quantitative analysis of the amount of molecule attached to the surface. More quantitative measurements are required, especially if this technique will be used to modify surfaces of polymeric scaffolds. This can be done by dissociating the TB molecules from the pMAA chains by treatment with dilute acetic acid solution. The absorbance of this dissociated TB in solution can be compared to a TB

concentration standard curve to obtain a fairly accurate estimate of the concentration of TB on the surface. This quantification method will work for any positively charged molecule as long as it has a 1:1 association with each –COOH group.

2. For other biomolecules, gravimetric analysis can provide accurate quantitative data. Accurate measurement of the change in weight of the sample after polymer grafting and after biomolecule attachment can be used to determine the exact amount of polymer and biomolecule on the surface. A study done by the Matsuda group has successfully demonstrated the use of the quartz crystal microbalance technique for such gravimetric measurements.[198]
3. Electrostatic attachment of biomolecules can be used as a drug delivery platform, as is commonly done by associating positively charged growth factors with negatively charged polysaccharides like heparin sulfate and heparin.[199] Such a drug delivery platform can be stimuli sensitive; pH in case of acidic monomers like pMAA and poly(acrylic acid). The release profiles can be easily tuned by changing various parameters like pH, grafted-chain density and chain MW. The effect of drug or biomolecule release can be tested by in vitro cell culture and *in vivo* experiments. Appropriate controls will be required and should consist of ungrafted PU substrates and unmodified polymer-grafted PU substrates to confirm that the PU substrate and the grafted polymer itself is not responsible for the observed cell behavior.
4. One of the main reasons for making the PU surface hydrophilic is to prevent non-specific protein adsorption. Therefore, a protein adsorption test using one or several ECM proteins like albumin, fibronectin or vitronectin followed by ELISA will prove the efficacy of grafted pMAA chains in preventing protein adsorption. Preliminary cell culture experiments must

be conducted using NIH3T3 fibroblasts, since even minimal amounts of adsorbed protein, undetectable by ELISA, might be enough for cell attachment.

5. If ELISA detects protein on the surface, or cell attachment occurs, it is probably because the charged nature of pMAA chains caused proteins to adsorb via electrostatic interactions. In such a scenario, grafting of a uncharged hydrophilic polymer like PEG or pHEMA can be attempted for better anti-fouling properties.
6. Possibility of covalent attachment of molecules must also be examined by attachment of a fluorescent dye molecule to the grafted polymer chains by using an appropriate conjugation chemistry. For example, if pMAA is the grafted polymer, N-hydroxysuccinimide (NHS) or carbonyldiimidazole (CDI) chemistry can be used, and if PEG or PHEMA is the grafted polymer, the CDI or dissucinimidyl carbonate (DSC) chemistry can be used to couple an amine-based dye.
7. If covalent attachment of the fluorescent dye is successful, further experiments can be conducted to attach bioactive molecules like drugs, hormones, peptides and proteins. Successful conjugation of the biomolecule can be verified by a general surface analytical technique like XPS, or ELISA in case of proteins. Finally, the accessibility and bioactivity of the conjugated biomolecules must be verified by their effect on cells which are known to respond that biomolecule.
8. Since UV-based grafting allows the use of photomasks, patterns and gradients of grafted polymer can be created. Visualization with a covalently conjugated fluorescent dye will provide the best proof of formation and fidelity of these patterns and gradients. Quantification of these gradients will not be possible with dye dissociation or gravimetric analysis described earlier. In this case, the PU surface roughness will have to be reduced to

a few nanometers, either by improving the crosslinking procedure or by polishing the surface after crosslinking.

9. Finally, patterns and gradients of conjugated biomolecules can be created, and then tested *in vitro* to study their effects on cell behavior.

6.3 Conclusions, Limitations and Recommendations for Creation of Anti-Biofouling Surfaces

Moving forward with the results obtained in the previous study, pMAA and pHEMA were grafted on glass surfaces to covalently immobilize noradrenaline (NA) in order to develop bioactive anti-biofouling surfaces for marine applications. This was successfully achieved by using suitable conjugation chemistries to covalently link the primary amine on NA molecules to the –COOH and –OH groups on pMAA and pHEMA chains, respectively. By immobilizing NA, leaching into water was prevented, a must for the ever stringent environmental norms put forth for anti-biofouling strategies. Additionally, immobilization ensured that the bioactivity was permanently maintained on the surface for long-term fouling deterrence.

Successful NA conjugation was verified by the significant increase in polymer layer thickness measured by AFM, and detection of a nitrogen peak in XPS scans, which were absent for control samples. Oyster hemocytes seeded onto NA-conjugated surfaces, underwent apoptosis, cytoskeletal degradation and structural disintegration. None of the control surfaces without NA were able to produce this destruction, with the hemocytes remaining healthy and viable. These cell-based assays demonstrated that accessibility and bioactivity of immobilized NA was retained, and the polymer itself did not have any effect on cell viability. Additionally, the concentration of conjugated NA was high enough to produce such pronounced results. Furthermore, sonication and extensive washing of all NA conjugated samples verified the

robustness of the grafted polymer layer, excellent stability of covalent conjugation bonds, and absence of nonspecifically bound NA which could have produced false positive results.

There are two limitations that need to be addressed. First, even though conjugation of NA was verified by AFM and XPS, the absolute concentration of NA on the surface was not determined. It would be advantageous to know the minimum NA concentration required to produce the observed cell apoptosis. This way, incorporation of excessive NA can be prevented in the next generation of bioactive marine coatings, to prevent or reduce potential ecological repercussions.

Second, effectiveness of immobilized NA to cause apoptosis in hemocytes is good as a proof of principle study, but carries little practical value. Preventing settlement of larvae of oysters, barnacles and other fouling animals carries more practical significance. Fortunately, it has already been proven that NA added in solution very effectively prevents larval settlement. The next logical step is to prove this with covalently immobilized NA.

Finally, bacterial biofilm formation is an important factor that assists in the larval settlement process. Therefore, the ideal anti-fouling surface should also prevent biofilm formation on the surface. Based on the above discussion, here are a few recommendations for future studies.

1. Determine the minimum concentration of immobilized NA required to induce apoptosis. To do this, create polymer thickness gradients and conjugate NA to create a concentration gradient of NA. Use the increase in thickness post-conjugation to determine the absolute NA concentration across the gradient. Seed hemocytes and use the NA concentration data to determine the minimum concentration of immobilized NA required to induce apoptosis.

2. Also determine the minimum concentration of NA required in solution to produce apoptosis. This value can be compared with the minimum immobilized NA concentration, to determine whether the immobilization procedure enhances or suppresses the biological effects of NA.
3. It is absolutely critical to test if immobilized NA can prevent larval settlement of marine biofouling organisms. Therefore initial anti-fouling tests should at least include oyster, barnacle and tube worm larvae, the most common foulers. Once these initial studies are successful, the test can be expanded to include other less common fouling organisms.
4. Effectiveness of unmodified hydrophilic pMAA and pHEMA brushes in reducing or eliminating bacterial growth can be tested. If not effective, then anti-bacterial agents like quaternary ammonium groups or magainin I[200] can be conjugated to the polymer chains along with NA, and tested for bacterial growth. Covalent immobilization will prevent leaching of the antibacterial molecules into water.
5. If this is not effective, special polymers with anti-bacterial properties like poly[2-(Methacryloyloxy)ethyl]trimethylammonium chloride[201] or poly(methacryloxylethyl benzyl dimethyl ammonium chloride)[202] can be grafted and tested for bacterial growth. Functional groups on these polymers can then be used to conjugate NA and tested for combined prevention of bacterial growth and larval settlement.
6. As described earlier in this chapter, practical limitations introduced by the sensitivity of SIPMP to atmospheric oxygen will make it difficult to graft polymers from surface areas as large as ships. Adding oxygen scavengers to the monomer solution prior to grafting from the ships surface may help solve this problem.

6.4 Conclusions, Limitations and Recommendations for Creation of Protein Gradients to Control Cell Behavior

The successful grafting of pMAA and pHEMA from glass surfaces, and covalent conjugation of biomolecules demonstrated in the previous study was used as the basis to develop protein concentration gradients to control cell behavior for tissue engineering applications. SIPMP allowed grafting of pMAA and pHEMA layers with homogeneous and gradient thickness profiles from a surface, which was verified by AFM thickness measurements. Since the concentration of functional side-groups should follow the polymer thickness, covalent conjugation of dansylcadavarine yielded homogeneous and gradient fluorescent intensity profiles for the corresponding polymer layers. NIH3T3 fibroblasts failed to adhere on unmodified pHEMA grafted surfaces, but did attach on bare glass, verifying the protein-resistant properties of pHEMA. It appeared that covalent conjugation of Fn to pHEMA using the DSC chemistry promoted NIH3T3 and B35 cell adhesion. Similar results were obtained with B35 cells on L1 conjugated surfaces. Unfortunately, even control samples promoted cell adhesion and proliferation, making it impossible to attribute cell adhesion to successful protein conjugation. This indicated protein adsorption due to deviation from the original pHEMA surface chemistry. Even if it were assumed that protein conjugation did occur, non-specific protein adsorption due to a change in surface chemistry after DSC treatment would negate the gradient effect. Taking extra care to eliminate impurities during DSC conjugation, and allowing complete hydrolysis of leftover activated groups may help partly alleviate this problem. The thiol-acrylate chemistry used as an alternative to the DSC also suffered from non-specific protein adsorption due to the hydrophobic nature of the acrylate groups. Furthermore, since the acrylate groups cannot be cleaved quickly enough, regaining the original pHEMA surface chemistry is not a possibility with

the thiol-acrylate procedure. Changing the acrylate groups to –OH by conjugating mercaptoethanol was not able to restore the protein resistant properties exhibited by unmodified pHEMA surfaces, resulting in cell adhesion and proliferation. The delicate nature of proteins prevents usage of sonication, a very effective technique to remove adsorbed molecules.

Finally, primary chick forebrain neurons seeded on L1 conjugated pHEMA surfaces failed to adhere and survive. The bioactivity of L1 would be in question, but neurons did adhere and extended neurites on the exposed glass surface (strip for AFM) where L1 adsorption had occurred. It is possible that L1 did conjugate to the pHEMA chains, but underwent conformational and structural changes making it unrecognizable by the neurons.

Based on the above discussion, here are some recommendations for future studies.

1. It is important to determine if incomplete hydrolysis of DSC activated –OH groups was responsible for the attachment of serum proteins on the pHEMA surface. Hydrolysis of the leftover activated groups should be allowed to proceed to completion by leaving the samples in buffer for 48 hours or longer. Retesting by seeding cells will verify if this procedure is enough to prevent the undesired protein attachment to the pHEMA chains.
2. Instead of using L1, peptide sequences that have the same or similar effects on neurons (like KYSFNYDGSE from NCAM[203], VFDNFVLK from tenascin[204], and YIGSR and SIKVAV from laminin) can be conjugated to the polymer chains. They can be subjected to sonication to remove non-specifically adsorbed peptide molecules without the concern of loss of peptide bioactivity. Such a technique was recently demonstrated by Harris et al., who created a concentration gradient of RGD and studied its effect on fibroblast adhesion.[55]

3. If use of whole proteins cannot be bypassed to produce the desired cell behavior, acrylate groups can be covalently coupled to the protein molecules via PEG-based spacers. These acrylated protein molecules can then be directly grafted from the surface. Some recent studies have successfully shown grafting of acrylated proteins and antibodies from polymer surfaces without loss of bioactivity using SIPMP [138, 150], thus eliminating the need for conjugation post-polymer grafting. A similar procedure can be attempted with proteins of interest to this study, like L1 for axonal guidance.
4. Once the protein conjugation procedure has been sorted out, gradients of L1 with different slopes and baseline values can be created. This can help identify the profile or group of profiles which are best for guiding and stimulating axonal growth.

Irrespective of whether acrylated proteins are grafted or peptides are conjugated, SIPMP still remains an excellent technique to modify surface properties. Where just prevention of protein adsorption is necessary, unmodified polymer layers can be used. Finally, with improvements in the protein immobilization procedure, homogeneous, patterned, gradient, and other complex concentration profiles of biomolecules can be created on the surface to control cell behavior.

Appendix A.

A.1 Epilogue

The focus of this dissertation is the use of SIPMP for surface modification of various biomaterials. One group of such biomaterials are degradable hydrogels, which are under intense investigation as tissue culture scaffolds as well as controlled drug delivery vehicles. PEG is the polymer of choice for synthesizing these hydrogels due to its hydrophilic nature and versatility in chain structure and MW. Short PLA and/or PGA chains are added into the crosslinked PEG matrix to make the chains hydrolytically degradable. Additionally, since PEG, PLA and PGA are all FDA approved, using these polymers to synthesize degradable hydrogels for biomedical applications quickens the development process and reduces expenses. However, just like any biomaterials, even PEG and PLA face long-term biocompatibility problems due to non-specific protein and cell interactions. Therefore, reducing protein adsorption and imparting bioactivity to the hydrogels surface to control cell behavior is required to improve clinical outcomes. Just like surface modification of PU surfaces discussed earlier, an iniferter like TED can be incorporated into PEG-PLA matrices crosslinked using UV light. A recent study has already demonstrated this by grafting crosslinked blocks of PEG hydrogels on top of a TED containing base PEG layer.[156, 195] This can be extended to graft polymer chains and use them to covalently conjugate biomolecules to control cell behavior. The following study is a preliminary step in understanding the degradation kinetics of such photo-crosslinked PEG-PLA hydrogels under various conditions and potentially developing statistical models that can be used to quickly develop hydrogels with specific properties. Future work can involve using SIPMP to improve surface properties of these hydrogels and possibly conjugating biomolecules to the surface before testing them for tissue engineering and drug delivery applications.

A.2 Influence of Network Structure on the Degradation of Photo-Cross-Linked PLA-b-PEG-b-PLA Hydrogels

A.2.1 Introduction

Hydrogels based on the free-radical polymerization and crosslinking of acrylated or methacrylated poly(lactic acid)-b-poly(ethylene glycol)-b-poly(lactic acid) (PLA-b-PEG-b-PLA) macromers were designed to maintain all the advantages of a PEG-based material while also permitting tunable degradability.[205] As the utilization of PLA-b-PEG-b-PLA gels has increased, this characteristic of tunable degradability has become extremely useful in the biomedical field to eliminate the need for physical removal of PLA-b-PEG-b-PLA implants as well as to modulate the delivery rates of drugs or growth rates of cells encapsulated within crosslinked PLA-b-PEG-b-PLA matrices. Therefore, it is important to understand the factors controlling the degradation behavior of chemically crosslinked PLA-b-PEG-b-PLA hydrogels.

According to previously developed degradation models, there are two main parameters that affect the form and rate of network degradation for chemically crosslinked PLA-b-PEG-b-PLA macromers.[206-208] The first is the hydrolysis kinetics of PLA ester bonds within the crosslinked hydrogels. The second is the physical structure of the gel. These two parameters are interdependent, making the entire gel degradation process very complex. Sawhney et al..[205] showed that increasing the molecular weight of the PEG segment decreases the crosslinking density (structural effect), which in turn increases the water content of PLA-b-PEG-b-PLA gels. Increases in water content increase the rate of hydrolysis of PLA ester bonds (kinetic effect) and the overall gel degradation rate.[205]

The ability to tailor hydrogel crosslinking density can also be used to control network mesh size and diffusivities of encapsulated solutes. Lu et al..[209] have shown that the initial

mesh size of the hydrogel network as well as the degradation rate affect the drug release profile. Faster degradation rates result in faster increases in mesh size and more rapid drug release. Metters et al..[208] demonstrated that changing the macromer weight percent during polymerization also affects the crosslinking density and the resulting water content of the degradable gel. Lowering the macromer content during gel fabrication lowers the crosslinking density of the hydrogel while increasing both its water content and degradation rate.[209-211]

In addition to its crosslinking density, water content, and elastic modulus, the chemical nature of a degradable PLA-b-PEG-b-PLA hydrogel also changes with degradation. For example, as PLA-b-PEG-b-PLA gels degrade, acidic species are generated along the backbone chains of the network. These immobilized anionic groups should make the swelling and degradation behavior of the resultant gels sensitive to changes in solution pH and ionic strength. Since previous studies of PLA-b-PEG-b-PLA hydrogel degradation behavior have been conducted at constant pH and ionic strength[205-209, 211-214], the results obtained from these investigations cannot provide insight as to how alterations in pH or ionic strength affect the kinetics of ester bond degradation or the nanoscopic architecture of the gel. To better understand the behavior of photo-crosslinked PLA-b-PEG-b-PLA hydrogels and to evaluate their potential as environmentally responsive biomaterials, the sensitivity of their degradation behavior to local changes in pH and ionic strength needs to be understood.

To help unravel the dependence of PLA-b-PEG-b-PLA hydrogel degradation behavior on macromer chemistry versus network structure, the goal of this work is to compare the pseudo first-order degradation kinetics of soluble PLA-b-PEG-b-PLA macromers to those of identical yet crosslinked macromers contained within insoluble, highly swollen gels. For this study, gels were synthesized from PLA-b-PEG-b-PLA macromers by photopolymerization and their hydrolytic

degradation was compared to the degradation of the same unpolymerized macromers in buffered solutions as a function of time. Mass-transfer effects are minimized in both cases due to the low macromer concentrations of the chosen solutions and highly swollen nature of the gels investigated.[208, 213] Degradation of uncrosslinked macromer in solution eliminates association of neighboring chains or gel structure. Therefore, any significant differences in degradation behavior between the soluble and insoluble systems can be attributed to the supramolecular character of the crosslinked gel. Such a direct comparison should provide a better understanding of the complex set of parameters controlling the process of hydrogel degradation, and enable one to independently design hydrogel chemistry and structure for specific applications.

A.2.2 Materials and Methods

A.2.2.1 Macromer Synthesis and Characterization

The detailed procedure for the synthesis of the PLA-b-PEG-b-PLA diacrylate macromer has been described previously.[205] Briefly, it was synthesized by first reacting 20gm of dry PEG 4600Da (Aldrich; Mn = 4600) with 3.13gm of D,L-lactide (Polysciences Inc., PA; MW=144.1Da) at 130°C to give PLA-b-PEG-b-PLA through a ring-opening polymerization. In the second step, this triblock macromer was dissolved in a minimum amount of dichloromethane (Fluka; Purity □ 98%) and end capped with acrylate functionalities by reaction with 2.83ml of acryloyl chloride (Aldrich; Purity > 98%) and 5.33ml of triethylamine (Aldrich; Purity = 99.5%) under vigorous agitation at room temperature for 4 hours. The synthesized macromer was then purified by precipitation in ice-cold ether followed by filtration. Remaining solvent was removed by drying the purified product under vacuum at room temperature for 48 hours. All materials were used as received.

H1 NMR (Bruker 300) analysis of the synthesized macromers dissolved in deuterated chloroform (Aldrich; Purity = 99.9%) was used to determine the number of lactic acid groups (j) added to each end of the 4600Da PEG chain and the percent acrylation of the final triblock macromer. The number of lactic acid groups j is also the number of ester bonds at each end of the 4600Da PEG chain. Characteristics of the three batches of PLA-b-PEG-b-PLA macromer synthesized for the current study are given in Table A.1.

Table A.1 H^1 NMR Characterization of PLA-b-PEG-b-PLA macromers

Macromer	Number of LA units per end group (*j*)	Percent Acrylation (%)
PEGPLA1	3.1	83
PEGPLA2	2.8	96
PEGPLA3	2.7	86

A.2.2.2 Hydrogel Polymerization

Hydrogels were synthesized by solution photopolymerization of PLA-b-PEG-b-PLA diacrylate macromer in deionized water. In brief, the macromer was dissolved in deionized water to form 7.0, 10, 20 or 30 wt% solutions by weight, which correspond to water contents of 93, 90, 80 and 70 wt%. Photoinitiator, Irgacure 2959 (Ciba, NY), was added to the solution at a final concentration of 0.5 wt%. This solution was then injected between two glass slides separated by 0.8mm Teflon® spacers. Photopolymerization and gel formation was initiated by exposure of this solution to 365nm UV light of intensity ~8.5mW/cm^2 for 10 minutes (Black-Ray: B 100 AP, Upland, CA, USA). Identical disk-shaped gel samples having a volume of ~160□l were then cut for subsequent degradation studies using a 5/16th inch hollow punch.

A.2.2.3 Hydrogel Degradation

To measure the effect of buffer pH on the rate of gel degradation, identical undegraded gel samples synthesized from a 30 wt% PLA-b-PEG-b-PLA macromer (PEGPLA3) solution were placed in a large excess of 50mM buffer (approximately 3 ml) at pH 2, 3, 4, 5 or 7.4 and allowed to degrade at a constant temperature of 37°C. The pH 2 and 3 buffer solutions were made using phosphoric acid (Sigma), the pH 7.4 buffer solution was made using sodium phosphate dibasic (Riedel-de Haën, Germany), while the pH 4 and 5 buffer solutions were made using acetic acid (Aldrich). Sodium chloride (Sigma-Aldrich) was added to all buffers to maintain a constant ionic strength of 0.135M. To measure the effect of ionic strength on the rate of gel degradation, additional gel samples synthesized from 30 wt% macromer (PEGPLA1) solution were placed in 7.4 pH buffer solutions with ionic strengths of 0.135M, 0.4M, 0.7M, 1M and 1.5M. Finally, to study the effect of water content on the rate of gel degradation, gel samples were synthesized from solutions of 7.0, 10, 20 and 30 wt% macromer (PEGPLA2) and allowed to degrade in 7.4 pH buffer with an ionic strength of 0.135M.

For each degradation experiment, gels were first allowed to equilibrate in buffer solution for 48 hours. After equilibration, the swollen weights of all gel samples were measured. Some gels were dried in vacuum for 2 days to provide corresponding dry weights. The ratio of the swollen gel weight before drying (S_w) to the polymer weight after drying (D_w) provided the mass swelling ratio (Q_m) and the percent initial water content by mass (*IWC*) for each gel as shown by Equations 1 and 2, respectively:

$$Q_m = \frac{S_w}{D_w} \qquad \text{Equation 1}$$

$$IWC = \frac{Q_{m,0} - 1}{Q_{m,0}} \times 100\% \qquad \text{Equation 2}$$

where, $Q_{m,0}$ is the initial, equilibrium mass swelling ratio measured after 48 hours in buffer. It should be noted that the hydrogel IWC may differ from that of the macromer solution used to make it due to swelling (or deswelling) during equilibration. The swollen weights of the remaining gels were measured at regular intervals during the degradation experiment. Additional gel samples were dried at regular intervals to obtain the characteristic mass loss profile for the experiment.

It has been previously established that the change in gel swelling ratio with time is related to the degradation rate of the PLA-b-PEG-b-PLA hydrogels and can be used to calculate the pseudo first-order degradation rate constant of the ester bonds present in the crosslinks of the highly swollen networks.[206-208, 210-217] This relation is based on the assumption that the water concentration and pH inside the gel remain approximately constant during degradation. This assumption is reasonably valid for highly swollen gels degraded in an excess of buffer. The Flory-Rehner equation relates the dynamic mass-swelling ratio of this degrading system to the time-dependent crosslinking density of the gel, as given by Equations 3 and 4 below[212, 215, 218]:

$$\nu_c = -\frac{\ln(1-v_2)+v_2+\chi_{12}v_2^2}{V_1\left(v_2^{1/3}-\frac{2v_2}{f_A}\right)} \qquad \text{Equation 3}$$

$$v_2 = \frac{1}{Q} = \frac{\bar{v}_2}{Q_m(1-\bar{v}_1+\bar{v}_2)} \qquad \text{Equation 4}$$

where ν_c is the gel crosslinking density, Q is the volumetric swelling ratio, v_2 is the polymer volume fraction in the hydrogel, $\bar{v}_1$ is the specific volume of water (1.006 cm^3/g at 37 °C), $\bar{v}_2$ is the specific volume of dried PEG (0.92 cm^3/g at 37 °C), χ_{12} is the Flory-Huggins

interaction parameter for a PEG-H_2O system (0.45[215, 219]), and f_A is the functionality of the PLA-b-PEG-b-PLA macromers (f_A = 4 for all divinyl macromers used in the current studies).

Assuming pseudo first-order degradation kinetics, the time-dependent decrease in PLA-b-PEG-b-PLA crosslinking density can be expressed mathematically as

$$\nu_c \propto e^{-2jk'_{gel}t}[\mathrm{A}]_0 \qquad \text{Equation 5}$$

where, k'_{gel} is the pseudo first-order degradation rate constant in hr^{-1}, $2j$ is the number of ester bonds per macromer, t is the degradation time in hours, and $[A]_0$ is the initial concentration of PLA-b-PEG-b-PLA diacrylate molecules in the system.[215]

Values of k'_{gel} were obtained by quantitatively matching theoretical and experimental values of ν_c. Equations 3 and 4 were first used to calculate experimental values of the crosslinking density ν_c from the gel mass swelling ratios (Q_m) obtained with Equation 1. Using the solver function in Microsoft® Excel the values of k'_{gel} and $[A_0]$ were then independently adjusted until the residual error between the experimental ν_c values and those predicted by Equation 5 were minimized. The solver used a quasi-Newtonian iteration algorithm with linear interpolation and forward differentials.

A.2.2.4 Solution Degradation

To measure the effect of buffer pH and water content on the degradation rates of soluble PLA-b-PEG-b-PLA, unpolymerized macromer was dissolved in buffer solutions at the same pH and ionic strengths as the previously described gel samples. 10 ml of macromer (PEGPLA1 or PEGPLA2) solutions at concentrations of 5.0, 10, 15 and 20 wt% were then allowed to degrade at 37°C. These solutions correspond to IWC of 95, 90, 85 and 80 wt%, respectively. Unlike the hydrogel measurements, the bulk water contents of these macromer solutions

remain constant throughout the degradation period. To measure the effect of ionic strength on the degradation rate of unpolymerized PLA-b-PEG-b-PLA, macromer (PEGPLA2) solutions at a concentration of 6.7 wt% (IWC = 93.3 wt%) were prepared and allowed to degrade in 7.4 pH buffer solutions at ionic strengths of 0.135M, 0.7M and 1.5M at 37°C.

Soluble macromer degradation was observed by the formation of lactic acid, a well-known degradation product of PLA-b-PEG-b-PLA hydrolysis. The time-dependent increase in lactic acid concentration of each solution was measured with a sensitivity of 0.01 g/L using a YSI 2700 SELECT Biochemistry Analyzer (YSI Inc., OH, USA). This analytical sensitivity is sufficient for this study, since 0.01g/L corresponds to only 0.2 % degradation for the 5 wt% macromer solution or just 0.03 % degradation for the 20 wt% solution. The change in lactic acid concentration with time was used to calculate the degradation rate constant for the linear macromer in solution by assuming pseudo first-order reaction kinetics. This is a valid assumption since both buffer pH and water content are constant during the experiment. A single molecule of lactic acid is produced from the diacrylated PLA-b-PEG-b-PLA macromer only upon cleavage of two adjacent ester bonds. According to previously published pseudo first-order kinetic models for PLA-b-PEG-b-PLA degradation[206-208, 214, 215], the statistical fraction of hydrolyzed or degraded ester bonds (PEster) is described by Equation 6:

$$P_{Ester} = 1 - \frac{[E]_t}{[E]_0} = 1 - e^{-k't} \qquad \text{Equation 6}$$

where [E]t is the ester bond concentration at time t, [E]0 is the maximum ester bond concentration at time t = 0, t is the degradation time, and k' is the pseudo first-order degradation rate constant. Release of one lactic acid molecule requires cleavage of two ester

bonds. Therefore, the pseudo first-order rate constant for degradation can be related to the growing concentration of lactic acid in solution by Equation 7:

$$P_{Ester}^{2} = \left(1 - \frac{[E]_t}{[E]_0}\right)^2 = \left(1 - e^{-k'_{soln} t}\right)^2 = \frac{[LA]_t}{[LA]_{max}} \qquad \text{Equation 7}$$

where [LA]t is the lactic acid concentration in the solution at time t, [LA]max is the final lactic acid concentration after the macromer is completely degraded, and k'soln is the pseudo first-order degradation rate constant.

A.2.3 Results and Discussion

A.2.3.1 Macromer Degradation

It is well established that hydrolysis of ester bonds is acid as well as base catalyzed.[220] Equation 8 represents the generalized kinetic equation for acid and base catalyzed hydrolysis of ester bonds such as those present within solubilized or crosslinked PLA-b-PEG-b-PLA macromers:

$$\frac{d[E]}{dt} = -k_{H^+}[H^+][H_2O][E] - k_{OH}[^-OH][H_2O][E] \qquad \text{Equation 8}$$

where, k_{H+} is the kinetic rate constant for acid-catalyzed hydrolysis, k_{-OH} is the kinetic rate constant for base-catalyzed hydrolysis, [E] is the concentration of ester bonds in the PLA segments at time *t*, [H_2O] is water concentration, and [H^+] is the hydronium ion concentration and [$^-$OH] is the hydroxyl ion concentration.

In the current study, [H^+] and [$^-$OH] remain essentially constant during the degradation of both the macromer solutions as well as hydrogels due to the use of excess buffer solutions to maintain a constant pH. Assuming no localized variations, [H_2O] also remains constant during degradation of solubilized macromers. [H_2O] does change as Q increases during hydrogel

degradation. However, for the highly swollen hydrogels used in the current study with large initial water contents, this change is relatively minor. For example, the water content within a gel with an initial Q = 5 (equivalent to an initial water content of 80 wt%) will increase, at most, by 20%. Likewise, gels with an initial Q > 10 will experience changes in water concentration of less than 10% over the entire course of degradation. Assuming these variations are acceptable for the current analysis Equation 8 can be simplified for the degradation of both soluble and crosslinked macromers to the following pseudo first-order kinetic equation[206-208, 213, 221]:

$$\frac{d[\mathrm{E}]}{dt} = -k'[\mathrm{E}] \qquad \text{Equation 9}$$

where, k' is the pseudo first-order rate constant equal to ($k_{H+}[H_2O][H^+] + k_{-OH}[H_2O][^-OH]$). Previously published studies on the degradation behavior of PLA oligomers and networks have clearly established the acceptance of using a pseudo first-order kinetic mechanism to accurately describe PLA hydrolysis kinetics under experimental conditions similar to those used in the current work.[222-226]

Equation 9 illustrates that although k' is constant during pseudo first-order macromer degradation, the degradation rate (d[E]/dt) varies with time. As the macromer degrades, the ester bond concentration and the degradation rate decrease. These changes make it difficult to quantitatively compare the degradation behavior of gels synthesized with various ester bond concentrations or degraded under different conditions. However, under the proper conditions discussed above (constant pH and high initial gel swelling) the pseudo first-order degradation rate constant (k') remains constant throughout the degradation process, making it a useful tool for assessing and comparing the characteristic degradation behavior of various systems. The impact of important system parameters (e.g., pH, water concentration) on the gel structure and

ester bond hydrolysis kinetics can be readily observed by monitoring apparent changes in *k'*. Furthermore, this analysis is applicable for comparing macromer degradation in solution and in highly swollen gels since *k'* is equivalent to both k'_{soln} and k'_{gel} in the appropriate environment.

A.2.3.2 Effect of pH

During degradation of soluble macromer, cleavage of the PLA ester bonds takes place through hydrolysis leading to the formation of PEG, lactic acid and polyacrylic acid as degradation products. For a single lactic acid molecule to be released, two adjacent ester bonds along the macromer chain must be broken. Therefore, as macromer degradation proceeds, the lactic acid concentration in solution increases in a sigmoidal fashion as shown in Figure A.1a. The value of k'soln for a given set of degradation conditions is obtained by fitting Equation 7 to the data, which provides a very good fit to the measured data, as shown in Figure A.1a. Additionally, the shift in the degradation curves shown in Figure A.1a demonstrate that the degradation rate of soluble macromer and the calculated value of the pseudo first-order rate constant (k'soln) depend strongly on the pH of the surrounding buffer solution.

Alternatively, degradation of PLA-b-PEG-b-PLA hydrogels takes place by cleavage of ester bonds located within the network crosslinks. In these gels, only one PLA ester bond needs to be cleaved to break a crosslink. However, the release of lactic acid from a degrading network can be a complex function of hydrolysis kinetics and mass transfer limitations. Therefore, for gel degradation it can be difficult to determine the degradation rate constant k'gel by direct measurement of degradation products such as lactic acid (LA). Instead, the change in mass swelling ratio with time is used to calculate k'gel using Equations 3-5[207, 208, 213, 215]. The time-dependent exponential growth in the mass swelling ratio of the gels produced by these equations provides a good fit to the experimental data as shown in Figure A.1b. Similar to the

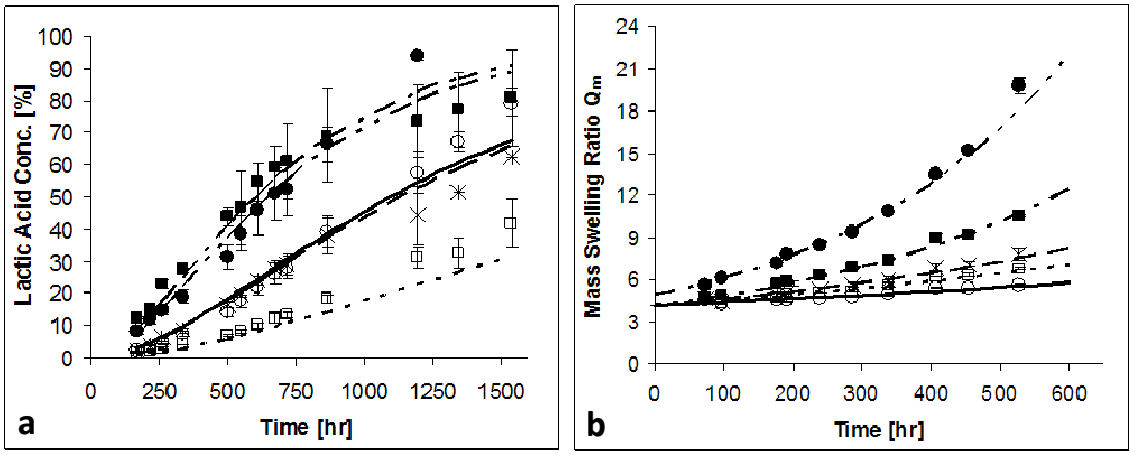

Figure A.1 Experimental measurements of hydrolytic degradation of PLA-b-PEG-b-PLA macromer at constant pH. Points show experimental data, while solid and dashed lines indicate model predictions. (a) Change in lactic acid concentration with time as soluble PLA-b-PEG-b-PLA macromer is hydrolytically degraded. (b) Mass swelling ratios of PLA-b-PEG-b-PLA gels as functions of degradation time. [(■,□ - □) pH 2; (○, □ □ □) pH 3; (□,- - -) pH 4; (✕,□ □) pH 5; (●,□ - - □)) pH 7.4, For all data: Solution: 10 wt% PEGPLA1, Gel: 30 wt% PEGPLA3; Ionic strength = 0.135M; n=3, error bars = ± std. dev.]

soluble degradation experiment, comparison of the multiple data sets in Figure A.1b demonstrate that the rate of gel degradation and the measured value of k'gel also depend strongly on buffer pH.

The effects of pH on k'soln and k'gel are summarized in Figure A.2. As buffer pH is increased from a value of 2.0 to 4.0, the calculated value of k'soln decreases. The k'soln then continually increases with buffer pH above 4.0. A minimum in k'soln is therefore observed to occur at pH 4, close to the pKa of lactic acid (pKa = 3.85). This pH-dependent minimum for the degradation rate constant is consistent with observations made by Schliecker et al..[222] and de Jong et al..[227] during the degradation of pure PLA networks. In these previous studies, a degradation rate minimum was observed for pure PLA at a buffer pH of 4.0. This minimum was hypothesized to occur due to the hydrolysis of PLA being both acid as well as base-catalyzed. According to degradation mechanisms provided by de Jong et al..[227] and Shih[228], at pH values below the pKa of lactic acid, proton catalysis dominates due to protonation of the acid

hydroxyl group leading to subsequent attack by H_2O and hence degradation. Similarly, at pH values above the pKa hydroxyl catalysis dominates due to nucleophilic attack by the hydroxyl end group on the second carbonyl group, also known as back-biting.[227, 229] Though the current gel networks are not pure PLA systems, obtaining similar trends in degradation behavior can be expected because of the PLA-mediated degradation of the PLA-b-PEG-b-PLA macromers.

Degradation of both crosslinked and soluble macromers occurs through hydrolysis of PLA ester bonds. As a result, the measured pseudo first-order rate constants for hydrogel degradation agree reasonably well with those obtained for the soluble system, even though the two kinetic parameters were calculated using different methods (Figure A.2). In addition, the range of values obtained in the current study for both degradation rate constants agrees with previously published results[208, 210]. The values for k'gel show a similar dependency on pH when compared to k'soln with a minimum occurring between pH 2 and 7.4 (Figure A.2). However, some differences do occur between the two data sets. The values of k'gel are consistently lower than those of k'soln at corresponding pH. One reason for this is that the initial water contents of the gels (79 wt% ± 1.5%) are lower than those of the macromer solutions (90 wt%) used in this experiment. In addition, the minimum value for k'gel is shifted to a lower pH value compared to that of k'soln. This shift of the observed minimum to a lower pH value is not

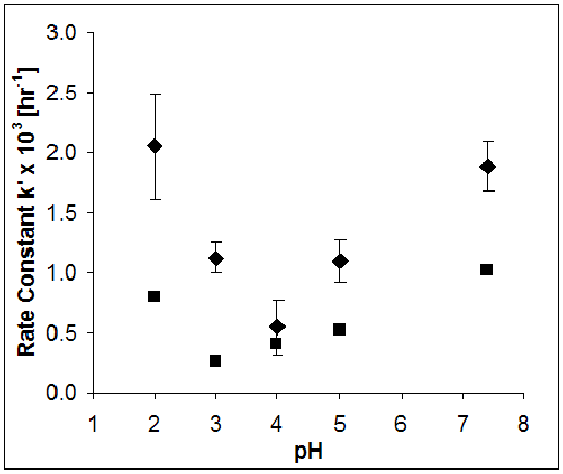

Figure A.2 Experimentally determined degradation rate constants for PLA-b-PEG-b-PLA macromers in solution (◆; k'soln) and in gels (■; k'gel) as functions of pH. For all data: Solution: 10 wt% PEGPLA1, Gel: 30 wt% PEGPLA3; Ionic strength = 0.135M; n=3, error bars = ± std. dev.]

consistent with pKa differences between linear and crosslinked polymers. Previous studies indicate the acidity of carboxy groups in hydrogels to be much lower than linear polymers of identical composition.[230] In other words, the apparent pKa's of carboxy groups in hydrogels are higher than those of linear polymers of the same composition. For example, the pKa's of poly(acrylic acid) hydrogels have been measured at pH values much higher than 5.0 compared to a value of 4.7 for soluble poly(acrylic acid)[231]. If the location of the k'gel minimum is simply a function of acid-group pKa, then it would be expected to shift to higher pH values in Figure A.2.

To understand why the pH dependence of k'soln and k'gel differ requires an analysis of the hydrogel structure and degradation kinetics. According to Equation 8, any change in the water content of crosslinked PLA-b-PEG-b-PLA networks will alter the local environment of the hydrolytically labile ester bonds and affect k'gel. While a non-degraded PLA-b-PEG-b-PLA gel is considered to be relatively non-ionic, the water content of partially degraded PLA-b-PEG-b-PLA networks varies strongly with pH due to ionization of weakly acidic pendant groups created during ester bond cleavage[232]. Scheme A.1 illustrates the impact of buffer pH and ionic strength on the swelling ratio (Q) and degradation rate constant (k'gel) of a partially degraded PLA-b-PEG-b-PLA gel network.

After hydrolysis of some fraction of PLA ester bonds in the crosslinks, network-immobilized acid groups are created – lactic acid groups at the ends of cleaved crosslinks and acrylic acid groups along the backbone chains. Polyacrylic acid has a pKa of 4.7[231] compared to a value of 3.85 for lactic acid. Therefore, in buffer solutions of pH greater than or equal to approximately 3.85 a significant portion of network-immobilized acid functionalities will be deprotonated, i.e. ionized. This ionization can alter the water content of the gel through two

distinct mechanisms. First, the immobilized negative charges repel one another, causing the crosslinked polymer chains to stretch to a higher degree and increased gel swelling to occur[233-236] ((B) in Scheme A.1). In addition, the excess negative charge inside the gel attracts positive counter-ions from the buffer into the swollen gel environment. The ionic concentration inside the gel becomes greater than the surrounding buffer. Transport of water from the surrounding solution into the hydrogel then occurs to balance the osmotic pressure difference.[232, 237] The end result is that the swelling of the partially ionized gel increases until the elastic forces of the stretched polymer network are in equilibrium with the increased osmotic forces.[238]

Therefore, while the water content of a single-phase macromer solution is fixed during degradation, the water concentration within a partially degraded PLA-b-PEG-b-PLA gel depends on local pH. Below the pKa of lactic acid (pH = 3.85) negligible ionization of network-immobilized lactic acid as well as poly(acrylic acid) groups occurs (part A in Scheme A.1). However, above pH 3.85 the degree of ionization and the amount of water transported inside the gel continuously increases. As a result, the values of k'_{gel} at pH values greater than 3.85 are increased compared to what they would be if ionization and additional water transport did not occur. This preferential increase in k'_{gel} values at higher pH adds to the inherent complexity of PLA degradation kinetics already observed in solution and results in shifting the pH at which the minimum kinetic constant value is observed from pH 4 to pH 3 (Figure A.2).

A.2.3.3 Effect of ionic strength

As depicted in Scheme A.1(C), if ionization does occur inside the gel network, then it should be possible to nullify the increased swelling of partially degraded PLA-b-PEG-b-PLA gels observed at higher pH by increasing the ionic strength of the surrounding buffer solution. As the

ionic strength of the buffer solution is raised, the osmotic pressure and degree of gel swelling should decrease.[232, 237] In addition, the excess negative charges produced in the hydrogel will be screened or masked by the increased concentration of positive ions in the buffer, thus reducing the repulsive forces and further decreasing gel swelling. As shown by Equations 8 and 9, this decrease in gel water content will ultimately lower the gel degradation rate and the observed k'gel.

To verify that the ionization of acid species within PLA-b-PEG-b-PLA hydrogels affects gel swelling and degradation behavior as described above, gels fabricated from 30 wt% macromer solutions were degraded in pH 7.4 buffer solutions of varying ionic strength. Within the range of pH values investigated, pH 7.4 represents the value where maximum ionization of the acrylic acid and lactic acid groups inside the partially degraded gel network occurs. Figure A.3 shows that under these conditions the initial water content of the hydrogels decreases with an increase in buffer ionic strength up to 1.5M. The relatively small decrease in gel water content of approximately 11% leads to a rather large 75% decrease in the measured degradation rate constant k'gel. This observed decrease in k'gel is much greater than the effect predicted by the pseudo first-order relationship that assumes k'gel to be directly proportional to gel water content (Equation 9).

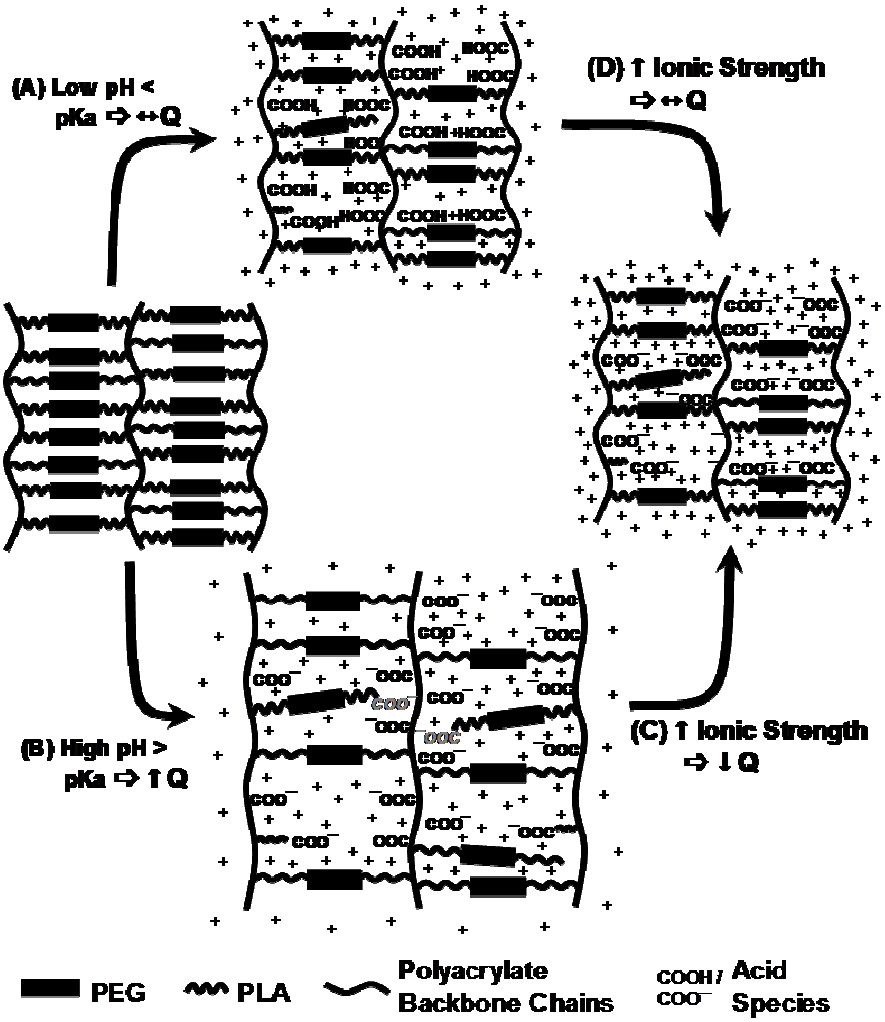

Scheme A.1 Sensitivity of PLA-b-PEG-b-PLA hydrogel swelling to solution pH and ionic strength: Partial hydrolysis of PLA ester bonds creates an anionic network (A) Network-immobilized acrylic acid and lactic acid species do not deprotonate at low pH (< pK_a). (B) At high pH values (> pK_a), these acid species deprotonate, leading to increased water contents, gel swelling ratios (Q), and kinetic rate constants (k'_{gel}). (C) Increased buffer ionic strength at high pH shields any charged groups present and leads to gel deswelling and lower values of k'_{gel}. (D) Increased buffer ionic strength at low pH has no effect on gel swelling or k'_{gel} due to absence of ionized acid species.

Contrary to what is observed with crosslinked macromer, no decrease in the degradation rate constant for the macromer solutions (k'soln) is observed when the solution ionic strength is increased except for a slight decrease at the highest ionic strength of 1.5M

(Figure A.3). This result is expected since no difference in osmotic pressure can be created in the single-phase soluble system and any repulsion between adjacent macromer molecules is minimized due to their high degree of mobility. Furthermore, when identical experiments were conducted in pH 2 buffer solutions where negligible ionization of the lactic or acrylic acid species occurs, increasing ionic strength had no significant effect on gel swelling or the degradation rate constants for the gel or solution-based systems (data not shown). These results indicate that ionic repulsion and osmotic pressure effects are significant only within crosslinked hydrogels at buffer pH values greater than the pK_a of the network-immobilized acid species.

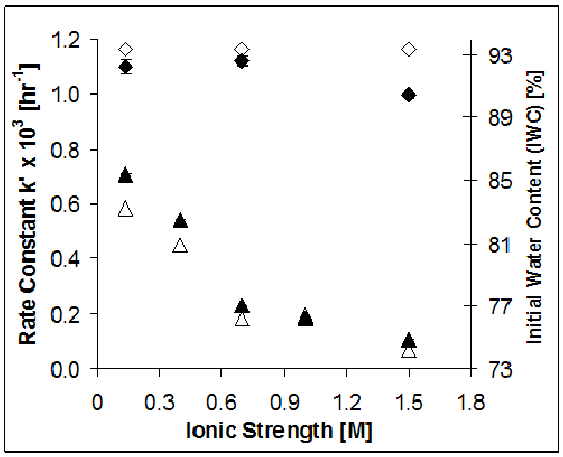

Figure A.3 Dependence of kinetic rate constants for PLA-b-PEG-b-PLA macromer degradation on buffer ionic strength: k'_{gel} (▲) and water content (△) for crosslinked gels. k'_{soln} (◆) and water content (◇) for macromer in solution. [For all data: Solution: 6.7 wt% PEGPLA2, Gel: 30 wt% PEGPLA1; pH = 7.4; n=3, error bars = ± std. dev.]

A.2.3.4 Effect of macromer concentration

The bulk water contents of the two-component macromer solutions are determined solely by their macromer concentrations. Therefore, to directly observe the effect of water content on the degradation rate constant of soluble macromers (k'soln), PLA-b-PEG-b-PLA solutions with macromer weight percents of 5, 10, 15 and 20 wt%, corresponding to water contents of 95, 90, 85 and 80 wt% were prepared and allowed to degrade in a well defined buffer solution (pH 7.4 and ionic strength 0.135M) at 37°C. As described above, the degradation rate constant k'soln was calculated by measuring the change in lactic acid concentration over time. The open symbols in Figure A.4 show the increase in k'soln with increase in water content.

Extrapolating from the experimental data point at 80% water content (k'soln = 8.2 x 10^{-4} hr^{-1}), measured values of k'soln increase proportionately with water content as predicted by the pseudo first-order kinetic assumption (dashed line). Similar values of k'soln are obtained using a second macromer, indicating that within the range of macromers tested (see Table A.1), variations in percent acrylation and PLA block size have no significant effect on the k'soln of macromer solutions with relatively high water contents (open triangles and open circles in Figure A.4).

Buffer ionic strength affects gel water content as shown previously in Figure A.3. Gel water content can also be varied by altering macromer concentration in the prepolymer solution. A lower macromer concentration during network formation leads to lower crosslinking densities due to a greater degree of macromer cyclization and relaxation of the backbone polymer chains.[208, 212-215, 239] As described by the Flory-Rehner equation[218] (Equation 3 and 4), lower crosslinking densities lead to higher gel swelling ratios and water contents. Therefore, to systematically vary the water content experienced by the PLA ester bonds during degradation while maintaining a constant pH and ionic strength, gels with initial water contents of 93, 91, 84, and 81 wt % were prepared using 7, 10, 20 and 30 wt % macromer solutions. As shown by the solid squares in Figure A.4, the values

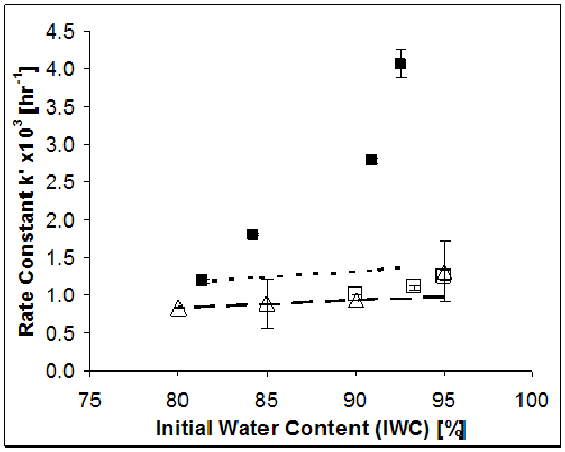

Figure A.4 Dependence of kinetic rate constants for PLA-b-PEG-b-PLA macromer degradation on water content: k'_{soln} for two soluble PLA-b-PEG-b-PLA macromers (△, PEGPLA1; □, PEGPLA2); k'_{gel} of crosslinked PLA-b-PEG-b-PLA macromer (■, PEGPLA2); Predicted behavior of k'_{soln} (- - -) and k'_{gel} (— - —) according to pseudo first-order kinetics of ester bond degradation. [All data at pH 7.4, Ionic Strength 0.135M, n=3, error bars = ± std. dev.]

of k'gel increase more rapidly with initial water content than the measured k'soln values. This dramatic increase results from a corresponding decrease in macromer concentration during network formation and is similar to the trend seen in Figure A.3 as ionic strength is decreased. The data in Figure A.4 indicate an decrease in water content of ~12% results in a significant 71% decrease in k'gel (from 1.2 x 10-3hr-1 to 4.1 x 10-3hr-1). Therefore, in gel form the pseudo first-order kinetic constant for hydrolysis is much more sensitive to water content than predicted by the kinetic theory or seen in soluble systems. Furthermore, the increased sensitivity of the degradation kinetics to changes in the local water concentration is independent of whether those changes are due to variations in ionic strength (environmental parameter) or macromer concentration (structural parameter).

A.2.4 Conclusions

Degradation behavior of PLA-b-PEG-b-PLA macromers in soluble form and insoluble, photocrosslinked form was compared by direct examination of the respective degradation kinetic constants, k'_{soln} and k'_{gel}. The time-dependent production of lactic acid from aqueous solutions of PLA-b-PEG-b-PLA was used to quantify k'_{soln}, while k'_{gel} was estimated from the change in the mass swelling ratio of photocrosslinked PLA-b-PEG-b-PLA gels with degradation time. Kinetic constants obtained from both systems under a variety of degradation conditions ranged from 1.7×10^{-4} to 4.1×10^{-3} hr^{-1} and were similar to one another and to previously reported values. Close examination of these kinetic constants demonstrates that network structure definitively influences macromer degradation behavior. Specifically, the apparent degradation kinetic constants of macromers assembled into crosslinked hydrogels are more sensitive to fluctuations in macromer chemistry as well as pH, ionic strength, and water content of the bulk environment compared to those of soluble macromers. Degradation of soluble

macromer was observed to be a complex function of pH, displaying a minimum value of k'_{soln} at pH 4, similar to previous observations of pure PLA systems. However, this minimum was shifted to pH 3 during degradation of crosslinked macromers. Increasing buffer ionic strength counteracted the charge repulsion and osmotic pressure effects occurring inside crosslinked PLA-b-PEG-b-PLA gels at high pH, decreasing gel swelling and k'_{gel}. However, increasing the buffer ionic strength had no effect on values of k'_{soln} and the rate of soluble macromer degradation. These experiments indicate that the difference between the pH-dependent degradation behavior of soluble versus crosslinked PLA-b-PEG-b-PLA macromers results from ionization of network-immobilized lactic acid and acrylic acid species that increases the water content of crosslinked PLA-b-PEG-b-PLA networks in all but strongly acidic solutions.

The results of the current studies also indicate the rate of PLA-b-PEG-b-PLA macromer degradation in a buffered solution at constant pH and temperature to be primarily a function of water content. For soluble macromer solutions, water content was shown to be a function of macromer concentration but not to vary to any significant extent with changes in ionic strength or pH. When the soluble macromer concentration was decreased, k'_{soln} increased linearly and in proportion to the corresponding increase in water content as predicted by the pseudo first-order kinetic equation. This behavior was independent of macromer chemistry within the range of macromers studied. However, increasing gel water content by decreasing macromer concentration during photocrosslinking of PLA-b-PEG-b-PLA hydrogels lead to an approximately six-fold greater increase in k'_{gel} than predicted by the pseudo first-order kinetic equation. The similar increases in k'_{gel} observed with a decrease in either ionic strength (environmental parameter) or macromer concentration (structural parameter) indicate that k'_{gel} for a given macromer is dependent on the absolute gel water content and independent of whether this

water concentration is manipulated by changes in solution or network properties. Unlike the soluble system, measured values of k'_{gel} vary significantly with slight changes in macromer chemistry. While water transport is identical in the highly swollen, crosslinked networks, slight differences in crosslinking density and network structure most likely affect the rates at which ionic degradation products are released from the gels. Differences in the concentration of ionic species within the degrading networks affect the response of the local gel environment to bulk solution conditions. Therefore, the results of this study indicate that the crosslinking of PLA-b-PEG-b-PLA macromers affects the rate and sensitivity of their hydrolytic degradation to bulk solution conditions such as water concentration, pH and ionic strength. These differences must be taken into account when designing crosslinked degradable gels for clinical applications and indicates their sensitivity to external stimuli as well as their potential as stimuli-responsive materials.

A.2.5 Acknowledgements

The authors thank Chien-Chi Lin for assistance with the synthesis of the PLA-b-PEG-b-PLA diacrylate macromers and Dr. Karen Burg and David Orr of the Department of Bioengineering at Clemson University for assistance with lactic acid measurements. Funding was provided for this work through a grant from the NSF-EPSCoR program and the Department of Chemical and Biomolecular Engineering at Clemson University.

7. References

1. Rao, C.R.K. and D.C. Trivedi, *Chemical and electrochemical depositions of platinum group metals and their applications.* Coordination Chemistry Reviews, 2005. **249**(5-6): p. 613-631.
2. Hirvonen, J.K., *Ion-Beam Processing for Surface Modification.* Annual Review of Materials Science, 1989. **19**: p. 401-417.
3. McCafferty, E., et al., *Naval Research Laboratory Surface Modification Program - Ion-Beam and Laser Processing of Metal-Surfaces for Improved Corrosion-Resistance.* Materials Science and Engineering, 1987. **86**: p. 1-17.
4. Schulz, U., *Review of modern techniques to generate antireflective properties on thermoplastic polymers.* Applied Optics, 2006. **45**(7): p. 1608-1618.
5. Cobley, A.J., *Alternative surface modification processes in metal finishing and electronic manufacturing industries.* Transactions of the Institute of Metal Finishing, 2007. **85**(6): p. 293-297.
6. Park, J.H., ed. *Chemical Vapor Deposition*. 1st ed., ed. J.H. Park. Vol. 2. 2001, ASM International. 482.
7. Asai, S. and Y. Wada, *Technology challenges for integration near and below 0.1 mu m.* Proceedings of the Ieee, 1997. **85**(4): p. 505-520.
8. Decker, C., *Kinetic study and new applications of UV radiation curing.* Macromolecular Rapid Communications, 2002. **23**(18): p. 1067-1093.
9. Bradley, E.L., W.A. Read, and L. Castle, *Investigation into the migration potential of coating materials from cookware products.* Food Additives and Contaminants, 2007. **24**(3): p. 326-335.
10. Begley, T.H., et al., *Perfluorochemicals: Potential sources of and migration from food packaging.* Food Additives and Contaminants, 2005. **22**(10): p. 1023-1031.
11. Paso, K., et al., *Novel Surfaces with Applicability for Preventing Wax Deposition: A Review.* Journal of Dispersion Science and Technology, 2009. **30**(6): p. 757-781.
12. Chiang, Y.-C., et al., *Sulfobetaine-grafted poly(vinylidene fluoride) ultrafiltration membranes exhibit excellent antifouling property.* Journal of Membrane Science, 2009. **339**(1-2): p. 151-159.
13. Niinomi, M., *Metallic biomaterials.* Journal of Artificial Organs, 2008. **11**(3): p. 105-110.
14. Liu, X.Y., P.K. Chu, and C.X. Ding, *Surface modification of titanium, titanium alloys, and related materials for biomedical applications.* Materials Science & Engineering R-Reports, 2004. **47**(3-4): p. 49-121.
15. Geetha, M., et al., *Ti based biomaterials, the ultimate choice for orthopaedic implants - A review.* Progress in Materials Science, 2009. **54**(3): p. 397-425.
16. Singh, R. and N.B. Dahotre, *Corrosion degradation and prevention by surface modification of biometallic materials.* Journal of Materials Science-Materials in Medicine, 2007. **18**(5): p. 725-751.
17. Turos, A., et al., *The effects of ion bombardment of ultra-high molecular weight polyethylene.* Nuclear Instruments & Methods in Physics Research Section B-Beam Interactions with Materials and Atoms, 2006. **249**: p. 660-664.
18. Tirrell, M., E. Kokkoli, and M. Biesalski, *The role of surface science in bioengineered materials.* Surface Science, 2002. **500**(1-3): p. 61-83.

19. Sevast'yanov, V.I. and V.N. Vasilets, *Plasmochemical modification of fluorocarbon polymers for creation of new hemocompatible materials.* Russian Journal of General Chemistry, 2009. **79**(3): p. 596-605.
20. Poncin-Epaillard, F. and G. Legeay, *Surface engineering of biomaterials with plasma techniques.* Journal of Biomaterials Science-Polymer Edition, 2003. **14**(10): p. 1005-1028.
21. Jian, Y., et al., *Fabrication and surface modification of macroporous poly(lactic acid) and poly(L-lactic-co-glycolic acid) (70/30) cell scaffolds for human skin fibroblast cell culture.* Journal of Biomedical Materials Research, 2002. **62**(3): p. 438-446.
22. Faucheux, N., et al., *Self-assembled monolayers with different terminating groups as model substrates for cell adhesion studies.* Biomaterials, 2004. **25**(14): p. 2721-2730.
23. Vallieres, K., E. Petitclerc, and G. Laroche, *Covalent grafting of fibronectin onto plasma-treated PTFE: Influence of the conjugation strategy on fibronectin biological activity.* Macromolecular Bioscience, 2007. **7**(5): p. 738-745.
24. Pasqui, D., A. Atrei, and R. Barbucci, *A novel strategy to obtain, a hyaluronan monolayer on solid substrates.* Biomacromolecules, 2007. **8**(11): p. 3531-3539.
25. Yanker, D.M. and J.A. Maurer, *Direct printing of trichlorosilanes on glass for selective protein adsorption and cell growth.* Molecular Biosystems, 2008. **4**(6): p. 502-504.
26. Scholl, M., et al., *Ordered networks of rat hippocampal neurons attached to silicon oxide surfaces.* Journal of Neuroscience Methods, 2000. **104**(1): p. 65-75.
27. Herbert, C.B., et al., *Micropatterning gradients and controlling surface densities of photoactivatable biomolecules on self-assembled monolayers of oligo(ethylene glycol) alkanethiolates.* Chemistry & Biology, 1997. **4**(10): p. 731-737.
28. Angus, H., R. Srinath, and C. Ashutosh, *In Pursuit of Zero: Polymer Brushes that Resist the Adsorption of Proteins.* Advanced Materials, 2009. **21**(23): p. 2441-2446.
29. Xia, N., et al., *Functionalized Poly(ethylene glycol)-Grafted Polysiloxane Monolayers for Control of Protein Binding.* Langmuir, 2002. **18**(8): p. 3255-3262.
30. Guo, Z., et al., *Self-assembly of silanated poly(ethylene glycol) on silicon and glass surfaces for improved haemocompatibility.* Applied Surface Science, 2009. **255**(15): p. 6771-6780.
31. Archambault, J.G. and J.L. Brash, *Protein resistant polyurethane surfaces by chemical grafting of PEO: amino-terminated PEO as grafting reagent.* Colloids and Surfaces B-Biointerfaces, 2004. **39**(1-2): p. 9-16.
32. Bozukova, D., et al., *Improved performances of intraocular lenses by poly(ethylene glycol) chemical coatings.* Biomacromolecules, 2007. **8**(8): p. 2379-2387.
33. Shoichet, M.S., et al., *Poly(Ethylene Oxide) Grafted Thermoplastic Membranes for Use as Cellular Hybrid Bioartificial Organs in the Central-Nervous-System.* Biotechnology and Bioengineering, 1994. **43**(7): p. 563-572.
34. Alcantar, N.A., E.S. Aydil, and J.N. Israelachvili, *Polyethylene glycol-coated biocompatible surfaces.* Journal of Biomedical Materials Research, 2000. **51**(3): p. 343-351.
35. McPherson, T.B., H.S. Shim, and K. Park, *Grafting of PEO to glass, nitinol, and pyrolytic carbon surfaces by gamma irradiation.* Journal of Biomedical Materials Research, 1997. **38**(4): p. 289-302.
36. Zhao, B. and W.J. Brittain, *Polymer brushes: surface-immobilized macromolecules.* Progress in Polymer Science, 2000. **25**(5): p. 677-710.

37. Raynor, J.E., et al., *Polymer brushes and self-assembled monolayers: Versatile platforms to control cell adhesion to biomaterials (Review).* Biointerphases, 2009. **4**(2): p. FA3-FA16.
38. Lee, S.-D., et al., *Plasma-induced grafted polymerization of acrylic acid and subsequent grafting of collagen onto polymer film as biomaterials.* Biomaterials, 1996. **17**(16): p. 1599-1608.
39. Ren, J.R., et al., *Surface modification of polyethylene terephthalate with albumin and gelatin for improvement of anticoagulation and endothelialization.* Applied Surface Science, 2008. **255**(2): p. 263-266.
40. Insup, N. and A.H. Jeffrey, *Photograft polymerization of acrylate monomers and macromonomers on photochemically reduced PTFE films.* Journal of Polymer Science Part A: Polymer Chemistry, 1997. **35**(16): p. 3467-3482.
41. Shin, Y.M., et al., *Modulation of spreading, proliferation, and differentiation of human mesenchymal stem cells on gelatin-immobilized poly(L-lactide-co-epsilon-caprolactone) substrates.* Biomacromolecules, 2008. **9**(7): p. 1772-1781.
42. Chang, Y., et al., *Biofouling-resistance expanded poly(tetrafluoroethylene) membrane with a hydrogel-like layer of surface-immobilized poly(ethylene glycol) methacrylate for human plasma protein repulsions.* Journal of Membrane Science, 2008. **323**(1): p. 77-84.
43. Ko, Y.G., et al., *Immobilization of poly(ethylene glycol) or its sulfonate onto polymer surfaces by ozone oxidation.* Biomaterials, 2001. **22**(15): p. 2115-2123.
44. Xu, J.M., et al., *Ozone-induced grafting phosphorylcholine polymer onto silicone film grafting 2-methacryloyloxyethyl phosphorylcholine onto silicone film to improve hemocompatibility.* Colloids and Surfaces B-Biointerfaces, 2003. **30**(3): p. 215-223.
45. Yuan, Y.L., et al., *Grafting sulfobetaine monomer onto silicone surface to improve haemocompatibility.* Polymer International, 2004. **53**(1): p. 121-126.
46. Yuan, Y.L., et al., *Surface modification of SPEU films by ozone induced graft copolymerization to improve hemocompatibility.* Colloids and Surfaces B-Biointerfaces, 2003. **29**(4): p. 247-256.
47. Yuan, Y.L., et al., *Polyurethane vascular catheter surface grafted with zwitterionic sulfobetaine monomer activated by ozone.* Colloids and Surfaces B-Biointerfaces, 2004. **35**(1): p. 1-5.
48. Yuan, J., et al., *Chemical graft polymerization of sulfobetaine monomer on polyurethane surface for reduction in platelet adhesion.* Colloids and Surfaces B-Biointerfaces, 2004. **39**(1-2): p. 87-94.
49. Shan, B., et al., *Ozone-induced grafting of a sulfoammonium zwitterionic polymer onto low-density polyethylene film for improving hemocompatibility.* Journal of Applied Polymer Science, 2006. **101**(6): p. 3697-3703.
50. Helary, G., et al., *A new approach to graft bioactive polymer on titanium implants: Improvement of MG 63 cell differentiation onto this coating.* Acta Biomaterialia, 2009. **5**(1): p. 124-133.
51. Jin, Z.L., et al., *Protein-resistant polyurethane prepared by surface-initiated atom transfer radical graft polymerization (ATRgP) of water-soluble polymers: Effects of main chain and side chain lengths of grafts.* Colloids and Surfaces B-Biointerfaces, 2009. **70**(1): p. 53-59.

52. Kizhakkedathu, J.N., et al., *Poly(oligo(ethylene glycol)acrylamide) Brushes by Surface Initiated Polymerization: Effect of Macromonomer Chain Length on Brush Growth and Protein Adsorption from Blood Plasma.* Langmuir, 2009. **25**(6): p. 3794-3801.
53. Andruzzi, L., et al., *Oligo(ethylene glycol) containing polymer brushes as bioselective surfaces.* Langmuir, 2005. **21**(6): p. 2495-2504.
54. Ignatova, M., et al., *Synthesis of copolymer brushes endowed with adhesion to stainless steel surfaces and antibacterial properties by controlled nitroxide-mediated radical polymerization.* Langmuir, 2004. **20**(24): p. 10718-10726.
55. Harris, B.P., et al., *Photopatterned Polymer Brushes Promoting Cell Adhesion Gradients.* Langmuir, 2006. **22**(10): p. 4467-4471.
56. Harris, B.P. and A.T. Metters, *Generation and Characterization of Photopolymerized Polymer Brush Gradients.* Macromolecules, 2006. **39**(8): p. 2764-2772.
57. Rahane, S.B., S.M. Kilbey, and A.T. Metters, *Kinetics of Surface-Initiated Photoiniferter-Mediated Photopolymerization.* Macromolecules, 2005. **38**(20): p. 8202-8210.
58. Chen, J.K., et al., *Using Solvent Immersion to Fabricate Variably Patterned Poly(methyl methacrylate) Brushes on Silicon Surfaces.* Macromolecules, 2008. **41**(22): p. 8729-8736.
59. Li, L.H., et al., *Fabrication of Thermoresponsive Polymer Gradients for Study of Cell Adhesion and Detachment.* Langmuir, 2008. **24**(23): p. 13632-13639.
60. Yebra, D.M., S. Kiil, and K. Dam-Johansen, *Antifouling technology - past, present and future steps towards efficient and environmentally friendly antifouling coatings.* Progress in Organic Coatings, 2004. **50**(2): p. 75-104.
61. Zhou, F., et al., *Influence of nitrogen ion implantation fluences on surface structure and tribological properties of SiC ceramics in water-lubrication.* Applied Surface Science, 2009. **255**(9): p. 5079-5087.
62. Hadjichristov, G.B., et al., *Silicon ion implanted PMMA for soft electronics.* Organic Electronics, 2008. **9**(6): p. 1051-1060.
63. Han, S., et al., *Polymer surface modification by plasma source ion implantation.* Surface & Coatings Technology, 1997. **93**(2-3): p. 261-264.
64. Pelletier, J. and A. Anders, *Plasma-based ion implantation and deposition: A review of physics, technology, and applications.* Ieee Transactions on Plasma Science, 2005. **33**(6): p. 1944-1959.
65. Erck, R.A., et al., *Ion-Beam-Assisted Surface Modifications for Friction and Wear Reduction.* Lubrication Engineering, 1992. **48**(4): p. 307-317.
66. Pogrebnjak, A.D. and Y.N. Tyurin, *Modification of material properties and coating deposition using plasma jets.* Physics-Uspekhi, 2005. **48**(5): p. 487-514.
67. Brown, I.G., *Cathodic arc deposition of films.* Annual Review of Materials Science, 1998. **28**: p. 243-269.
68. Radhakrishnan, S., N. Sonawane, and C.R. Siju, *Epoxy powder coatings containing polyaniline for enhanced corrosion protection.* Progress in Organic Coatings, 2009. **64**(4): p. 383-386.
69. Masson, F., et al., *UV-curable formulations for UV-transparent optical fiber coatings I. Acrylic resins.* Progress in Organic Coatings, 2004. **49**(1): p. 1-12.
70. Hilal, N., et al., *Methods employed for control of fouling in MF and UF membranes: A comprehensive review.* Separation Science and Technology, 2005. **40**(10): p. 1957-2005.

71. Yu, H.-Y., et al., *Thermo- and pH-responsive polypropylene microporous membrane prepared by the photoinduced RAFT-mediated graft copolymerization.* Journal of Membrane Science. **In Press, Accepted Manuscript**.
72. Anderson, J.M., *Biological responses to materials.* Annual Review of Materials Research, 2001. **31**: p. 81-110.
73. de Jonge, L.T., et al., *Organic-inorganic surface modifications for titanium implant surfaces.* Pharmaceutical Research, 2008. **25**(10): p. 2357-2369.
74. Bielinski, D.M., et al., *Influence of ion bombardment on tribological properties of UHMWPE.* Tribology Letters, 2006. **23**(2): p. 139-143.
75. Lipinski, P., et al., *Biomedical aspects of ion bombardment of polyethylene.* Vacuum, 2009. **83**: p. S200-S203.
76. Bi, H.Y., et al., *Deposition of PEG onto PMMA microchannel surface to minimize nonspecific adsorption.* Lab on a Chip, 2006. **6**(6): p. 769-775.
77. Chen, H., et al., *Biocompatible polymer materials: Role of protein-surface interactions.* Progress in Polymer Science, 2008. **33**(11): p. 1059-1087.
78. Liu, J.K., et al., *Surface-modified poly(methyl methacrylate) capillary electrophoresis microchips for protein and peptide analysis.* Analytical Chemistry, 2004. **76**(23): p. 6948-6955.
79. Ghanbari, H., et al., *Polymeric heart valves: new materials, emerging hopes.* Trends in Biotechnology, 2009. **27**(6): p. 359-367.
80. Sydow-Plum, G. and M. Tabrizian, *Review of stent coating strategies: clinical insights.* Materials Science and Technology, 2008. **24**(9): p. 1127-1143.
81. Yin, M., et al., *Development of mussel adhesive polypeptide mimics coating for in-situ inducing re-endothelialization of intravascular stent devices.* Biomaterials, 2009. **30**(14): p. 2764-2773.
82. de Mel, A., et al., *Biofunctionalization of Biomaterials for Accelerated in Situ Endothelialization: A Review.* Biomacromolecules, 2008. **9**(11): p. 2969-2979.
83. Schmidt, C.E. and J.B. Leach, *Neural tissue engineering: Strategies for repair and regeneration.* Annual Review Of Biomedical Engineering, 2003. **5**: p. 293-347.
84. Mai, J., et al., *Axon Initiation and Growth Cone Turning on Bound Protein Gradients.* Journal of Neuroscience, 2009. **29**(23): p. 7450-7458.
85. Baier, H. and F. Bonhoeffer, *Axon Guidance by Gradients of a Target-Derived Component.* Science, 1992. **255**(5043): p. 472-475.
86. Cao, X. and M.S. Shoichet, *Investigating the synergistic effect of combined neurotrophic factor concentration gradients to guide axonal growth.* Neuroscience, 2003. **122**(2): p. 381-389.
87. Li, G.N., J. Liu, and D. Hoffman-Kim, *Multi-molecular gradients of permissive and inhibitory cues direct neurite outgrowth.* Annals of Biomedical Engineering, 2008. **36**(6): p. 889-904.
88. Tan, J. and J.L. Brash, *Nonfouling biomaterials based on polyethylene oxide-containing amphiphilic triblock copolymers as surface modifying additives: Adsorption of proteins from human plasma to copolymer/polyurethane blends.* Journal of Biomedical Materials Research Part A, 2009. **90A**(1): p. 196-204.
89. Chen, H., M.A. Brook, and H. Sheardown, *Silicone elastomers for reduced protein adsorption.* Biomaterials, 2004. **25**(12): p. 2273-2282.

90. Place, E.S., et al., *Synthetic polymer scaffolds for tissue engineering.* Chemical Society Reviews, 2009. **38**(4): p. 1139-1151.
91. Place, E.S., N.D. Evans, and M.M. Stevens, *Complexity in biomaterials for tissue engineering.* Nature Materials, 2009. **8**(6): p. 457-470.
92. Ishihara, K., et al., *Polyethylene/phospholipid polymer alloy as an alternative to poly(vinylchloride)-based materials.* Biomaterials, 2004. **25**(6): p. 1115-1122.
93. Wang, S.G., W.J. Cui, and J.Z. Bei, *Bulk and surface modifications of polylactide.* Analytical and Bioanalytical Chemistry, 2005. **381**(3): p. 547-556.
94. Lee, H.J., et al., *Platelet and bacterial repellence on sulfonated poly(ethylene glycol)-acrylate copolymer surfaces.* Colloids and Surfaces B-Biointerfaces, 2000. **18**(3-4): p. 355-370.
95. Mrksich, M. and G.M. Whitesides, *Using self-assembled monolayers to understand the interactions of man-made surfaces with proteins and cells.* Annual Review of Biophysics and Biomolecular Structure, 1996. **25**: p. 55-78.
96. Alves, C.M., et al., *Plasma surface modification of poly(D,L-lactic acid) as a tool to enhance protein adsorption and the attachment of different cell types.* Journal of Biomedical Materials Research Part B-Applied Biomaterials, 2008. **87B**(1): p. 59-66.
97. Yoshinari, M., et al., *Adsorption behavior of antimicrobial peptide histatin 5 on PMMA.* Journal of Biomedical Materials Research Part B-Applied Biomaterials, 2006. **77B**(1): p. 47-54.
98. Hayat, U., et al., *Esca Investigation of Low-Temperature Ammonia Plasma-Treated Polyethylene Substrate for Immobilization of Protein.* Biomaterials, 1992. **13**(11): p. 801-806.
99. Siow, K.S., et al., *Plasma methods for the generation of chemically reactive surfaces for biomolecule immobilization and cell colonization - A review.* Plasma Processes and Polymers, 2006. **3**(6-7): p. 392-418.
100. Sivaraman, B., K.P. Fears, and R.A. Latour, *Investigation of the Effects of Surface Chemistry and Solution Concentration on the Conformation of Adsorbed Proteins Using an Improved Circular Dichroism Method.* Langmuir, 2009. **25**(5): p. 3050-3056.
101. Ostuni, E., et al., *A survey of structure-property relationships of surfaces that resist the adsorption of protein.* Langmuir, 2001. **17**(18): p. 5605-5620.
102. Ostuni, E., et al., *Self-assembled monolayers that resist the adsorption of proteins and the adhesion of bacterial and mammalian cells.* Langmuir, 2001. **17**(20): p. 6336-6343.
103. Kristin, B.M., U. Tatiana, and W.G. David, *Modulating fibroblast adhesion, spreading, and proliferation using self-assembled monolayer films of alkylthiolates on gold.* Journal of Biomedical Materials Research, 2000. **50**(3): p. 428-439.
104. Roberts, C., et al., *Using Mixed Self-Assembled Monolayers Presenting RGD and (EG)3OH Groups To Characterize Long-Term Attachment of Bovine Capillary Endothelial Cells to Surfaces.* Journal of the American Chemical Society, 1998. **120**(26): p. 6548-6555.
105. Mahapatro, A., et al., *Drug delivery from therapeutic self-assembled monolayers (T-SAMs) on 316L stainless steel.* Current Topics in Medicinal Chemistry, 2008. **8**(4): p. 281-289.
106. Bain, J.R. and A.S. Hoffman, *Tissue-culture surfaces with mixtures of aminated and fluorinated functional groups. Part 2. Growth and function of transgenic rat insulinoma*

cells (betaG I/17). Journal of Biomaterials Science, Polymer Edition, 2003. **14**: p. 341-367.
107. Pitt, W.G., et al., *Attachment of hyaluronan to metallic surfaces.* Journal of Biomedical Materials Research Part A, 2004. **68A**(1): p. 95-106.
108. Chaki, N.K. and K. Vijayamohanan, *Self-assembled monolayers as a tunable platform for biosensor applications.* Biosensors and Bioelectronics, 2002. **17**(1-2): p. 1-12.
109. Moore, E., D. O'Connell, and P. Galvin, *Surface characterisation of indium-tin oxide thin electrode films for use as a conducting substrate in DNA sensor development.* Thin Solid Films, 2006. **515**(4): p. 2612-2617.
110. Tlili, A., et al., *A novel silicon nitride biosensor for specific antibody-antigen interaction.* Materials Science & Engineering C-Biomimetic and Supramolecular Systems, 2005. **25**(4): p. 490-495.
111. Falconnet, D., et al., *Surface engineering approaches to micropattern surfaces for cell-based assays.* Biomaterials, 2006. **27**(16): p. 3044-3063.
112. Jung, D.R., et al., *Topographical and physicochemical modification of material surface to enable patterning of living cells.* Critical Reviews in Biotechnology, 2001. **21**(2): p. 111-154.
113. Christopher, S.C., et al., *Micropatterned Surfaces for Control of Cell Shape, Position, and Function.* Biotechnology Progress, 1998. **14**(3): p. 356-363.
114. Zhang, S., et al., *Biological surface engineering: a simple system for cell pattern formation.* Biomaterials, 1999. **20**(13): p. 1213-1220.
115. Klein, C.L., M. Scholl, and A. Maelicke, *Neuronal networks in vitro: formation and organization on biofunctionalized surfaces.* Journal of Materials Science: Materials in Medicine, 1999. **10**(12): p. 721-727.
116. Hypolite, C.L., et al., *Formation of Microscale Gradients of Protein Using Heterobifunctional Photolinkers.* Bioconjugate Chemistry, 1997. **8**(5): p. 658-663.
117. Otsuka, H., Y. Nagasaki, and K. Kataoka, *Surface characterization of functionalized polylactide through the coating with heterobifunctional poly(ethylene glycol)/polylactide block copolymers.* Biomacromolecules, 2000. **1**(1): p. 39-48.
118. Bearinger, J.P., et al., *Chemisorbed poly(propylene sulphide)-based copolymers resist biomolecular interactions.* Nat Mater, 2003. **2**(4): p. 259-264.
119. Emmenegger, C.R., et al., *Interaction of Blood Plasma with Antifouling Surfaces.* Langmuir, 2009. **25**(11): p. 6328-6333.
120. Wyszogrodzka, M. and R. Haag, *Synthesis and Characterization of Glycerol Dendrons, Self-Assembled Monolayers on Gold: A Detailed Study of Their Protein Resistance.* Biomacromolecules, 2009. **10**(5): p. 1043-1054.
121. Caro, A., et al., *Grafting of Lysozyme and/or Poly(ethylene glycol) to Prevent Biofilm Growth on Stainless Steel Surfaces.* Journal of Physical Chemistry B, 2009. **113**(7): p. 2101-2109.
122. Gombotz, W.R., et al., *Protein Adsorption to Poly(Ethylene Oxide) Surfaces.* Journal of Biomedical Materials Research, 1991. **25**(12): p. 1547-1562.
123. Thierry, B., et al., *Biomimetic Hemocompatible Coatings through Immobilization of Hyaluronan Derivatives on Metal Surfaces.* Langmuir, 2008. **24**(20): p. 11834-11841.

124. Adden, N., et al., *Screening of photochemically grafted polymer films for compatibility with osteogenic precursor cells.* Journal of Biomaterials Science-Polymer Edition, 2007. **18**(3): p. 303-316.
125. To, Y., et al., *Surface modification of plastic, glass and titanium by photoimmobilization of polyethylene glycol for antibiofouling.* Acta Biomaterialia, 2007. **3**(6): p. 1024-1032.
126. Pandiyaraj, K.N., et al., *Glow discharge plasma-induced immobilization of heparin and insulin on polyethylene terephthalate film surfaces enhances anti-thrombogenic properties.* Materials Science & Engineering C-Biomimetic and Supramolecular Systems, 2009. **29**(3): p. 796-805.
127. Insup, N., et al., *Surface modification of poly(tetrafluoroethylene)with benzophenone and sodium hydride by ultraviolet irradiation.* Journal of Polymer Science Part A: Polymer Chemistry, 1997. **35**(8): p. 1499-1514.
128. Ma, Z.W., Z.W. Mao, and C.Y. Gao, *Surface modification and property analysis of biomedical polymers used for tissue engineering.* Colloids and Surfaces B-Biointerfaces, 2007. **60**(2): p. 137-157.
129. Patten, T.E. and K. Matyjaszewski, *Atom transfer radical polymerization and the synthesis of polymeric materials.* Advanced Materials, 1998. **10**(12): p. 901-+.
130. Wang, J.S. and K. Matyjaszewski, *Controlled Living Radical Polymerization - Halogen Atom-Transfer Radical Polymerization Promoted by a Cu(I)Cu(Ii) Redox Process.* Macromolecules, 1995. **28**(23): p. 7901-7910.
131. Hoshi, T., et al., *Protein adsorption resistant surface on polymer composite based on 2D- and 3D-controlled grafting of phospholipid moieties.* Applied Surface Science, 2008. **255**(2): p. 379-383.
132. Zhang, F., et al., *Functionalization of titanium surfaces via controlled living radical polymerization: From antibacterial surface to surface for osteoblast adhesion.* Industrial & Engineering Chemistry Research, 2007. **46**(26): p. 9077-9086.
133. Zainuddin, et al., *PHEMA hydrogels modified through the grafting of phosphate groups by ATRP support the attachment and growth of human corneal epithelial cells.* Journal of Biomaterials Applications, 2008. **23**(2): p. 147-168.
134. Sun, X.F., J.K. Liu, and M.L. Lee, *Surface modification of polymer microfluidic devices using in-channel atom transfer radical polymerization.* Electrophoresis, 2008. **29**(13): p. 2760-2767.
135. Nakayama, Y. and T. Matsuda, *Surface macromolecular architectural designs using photo-graft copolymerization based on photochemistry of benzyl N,N-diethyldithiocarbamate.* Macromolecules, 1996. **29**(27): p. 8622-8630.
136. Higashi, J., et al., *High-Spatioresolved Microarchitectural Surface Prepared by Photograft Copolymerization Using Dithiocarbamate: Surface Preparation and Cellular Responses.* Langmuir, 1999. **15**(6): p. 2080-2088.
137. Michael, H., M. Norbert, and L. Robert, *Oxygen scavengers and sensitizers for reduced oxygen inhibition in radical photopolymerization.* Journal of Polymer Science Part A: Polymer Chemistry, 2008. **46**(20): p. 6916-6927.
138. Sebra, R.P., et al., *Controlled polymerization chemistry to graft architectures that influence cell-material interactions.* Acta Biomaterialia, 2007. **3**(2): p. 151-161.

139. Vasita, R., K. Shanmugam, and D.S. Katti, *Improved biomaterials for tissue engineering applications: Surface modification of polymers.* Current Topics in Medicinal Chemistry, 2008. **8**(4): p. 341-353.
140. Archambault, J.G. and J.L. Brash, *Protein repellent polyurethane-urea surfaces by chemical grafting of hydroxyl-terminated poly(ethylene oxide): effects of protein size and charge.* Colloids and Surfaces B-Biointerfaces, 2004. **33**(2): p. 111-120.
141. Sheu, M.S., A.S. Hoffman, and J. Feijen, *A Glow-Discharge Treatment to Immobilize Poly(Ethylene Oxide) Poly(Propylene Oxide) Surfactants for Wettable and Nonfouling Biomaterials.* Journal of Adhesion Science and Technology, 1992. **6**(9): p. 995-1009.
142. Osterberg, E., et al., *Protein-Rejecting Ability of Surface-Bound Dextran in End-on and Side-on Configurations - Comparison to Peg.* Journal of Biomedical Materials Research, 1995. **29**(6): p. 741-747.
143. Lin, C.H., et al., *Hemocompatibility and cytocompatibility of styrenesulfonate-grafted PDMS-polyurethane-HEMA hydrogel.* Colloids and Surfaces B-Biointerfaces, 2009. **70**(1): p. 132-141.
144. Liu, S.X., J.T. Kim, and S. Kim, *Effect of polymer surface modification on polymer-protein interaction via hydrophilic polymer grafting.* Journal of Food Science, 2008. **73**(3): p. E143-E150.
145. Alves, P., et al., *Surface modification and characterization of thermoplastic polyurethane.* European Polymer Journal, 2009. **45**(5): p. 1412-1419.
146. Liu, F., et al., *Surface immobilization of polymer brushes onto porous poly(vinylidene fluoride) membrane by electron beam to improve the hydrophilicity and fouling resistance.* Polymer, 2007. **48**(10): p. 2910-2918.
147. Saito, N., S. Yamashita, and T. Matsuda, *Laser-irradiation-induced surface graft polymerization method.* Journal of Polymer Science Part a-Polymer Chemistry, 1997. **35**(4): p. 747-750.
148. Sebra, R.P., K.S. Anseth, and C.N. Bowman, *Integrated surface modification of fully polymeric microfluidic devices using living radical photopolymerization chemistry.* Journal of Polymer Science Part a-Polymer Chemistry, 2006. **44**(4): p. 1404-1413.
149. Rahane, S.B., et al., *Swelling behavior of multiresponsive poly(methacrylic acid)-block-poly (N-isopropylacrylamide) brushes synthesized using surface-initiated photoiniferter-mediated photopolymerization.* Advanced Functional Materials, 2008. **18**(8): p. 1232-1240.
150. Sebra, R.P., et al., *Surface grafted antibodies: Controlled architecture permits enhanced antigen detection.* Langmuir, 2005. **21**(24): p. 10907-10911.
151. Lee, H.J. and T. Matsuda, *Surface photograft polymerization on segmented polyurethane using the iniferter technique.* Journal of Biomedical Materials Research, 1999. **47**(4): p. 564-567.
152. Gupta, B., et al., *Plasma-induced craft polymerization of acrylic acid onto poly(ethylene terephthalate) films.* Journal of Applied Polymer Science, 2001. **81**(12): p. 2993-3001.
153. Kim, J.H., et al., *Surface modification of nanofiltration membranes to improve the removal of organic micro-pollutants (EDCs and PhACs) in drinking water treatment: Graft polymerization and cross-linking followed by functional group substitution.* Journal of Membrane Science, 2008. **321**(2): p. 190-198.

154. Luo, N., et al., *Surface-initiated photopolymerization of poly(ethylene glycol) methyl ether methacrylate on a diethyldithiocarbamate-mediated polymer substrate.* Macromolecules, 2002. **35**(7): p. 2487-2493.
155. Nakayama, Y., et al., *Spatio-resolved hyperbranched graft polymerized surfaces by iniferter-based photograft copolymerization.* Langmuir, 2002. **18**(7): p. 2601-2606.
156. Ward, J.H., R. Bashir, and N.A. Peppas, *Micropatterning of biomedical polymer surfaces by novel UV polymerization techniques.* Journal of Biomedical Materials Research, 2001. **56**(3): p. 351-360.
157. Sebra, R.P., et al., *Synthesis and photografting of highly pH-responsive polymer chains.* Sensors and Actuators B-Chemical, 2006. **119**(1): p. 127-134.
158. Diamanti, S., et al., *Reactive patterning via post-functionalization of polymer brushes utilizing disuccinimidyl carbonate activation to couple primary amines.* Polymer, 2008. **49**(17): p. 3770-3779.
159. Almeida, E., T.C. Diamantino, and O. de Sousa, *Marine paints: The particular case of antifouling paints.* Progress in Organic Coatings, 2007. **59**(1): p. 2-20.
160. Yu, J., *Biodegradation-based polymer surface erosion and surface renewal for foul-release at low ship speeds.* Biofouling, 2003. **19**: p. 83-90.
161. Dafforn, K.A., T.M. Glasby, and E.L. Johnston, *Differential effects of tributyltin and copper antifoulants on recruitment of non-indigenous species.* Biofouling, 2008. **24**(1): p. 23-33.
162. Burgess, J.G., et al., *The development of a marine natural product-based antifouling paint.* Biofouling, 2003. **19**: p. 197-205.
163. Rittschof, D., *Natural product antifoulants: One perspective on the challenges related to coatings development.* Biofouling, 2000. **15**(1-3): p. 119-127.
164. Coon, S.L. and D.B. Bonar, *Pharmacological evidence that □-adrenoceptors mediate metamorphosis of the pacific oyster, Crassostrea gigas.* Neuroscience, 1987. **23**(3): p. 1169-1174.
165. Coon, S.L., D.B. Bonar, and R.M. Weiner, *Chemical production of cultchless oyster spat using epinephrine and norepinephrine.* Aquaculture 1986. **58**: p. 255-262
166. Coon, S.L., D.B. Bonar, and R.M. Weiner, *Induction of settlement and metamorphosis of the Pacific oyster, Crassostrewa gigas (thunberg), by L-dopa and catecholamines.* Journal of experimental marine biology and ecology 1985. **94**(1-2-3): p. 211-221
167. Yamamoto, H., et al., *Roles of dopamine and serotonin in larval attachment of the barnacle, Balanus amphitrite.* Journal of Experimental Zoology, 1999. **284**(7): p. 746-758.
168. Dahms, H.-U., T. Jin, and P.-Y. Qian, *Adrenoceptor Compounds Prevent the Settlement of Marine Invertebrate Larvae: Balanus amphitrite (Cirripedia), Bugula neritina (Bryozoa) and Hydroides elegans (Polychaeta).* Biofouling, 2004. **20**(6): p. 313 - 321.
169. Dahlström, M., et al., *Surface active adrenoceptor compounds prevent the settlement of cyprid larvae of Balanus improvisus. Biofouling* Biofouling, 2000. **16**(4): p. 191-203.
170. Dahlström, M., et al., *Evidence for different pharmacological targets for imidazoline compounds inhibiting settlement of the barnacle Balanus improvisus.* Journal of Experimental Zoology Part A: Comparative Experimental Biology, 2005. **303A**(7): p. 551-562.
171. Gohad, N., *Development of a novel fouling deterrence strategy by understanding the effect of noradrenaline on the cells of Eastern oyster, Crassostrea virginica and cypris*

larvae of the Striped Barnacle, Balanus amphitrite, in *Biological Sciences*. 2008, Clemson University: Clemson. p. 121.
172. Gohad, N.V., *Development Of A Novel Fouling Deterrence Strategy By Understanding The Effect Of Noradrenaline On The Cells Of Eastern Oyster, Crassostrea Virginica And Cypris Larvae Of The Striped Barnacle, Balanus Amphitrite*, in *Biological Sciences*. 2008, Clemson University: Clemson.
173. Mrksich, M., *Tailored substrates for studies of attached cell culture.* Cellular and Molecular Life Sciences, 1998. **54**(7): p. 653-662.
174. Lacoste, A., A. Cueff, and S. Poulet, A., *P35-sensitive caspases, MAP kinases and Rho modulate □-adrenergic induction of apoptosis in mollusc immune cells.* Journal of Cell Science, 2002. **115**: p. 761-768.
175. Lacoste, A., et al., *Stress and stress-induced neuroendocrine changes increase the susceptibility of juvenile oysters (Crassostrea gigas) to Vibrio splendidus.* Appl Environ Microbiol, 2001. **67**(5): p. 2304-9.
176. Lacoste, A., et al., *Evidence for a form of adrenergic response to stress in the mollusc Crassostrea gigas.* J Exp Biol, 2001. **204**(Pt 7): p. 1247-55.
177. de Boer, B., et al., *"Living" free radical photopolymerization initiated from surface-grafted iniferter monolayers.* Macromolecules, 2000. **33**(2): p. 349-356.
178. Neri, S., et al., *Calcein-Acetyoxymethyl Cytotoxicity Assay: Standardization of a Method Allowing Additional Analyses on Recovered Effector Cells and Supernatants.* Clin. Diagn. Lab. Immunol., 2001. **8**(6): p. 1131-1135.
179. Hofer, M., N. Moszner, and R. Liska, *Oxygen Scavengers and Sensitizers for Reduced Oxygen Inhibition in Radical Photopolymerization.* Journal of Polymer Science Part a-Polymer Chemistry, 2008. **46**(20): p. 6916-6927.
180. Vencel, T., et al., *Oxygen exclusion from the organic solvents using ultrasound and comparison with other common techniques used in photochemical experiments.* Chemical Papers-Chemicke Zvesti, 2005. **59**(4): p. 271-274.
181. Gao, B., W. Bengt, and K.B. Wessléen, *Amphiphilic comb-shaped polymers from poly(ethylene glycol) macromonomers.* Journal of Polymer Science Part A: Polymer Chemistry, 1992. **30**(9): p. 1799-1808.
182. Hermanson, G.T., *Bioconjugate Techniques*. 2nd ed. 2008: Academic Press. 1323.
183. Laurencin, C.T., *Bone Graft Substitutes*, ed. C.T. Laurencin. 2003, West Conshohocken: ASTM International. 319.
184. Stevens, M.M., et al., *In vivo engineering of organs: The bone bioreactor.* Proceedings of the National Academy of Sciences of the United States of America, 2005. **102**(32): p. 11450-11455.
185. Breitbach, M., et al., *Potential risks of bone marrow cell transplantation into infarcted hearts.* Blood, 2007. **110**(4): p. 1362-1369.
186. Meiners, S. and M.L.T. Mercado, *Functional peptide sequences derived from extracellular matrix glycoproteins and their receptors - Strategies to improve neuronal regeneration.* Molecular Neurobiology, 2003. **27**(2): p. 177-195.
187. Vogel, V. and G. Baneyx, *The tissue engineering puzzle: A molecular perspective.* Annual Review of Biomedical Engineering, 2003. **5**: p. 441-463.
188. Wolman, M.A., et al., *Semaphorin3D regulates axon-axon interactions by modulating levels of l1 cell adhesion molecule.* Journal of Neuroscience, 2007. **27**(36): p. 9653-9663.

189. Miura, M., et al., *Functional expression of a full-length cDNA coding for rat neural cell adhesion molecule L1 mediates homophilic intercellular adhesion and migration of cerebellar neurons.* Journal of Biological Chemistry, 1992. **267**(15): p. 10752-10758.
190. Webb, K., et al., *Substrate-bound human recombinant L1 selectively promotes neuronal attachment and outgrowth in the presence of astrocytes and fibroblasts.* Biomaterials, 2001. **22**(10): p. 1017-1028.
191. Azemi, E., et al., *Surface immobilization of neural adhesion molecule L1 for improving the biocompatibility of chronic neural probes: In vitro characterization.* Acta Biomaterialia, 2008. **4**(5): p. 1208-1217.
192. Cribb, R.C., et al., *Baculovirus expression and bioactivity of a soluble 140 kDa extracellular cleavage fragment of L1 neural cell adhesion molecule.* Protein Expression and Purification, 2008. **57**(2): p. 172-179.
193. O'Reilly, D.R., L.K. Miller, and V.A. Luckow, *Baculovirus Expression Vectors: A Laboratory Manual*, ed. V.A. Luckow. 1994: Oxford University Press, US. 368.
194. Mei, Y., et al., *Tuning Cell Adhesion on Gradient Poly(2-hydroxyethyl methacrylate)-Grafted Surfaces.* Langmuir, 2005. **21**(26): p. 12309-12314.
195. Peppas, N.A. and J.H. Ward, *Biomimetic materials and micropatterned structures using iniferters.* Advanced Drug Delivery Reviews, 2004. **56**(11): p. 1587-1597.
196. Luo, N., et al., *A methacrylated photoiniferter as a chemical basis for microlithography: Micropatterning based on photografting polymerization.* Macromolecules, 2003. **36**(18): p. 6739-6745.
197. Reddy, S.K., et al., *Living radical photopolymerization induced grafting on thiol-ene based substrates.* Journal of Polymer Science Part a-Polymer Chemistry, 2005. **43**(10): p. 2134-2144.
198. Nakayama, Y. and T. Matsuda, *In situ observation of dithiocarbamate-based surface photograft copolymerization using quartz crystal microbalance.* Macromolecules, 1999. **32**(16): p. 5405-5410.
199. Silva, A.K.A., et al., *Growth Factor Delivery Approaches in Hydrogels.* Biomacromolecules, 2009. **10**(1): p. 9-18.
200. Glinel, K., et al., *Antibacterial and Antifouling Polymer Brushes Incorporating Antimicrobial Peptide.* Bioconjugate Chemistry, 2009. **20**(1): p. 71-77.
201. Yuan, S.J., et al., *Inorganic-Organic Hybrid Coatings on Stainless Steel by Layer-by-Layer Deposition and Surface-Initiated Atom-Transfer-Radical Polymerization for Combating Biocorrosion.* Acs Applied Materials & Interfaces, 2009. **1**(3): p. 640-652.
202. Xing, X.D., et al., *Preparation and Antibacterial Function of Quaternary Ammonium Salts Grafted Cellulose Fiber Initiated by Fe2+-H2O2 Redox.* Journal of Macromolecular Science Part a-Pure and Applied Chemistry, 2009. **46**(5): p. 560-565.
203. Rao, Y., et al., *Identification of a Peptide Sequence Involved in Homophilic Binding in the Neural Cell-Adhesion Molecule Ncam.* Journal of Cell Biology, 1992. **118**(4): p. 937-949.
204. Meiners, S., M.S.A. Nur-E-Kamal, and M.L.T. Mercado, *Identification of a neurite outgrowth-promoting motif within the alternatively spliced region of human tenascin-C.* Journal of Neuroscience, 2001. **21**(18): p. 7215-7225.
205. Sawhney, A.S., C.P. Pathak, and J.A. Hubbell, *Bioerodible Hydrogels Based on Photopolymerized Poly(Ethylene Glycol)-Co-Poly(Alpha-Hydroxy Acid) Diacrylate Macromers.* Macromolecules, 1993. **26**(4): p. 581-587.

206. Martens, P., et al., *A generalized bulk-degradation model for hydrogel networks formed from multivinyl cross-linking molecules.* Journal of Physical Chemistry B, 2001. **105**(22): p. 5131-5138.
207. Metters, A.T., K.S. Anseth, and C.N. Bowman, *A statistical kinetic model for the bulk degradation of PLA-b-PEG-b-PLA hydrogel networks: Incorporating network non-idealities.* Journal of Physical Chemistry B, 2001. **105**(34): p. 8069-8076.
208. Metters, A.T., C.N. Bowman, and K.S. Anseth, *A statistical kinetic model for the bulk degradation of PLA-b-PEG-b-PLA hydrogel networks.* Journal of Physical Chemistry B, 2000. **104**(30): p. 7043-7049.
209. Lu, S.X. and K.S. Anseth, *Release behavior of high molecular weight solutes from poly(ethylene glycol)-based degradable networks.* Macromolecules, 2000. **33**(7): p. 2509-2515.
210. Anseth, K.S., et al., *In situ forming degradable networks and their application in tissue engineering and drug delivery.* Journal of Controlled Release, 2002. **78**(1-3): p. 199-209.
211. Mason, M.N., et al., *Predicting controlled-release behavior of degradable PLA-b-PEG-b-PLA hydrogels.* Macromolecules, 2001. **34**(13): p. 4630-4635.
212. Metters, A.T., C.N. Bowman, and K.S. Anseth, *Verification of scaling laws for degrading PLA-b-PEG-b-PLA hydrogels.* Aiche Journal, 2001. **47**(6): p. 1432-1437.
213. Metters, A.T., K.S. Anseth, and C.N. Bowman, *Fundamental studies of a novel, biodegradable PEG-b-PLA hydrogel.* Polymer, 2000. **41**(11): p. 3993-4004.
214. Martens, P., T. Holland, and K.S. Anseth, *Synthesis and characterization of degradable hydrogels formed from acrylate modified poly(vinyl alcohol) macromers.* Polymer, 2002. **43**(23): p. 6093-6100.
215. Metters, A. and J. Hubbell, *Network formation and degradation behavior of hydrogels formed by Michael-type addition reactions.* Biomacromolecules, 2005. **6**(1): p. 290-301.
216. Martens, P.J., S.J. Bryant, and K.S. Anseth, *Tailoring the degradation of hydrogels formed from multivinyl poly(ethylene glycol) and poly(vinyl alcohol) macromers for cartilage tissue engineering.* Biomacromolecules, 2003. **4**(2): p. 283-292.
217. Martens, P.J., C.N. Bowman, and K.S. Anseth, *Degradable networks formed from multi-functional poly(vinyl alcohol) macromers: comparison of results from a generalized bulk-degradation model for polymer networks and experimental data.* Polymer, 2004. **45**(10): p. 3377-3387.
218. Flory, P.J., *Principles of Polymer Chemistry*. 1953, Ithaca, NY: Cornell University Press. 688.
219. Eliassi, A., H. Modarress, and G.A. Mansoori, *Measurement of activity of water in aqueous poly(ethylene glycol) solutions (Effect of excess volume on the Flory-Huggins chi-parameter).* Journal of Chemical and Engineering Data, 1999. **44**(1): p. 52-55.
220. Gopferich, A., *Polymer degradation and erosion: Mechanisms and applications.* European Journal Of Pharmaceutics And Biopharmaceutics, 1996. **42**(1): p. 1-11.
221. Loh, X.J., et al., *The in vitro hydrolysis of poly(ester urethane)s consisting of poly[(R)-3-hydroxybutyrate] and poly(ethylene glycol).* Biomaterials, 2006. **27**(9): p. 1841-1850.
222. Schliecker, G., et al., *Characterization of a homologous series of D,L-lactic acid oligomers; a mechanistic study on the degradation kinetics in vitro.* Biomaterials, 2003. **24**(21): p. 3835-3844.

223. Neradovic, D., et al., *Degradation mechanism and kinetics of thermosensitive polyacrylamides containing lactic acid side chains.* Macromolecules, 2003. **36**(20): p. 7491-7498.
224. Maniar, M.L., D.S. Kalonia, and A.P. Simonelli, *Determination Of Specific Rate Constants Of Specific Oligomers During Polyester Hydrolysis.* Journal Of Pharmaceutical Sciences, 1991. **80**(8): p. 778-782.
225. Lee, J.W. and J.A. Gardella, *In vitro hydrolytic surface degradation of poly(glycolic acid): Role of the surface segregated amorphous region in the induction period of bulk erosion.* Macromolecules, 2001. **34**(12): p. 3928-3937.
226. Amado, E. and J. Kressler, *Synthesis and hydrolysis of alpha,omega-perfluoroalkyl-functionalized derivatives of poly(ethylene oxide).* Macromolecular Chemistry And Physics, 2005. **206**(8): p. 850-859.
227. de Jong, S.J., et al., *New insights into the hydrolytic degradation of poly(lactic acid): participation of the alcohol terminus.* Polymer, 2001. **42**(7): p. 2795-2802.
228. Shih, C., *Chain-End Scission In Acid-Catalyzed Hydrolysis Of Poly(D,L-Lactide) In Solution.* Journal Of Controlled Release, 1995. **34**(1): p. 9-15.
229. Noda, M., *Organotin(IV) compounds as intramolecular transesterification catalysts in thermal depolymerization of poly(L-lactic acid) oligomer to form LL-lactide.* Preparative Biochemistry & Biotechnology, 1999. **29**(4): p. 333-338.
230. Pradny, M. and J. Kopecek, *Hydrogels For Site-Specific Oral Delivery - Poly[(Acrylic Acid)-Co-(Butyl Acrylate)] Cross-Linked With 4,4'-Bis(Methacryloylamino)Azobenzene.* Makromolekulare Chemie-Macromolecular Chemistry And Physics, 1990. **191**(8): p. 1887-1897.
231. Lee, J.W., et al., *Synthesis and characteristics of interpenetrating polymer network hydrogel composed of chitosan and poly(acrylic acid).* Journal Of Applied Polymer Science, 1999. **73**(1): p. 113-120.
232. English, A.E., T. Tanaka, and E.R. Edelman, *Polyelectrolyte hydrogel instabilities in ionic solutions.* Journal of Chemical Physics, 1996. **105**(23): p. 10606-10613.
233. De, S.K., et al., *Equilibrium swelling and kinetics of pH-responsive hydrogels: Models, experiments, and simulations.* Journal of Microelectromechanical Systems, 2002. **11**(5): p. 544-555.
234. Kim, B. and N.A. Peppas, *Poly(ethylene glycol)-containing hydrogels for oral protein delivery applications.* Biomedical Microdevices, 2003. **5**(4): p. 333-341.
235. Kim, B. and N.A. Peppas, *Complexation phenomena in pH-responsive copolymer networks with pendent saccharides.* Macromolecules, 2002. **35**(25): p. 9545-9550.
236. Kim, B. and N.A. Peppas, *Synthesis and characterization of pH-sensitive glycopolymers for oral drug delivery systems.* Journal Of Biomaterials Science-Polymer Edition, 2002. **13**(11): p. 1271-1281.
237. Qu, X., A. Wirsen, and A.C. Albertsson, *Synthesis and characterization of pH-sensitive hydrogels based on chitosan and D,L-lactic acid.* Journal of Applied Polymer Science, 1999. **74**(13): p. 3193-3202.
238. Herber, S., et al., *Study of chemically induced pressure generation of hydrogels under isochoric conditions using a microfabricated device.* Journal of Chemical Physics, 2004. **121**(6): p. 2746-2751.

239. Brannonpeppas, L. and N.A. Peppas, *Equilibrium Swelling Behavior of Ph-Sensitive Hydrogels. Chemical Engineering Science*, 1991. **46**(3): p. 715-722.